UNIVERSIDADE DA BEIRA INTERIOR
Engenharia

3D Computational Simulation and Experimental Characterization of Polymeric Stochastic Network Materials: Case Studies in Reinforced *Eucalyptus* Office Paper and Nanofibrous Materials

Joana Maria Rodrigues Curto

Tese para a obtenção do Grau de Doutor em
Engenharia do Papel
(3º ciclo de estudos)

Orientador: Professor Doutor Rogério Manuel dos Santos Simões
Co-orientador: Professor Doutor António Torres Garcia Portugal

Covilhã, Abril de 2012

Dedication

To Miguel, Carolina and Nuno.

To my Parents, Maria José and José Curto.

To my family and friends.

Acknowledgements

It would not have been possible to write this thesis without the help and support of Universidade da Beira Interior and Professor Manuel José Santos Silva, Coordinator of the Textile and Paper Materials Research Unit.

I am deeply grateful to Professor Rogério Simões and Professor António Portugal for the thesis supervision and valuable lessons.
I want to thank Professor Eduardo Trincão Conceição for his outstanding work developing the 3D Simulator, computational model implementation and fruitful discussions.

I also want to thank Professor Drean from ENSISA for the collaboration and nanowebs production.

My gratitude for the generous contribution of Eng. Cristina Gil, as well as for the friendly work environment in Paper, Chemistry and Textile Departments.

Acknowledgments to my Professors, especially Professors Silvy, Ana Paula, Nasceur and Almiro, references in my learning process.

Abstract

The properties of stochastic fibrous materials like paper and nanowebs are highly dependent on those fibers from which the network structure is made.

This work contributes to a better understanding of the effect of fiber properties on the network structural properties, using an original 3D fibrous material model with experimental validation, and its application to different fibrous materials used in reinforced *Eucalyptus* office paper and nanofibrous networks.

To establish the relationships between the fiber and the final structural material properties, an experimental laboratorial plan has been executed for a reinforced fibrous structure, and a physical based 3D model has been developed and implemented. The experimental plan was dedicated to an important Portuguese material: the reinforced *Eucalyptus* based office paper. Office paper is the principal Portuguese paper industry product. This paper is mainly produced from *Eucalyptus globulus* bleached kraft pulp with a small incorporation of a softwood pulp to increase paper strength. It is important to access the contribution of different reinforcement pulp fibers with different biometry and coarseness to the final paper properties. The two extremes of reinforcement pulps are represented by a *Picea abies* kraft softwood pulp, usually considered the best reinforcement fiber, and the Portuguese pine *Pinus pinaster* kraft pulp.

Fiber flexibility was determined experimentally using the Steadman and Luner method with a computerized acquisition device. When comparing two reinforcement fibers, the information about fiber flexibility and biometry is determinant to predict paper properties. The values presented correspond to the two extremes of fibers available as reinforcement fibers, regarding wall thickness, beating ability and flexibility values. *Pinus pinaster* has the thickest fiber wall, and consequently it is less flexible than the thinner wall fibers: *Pinus sylvestris* and *Picea abies*. Experimental results for the evolutions of paper properties, like paper apparent density, air permeability, tensile and tear strength, together with fiber flexibility for the two reinforcement fibers, constitute valuable information, also applicable for other reinforcement fibers, with fiber walls dimensions in this range.

After having quantified the influence of fiber flexibility, we identified that this is as a key physical property to be included in our structural model. Therefore, we chose to develop a 3D network model that includes fiber bending in the z direction as an important parameter. The inclusion of fiber flexibility was done for the first time by Niskanen, in a model known as the KCL-Pakka model. We propose an extension of this model, with improvements on the fiber model, as well as an original computational implementation. A simulator has been developed

from scratch and the results have been validated experimentally using handmade laboratory structures made from *Eucalyptus* fibers (hardwood fibers), and also *Pinus pinaster*, *Pinus Sylvestris* and *Picea abies* fibers, which are representative reinforcement fibers. Finally, the model was modified and extended to obtain an original simulator to nanofibrous materials, which is also an important innovation.

In the network model developed in this work, the structure is formed by the sequential deposition of fibers, which are modeled individually. The model includes key papermaking fiber properties like morphology, flexibility, and collapsibility and process operations such as fiber deposition, network forming or densification. For the first time, the model considers the fiber microstructure level, including lumen and fiber wall thickness, with a resolution up to 0.05μm for the paper material case and 0.05nm for the nanofibrous materials.

The computational simulation model was used to perform simulation studies. In the case of paper materials, it was used to investigate the relative influence of fiber properties such as fiber flexibility, dimensions and collapsibility. The developed multiscale model gave realistic predictions and enabled us to link fiber microstructure and paper properties.

In the case of nanofibrous materials, the 3D network model was modified and implemented for Polyamide-6 electrospun and cellulose nanowebs. The influence of computational fiber flexibility and dimensions was investigated. For the Polyamide-6 electrospun network experimental results were compared visually with simulation results and similar evolutions were observed. For cellulose nanowebs the simulation study used literature data to obtain the input information for the nanocellulose fibers. The design of computer experiments was done using a space filling design, namely the Latin hypercube sampling design, and the simulations results were organized and interpreted using regression trees.

Both the experimental characterization, and computational modeling, contributed to study the relationships between the polymeric fibers and the network structure formed.

Keywords

3D Network Materials Modeling, Flexibility, *Eucalyptus*, Reinforcement Fibers, Paper, Nanofibrous Materials Simulation, Polyamide-6 nanofibers

Resumo

As propriedades de materiais estocásticos constituídos por fibras, tais como o papel ou nanoredes poliméricas, dependem fortemente das fibras a partir das quais a estrutura em rede se forma.

Este trabalho contribui para uma melhor compreensão da influência das propriedades das fibras nas propriedades estruturais das redes, utilizando um modelo original 3D para materiais constituídos por fibras, com validação experimental, bem como a sua aplicação aos materiais utilizados no papel de escritório de *Eucalyptus*, com fibras de reforço, e a redes de nanofibras.

Para estabelecer as relações entre a fibra e as propriedades estruturais do material, executou-se um planeamento experimental para uma estrutura fibrosa reforçada, e desenvolveu-se e implementou-se um modelo 3D de base física. O plano experimental teve como objecto um material relevante em Portugal: o papel de escritório de *Eucalyptus* com fibras de reforço. O papel de escritório é o produto principal da indústria de papel Portuguesa. Este tipo de papel é produzido a partir da pasta kraft branqueada de *Eucalyptus globulus*, com incorporação de uma pequena quantidade de pasta de reforço, "softwood", para melhorar a resistência do papel. É importante avaliar a contribuição de diferentes fibras de reforço, com biometria e massas linear distinta, nas diferentes propriedades finais do papel. Os dois extremos das fibras de reforço estão representados pela pasta kraft de *Picea abies*, usualmente considerada a melhor fibra de reforço, e a pasta kraft Portuguesa de *Pinus pinaster*.

A flexibilidade da fibra determinou-se experimentalmente utilizando o método de Steadman e Luner, com um dispositivo de aquisição automatizado. A informação relativa à flexibilidade e biometria da fibra é fundamental para inferir sobre as propriedades do papel. Os valores determinados correspondem a valores dos extremos, paras as fibras de reforço disponíveis no mercado, no que diz respeito a espessura de parede, refinabilidade e valores de flexibilidade. Pode considerar-se a fibra de *Pinus pinaster* num extremo, sendo a fibra de paredes mais espessas, e consequentemente menos flexível que as fibras de paredes mais finas: *Pinus sylvestris* e *Picea abies*. Desta forma, os resultados experimentais obtidos para estas fibras, relativos à evolução de propriedades do papel, nomeadamente densidade, permeabilidade ao ar, resistência à tracção e ao rasgamento, entre outros, constituem informação importante que pode ser aplicada a outras fibras de reforço, que se situem nesta gama.

Como consequência lógica da identificação da flexibilidade da fibra como uma propriedade física determinante, e após a quantificação experimental, a escolha do modelo de papel recaiu sobre um modelo que inclui a flexibilidade como propriedade chave. Assim, desenvolvemos um modelo 3D que inclui a flexão das fibras na direcção transversal, isto é, a direcção da espessura do papel, também reconhecida como direcção da coordenada z. A inclusão da flexibilidade da fibra baseia-se no modelo de Niskanen, conhecido como o modelo

KCL-Pakka. Apresenta-se uma extensão deste modelo, com modificações no modelo da fibra, bem como uma implementação computacional original. Desenvolveu-se um simulador para matérias em rede, que se validou com resultados experimentais. Efectuaram-se, também, as modificações necessárias para obter um simulador para nanomateriais, o que constitui uma inovação relevante.

No modelo deste trabalho, desenvolvido para materiais fibrosos em rede, as fibras modelam-se individualmente e a estrutura forma-se sequencialmente pela sua deposição e conformação à estrutura existente. O modelo inclui propriedades das fibras determinantes, tais como morfologia, flexibilidade e colapsabilidade. Bem como etapas do processo, nomeadamente a deposição das fibras e a formação da rede, isto é, a densificação da estrutura. De uma forma original, o modelo da fibra inclui a espessura do lúmen e da parede da fibra, com uma resolução de 0.05μm para as fibras do papel e 0.05nm no caso das nanofibras.

O modelo computacional desenvolvido utilizou-se na realização de estudos de simulação. No caso dos materiais papeleiros, utilizou-se para investigar a influência das propriedades das fibras, tendo-se obtido previsões realistas.

No caso dos nanomateriais, o modelo foi modificado e implementado para as fibras electrofiadas de Poliamida-6 e redes de nanocelulose.

O plano de experiencias computacionais utilizou uma distribuição no espaço "Latin hypercube" e os resultados das simulações organizaram-se recorrendo a árvores de regressão.

Tanto a caracterização experimental, como a modelação computacional, contribuíram com valiosa informação para o estudo das relações entre as fibras poliméricas e as estruturas em rede por elas formadas.

Palavras chave

Modelação 3D de materiais em rede, Flexibilidade, *Eucalyptus,* Fibras de reforço, Papel, Simulação de nanomateriais, Nanofibras de poliamida-6

Table of Contents

List of publications

1. CURTO, J.M.R., CONCEIÇÃO, E.L.T., PORTUGAL, A.T.G. and SIMÕES, R.M.S., 2011d. The Influence of *Eucalyptus* and reinforcement fibers flexibility on paper properties: experimental and 3D paper model evaluation. In Proceedings of the 5th ICEP International Colloquium on Eucalyptus Pulp held in May 9-12, Porto Seguro, Brazil (2011).

2. CURTO, J.M.R, CONCEIÇÃO, E.L.T., PORTUGAL, A.T.G. and SIMÕES, R.M.S., 2010a. Comparative study of fibres for Eucalyptus globulus based paper using experimental characterization and 3D paper modeling. In Proceedings of the 2nd "Simpósio de Materiais Texteis e Papeleiros", Universidade da Beira Interior, Covilhã, Portugal (2010). ISBN: 978-989-654-074-6.

3. CURTO, J.M.R, GIL, C., CONCEIÇÃO, E.L.T., PORTUGAL, A.T.G. and SIMÕES, R.M.S., 2009a. "Estudo comparativo de incorporação de fibra de *Pinus pinaster* branqueada no papel de *Eucalyptus globulus*". *Revista Pasta e Papel* (2009): pp. 52-57.

4. CURTO, J.M.R, CONCEIÇÃO, E.L.T., PORTUGAL, A.T.G. and SIMÕES, R.M.S., 2011c. Three dimensional modeling of fibrous materials and experimental validation. *Materialwissenschaft und Werstofftechnik, Materials Science and Engineering Technology*, Wiley-vch, Germany, Wiley-Blackwell, USA, vol.42 no.5 (2011): pp. 370-374. ISSN: 0933-5137 (Print). ISSN 1521-4052 (Online). ISI IDS no.: 762EM.

5. CONCEIÇÃO, E.L.T., CURTO, J.M.R, SIMÕES, R.M.S and PORTUGAL, A.T.G., 2010. Coding a simulation model of the 3D structure of paper. In Proceedings of the 2nd International Symposium on Computational Modeling of Objects represented in Images, CompIMAGE 2010, USA. *Lecture Notes in Computer Science*, Barneva; R.P. *et al*. (Eds.), Springer-Verlag Berlin, vol.60 no.26 (2010): pp. 299–310. ISBN: 978-3-642-12711-3. ISI Document Delivery No.: BPJ99.

6. CONCEIÇÃO, E.L.T., CURTO, J.M.R., SIMÕES, R.M.S. and PORTUGAL, A.T.G, Parallelization of a parameter estimation problem in a 3D model of paper. In Proceedings of the "Congresso de Métodos Numéricos de Engenharia", CMNE, APMATC, Coimbra, Portugal, 14-17 July, vol.1 (2011).

7. CURTO, J. M. R., HEKMATI, A.H., DREAN, J.Y, CONCEIÇÃO, E.L.T., PORTUGAL, A.T.G., SIMÕES, R.M.S. and SANTOS SILVA, M.J., 2011b. Three dimensional polyamide-6 nanowebs modeling and simulation. In Proceedings of the 11th World Textile Conference, AUTEX 2011 (Association of Universities for Textiles), Mulhouse, ENSISA (École Nationale Supérieure d'Ingénieurs Sud Alsace), France, June, vol.2 (2011): pp. 639-643. ISNB: 978-2-7466-2858-8.

8. CURTO, J.M.R, CONCEIÇÃO, E.L.T., PORTUGAL, A.T.G. and SIMÕES, R.M.S., 2011a. The fiber properties influence on a three dimensional web model: reinforced office paper and cellulose nanowebs case studies. In Proceedings of the 5th International Conference on Advanced Computational Engineering and Experimenting, ACE-X2011, Algarve, Portugal (2011). Abstract.
   Best Paper Young Scientist Award, Springer.

Chapter 1 Introduction

In the science and engineering of materials there has been increasing interest in the design and production of enhanced materials, especially materials based on multi scaled structure organization. Traditional fibrous stochastic materials like paper, advanced materials like composites, and new materials like nanowebs are structured materials, its study can beneficiate from an integrative approach, where the physical knowledge of different scales is considered.

Following this philosophy, our work is focused on the structural properties of materials at different scales, departing from the fiber and building the network, for macro and nanomaterials. Our goal was to use experimental characterization and computational modeling, to study the relationships between polymeric fiber raw materials, process and final material properties.

Initially, in this work, we will concentrate on the properties of paper as the most common stochastic fibrous material used in society and industry, but there is a larger family of materials that exhibit similar structural characteristics. To illustrate these network materials micrographs several stochastic fibrous materials, including paper, are shown in Figure 1. From left to right and top to bottom: carbon fiber web, used in fuel cell applications (Eichhorn and Sampson, 2005); glass fiber network, used in laboratory filter applications (Eichhorn and Sampson, 2005); 60g/m^2 Eucalyptus laboratory handmade ISO Standard paper sheet, produced for this work at UBI; electrospun polyamide-6 network, produced by Ensisa for this work.

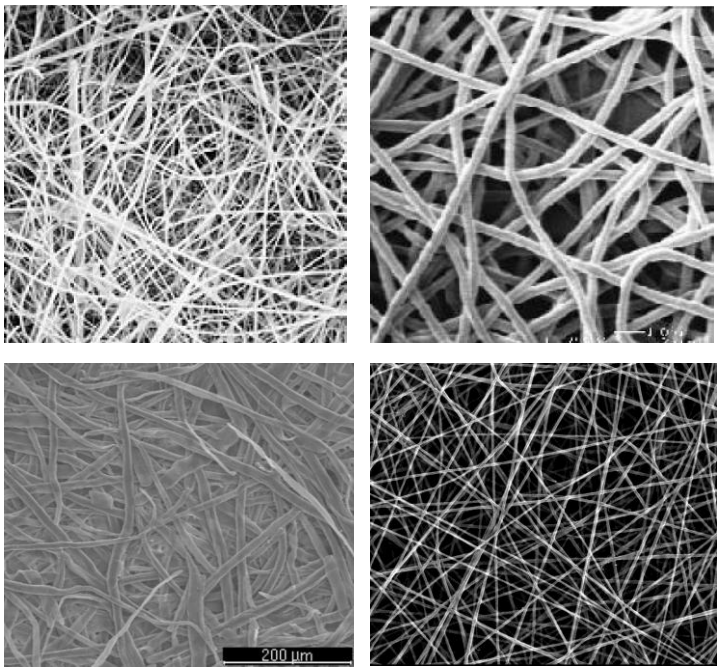

Figure 1. Polymeric stochastic network materials

1.1 Motivation and Objectives

Paper is a material present in our daily life that has great importance in communication and transmission of human knowledge. That is one of the reasons why paper consumption is used as an indicator of the economic development of a country. In the case of Portugal, both forest and cellulose pulp and paper industries play a prominent role on the Portuguese economy.

The research scope of this work is inserted in the research activities of Textile and Paper Research Unity of Beira Interior University and Research Center for Chemical Process Engineering and Forest Products of University of Coimbra and focus in raw materials and processes that are important to the national industry. In this domain, we have identified several research questions related to the way fibers respond to various operations of the papermaking process and how their properties influence the network structure. As a contribution to link fiber properties and paper structural properties our research goal was to develop a model that simulates the fibrous network structure present in paper materials. In this structure each fiber is modeled individually using an innovating fiber model that includes fiber structure (fiber length, fiber width, fiber wall and fiber lumen), and also the fiber mechanical behavior, this is, the bending in z direction and adjustment to the structure.

The modeling of materials is nowadays an important tool in developing and designing materials with enhanced performance and/or new functionalities. In the developing process of new materials this kind of tools can reduce significantly the experimental work, enabling better design of the experimental tests, and simulating the contribution of new components on the global performance or on specific properties. Despite the recognition of its importance and progresses that have recently been made in the area of fibrous materials modeling, there is no code available, and some key parameters of the fibers and/or formation process are not included in the models presented in literature. So, the objective of the present thesis is to develop a model, using a versatile programming language (MatLab), able to be extended to include additional parameters. The goal is to simulate the structure of paper materials, using as inputs the morphological properties of fibers, and also including the mechanical response of the fibers to compression and flexion (such as fiber collapsibility and fiber flexibility). Initially, in its basic form, the output of the model, chosen to be representative of the paper structure, was paper thickness (at a given grammage), paper porosity, and relative bonded area of fibers in paper. In the present, other structural properties like coverage, inter fiber and intrafibre porosity, number of crossings per fiber and local thickness have been introduced. Also two extensions have been accomplished deriving from the first implementation. The model has been extended to simulate paper formation, with the inclusion of sedimentation rules, and also has been extended to other fibrous materials, such as nanowebs.

To accomplish these general objectives, a combined experimental and computational simulation approach was used. The experimental part aims to provide information about the

key fiber parameters, their corresponding range of variation, and their influence on the structural and mechanical properties of the papers. To achieve this goal, experimental work was carried out, using pulp fibers with markedly different morphological and mechanical properties (*Eucalyptus globulus, Pinus pinaster, Pinus sylvestris* and *Picea abies*). Office paper is mostly formed by hardwood fibers, for example *Eucalyptus* fibers, with a small percentage of reinforcement fibers, usually softwood fibers. *Eucalyptus globulus* is well recognized as a good quality fiber for office paper and has consequently been chosen to be the hardwood pulp fiber of this work. At the beginning of this work, in spite of having around 32% of *Pinus pinaster* forest, Portugal didn't produce bleached softwood fibers and needed to import all the reinforcement fibers to be included in office paper. Accordingly, there was a scientific and industrial interest in studying *Pinus pinaster* bleached fibers and compare it with reference reinforcement fibers available on the market. From previous studies (Curto *et al.*, 2007; Curto and Simões, 2005; Curto *et al.*, 2003a) we were able to conclude that *Pinus pinaster* has the thickest fiber wall, presenting the highest coarseness. The other reinforcement fibers were selected because they were considered ideally reinforcement fibers and presented thinner fiber walls (*Pinus sylvestris* and *Picea abies*). In the present thesis, experimental work was carried on to quantify the influence of several stock fiber preparation operations, particularly beating, on fiber flexibility, measured by the Steadman and Luner method. Experimental results were used to provide realistic input ranges for the model, and also for validation. Paper thickness (at a given basic weight), or the corresponding apparent porosity (based on paper apparent density and assuming a value of 1.53 for polysaccharides density) were compared with the paper model outputs.

As the market papers are made from a mixture of fibers, as it is the case of office paper, it is of industrial and scientific interest, to investigate the topic of fibers mixture. Relevant experimental work was carried out, using mixture of *Eucalyptus globulus* pulp fibers and softwood pulp fibers in different proportions. The next step will be to use them to define input ranges and also compare with simulation results. In this thesis we didn´t include simulations of pulp mixtures. These simulations, as well as the comparison with experimental data already obtained will, deserve our attention in a near future. Also for the future, additional advantage will occur if the model could be extended, in order to simulate the corresponding mechanical performance of the paper materials. At this respect, the relative bonded area (ratio between the fibers bonded area and the total surface area of the fibers) will be a crucial structural parameter, and also de number of crossings per fiber (parameter recently added to the model) to simulate the stress distribution between fibers in the structure.

Concerning the extension to other materials, the goal for this thesis is to present the model extension for fibrous nanomaterials, and to realize a simulation study that is indicative of its possibilities. If paper had a major contribution to the advance of knowledge and culture in our society, nanomaterials are pointed as key materials for the future technologic development. It is consensual that the study and discovery of novel materials, processes, and

phenomena at the nanoscale will have a profound impact on our economy and society in the near future. The research and development in nanotechnology will lead to potential breakthroughs in areas such as nanoelectronics, medicine and healthcare, energy, biotechnology, information technology and national security, in a revolution comparable to the industrial revolution (Kornev *et al*, 2009; Barnes *et al*, 2007; Paiva *et al*, 2007; Ma *et al*., 2005; Jayaraman *et al*, 2004; Silva *et al*., 2011).

1.2 Document organization

Chapter 1 contains the introduction, including objectives and motivation, and also the document organization. Chapter 2 describes the cellulose materials with all the structural levels contributing to fiber properties, from the organization of polymeric chains to the higher structural levels, like microfibrils, fiber walls, etc. Chapter 3 reviews and discusses the literature of 3D network materials modeling. Chapter 4 includes the list of Publications and also the Publications presented as a part of this thesis. Chapter 5 is dedicated to conclusions and future work. The thesis document finalizes with the list of References.

The objective of this work was to study how different fiber properties influence the network properties, for paper (Publications 1, 2, 3 and 4) and nanofibrous materials (Publication 7 and the Abstract of the 8th Publication). Publications 5 and 6 present the developed web model and the most relevant programming code.

The determination of relationships between the fibers and the structure built by them was done, both experimentally and, with the simulation model for paper fibers (Publications 1, 2 and 4). The experimental part aims to provide information about the key fiber parameters, including fiber flexibility and fiber collapse, their corresponding range of variation, and their influence on the structural and mechanical properties of the papers. To achieve this goal, experimental work was carried out, using pulp fibers with markedly different morphological and mechanical properties (*Eucalyptus globulus, Pinus pinaster, Pinus sylvestris* and *Picea abies*). Publication 1 is dedicated to fiber flexibility: the methodology for measuring fiber flexibility; experimental results for Eucalyptus fibers and the two extremes of reinforcement fibers; and the use of fiber flexibility in the paper model. Publication 2 is dedicated to the influence of fiber properties on web structure. The SEM is used to obtain information about the transversal or Z dimension of paper. The degree of collapse is determined and used as input in the paper model to predict the paper thickness. A simulation study is presented to separate the influence of fiber flexibility and fiber collapse on paper thickness. Publication 3 presents the experimental characterization for the reinforced *Eucalyptus globulus* office paper with the mixture of reinforcement fibers on different proportions and the determination of structural and mechanical paper properties. At the present stage Publication 3 consists exclusively of an experimental characterization but we intend to use this experimental data as input on the paper model, and to validate the model for pulp

mixtures, in future work. Publication 4 presents the paper model, its inputs, outputs and extensions, as well as experimental validation and simulation studies. Publication 5 complements the model presentation with Matlab implementations and the extension that includes formation parameters and sedimentation rules. Publication 6 presents the programming code to the parallelization approach. Publication 7 presents the model extension to electrospun nanofibrous materials and a simulation study to a nanofibrous material: the polyamide-6 nanofibrous network. Publication 8, from which we present the Abstract, is dedicated to cellulose nanowebs.

Chapter 2 Natural cellulosic fibers

Natural cellulosic fibers are the most important raw materials of paper and paperboard, as well as of many hygiene products. The most usual source is wood. These fibers are obtained from woods using chemical, mechanical or chemo-mechanical processes. Wood raw material provenience has a very significant effect on the properties of the received fibers, as does the process used in their separation and pulp and paper manufacturing. The main chemical components of fibers are cellulose, hemicelluloses and lignin. Fibers are structured materials where the polymeric components have spatial arrangements in different scales (Figure 2).

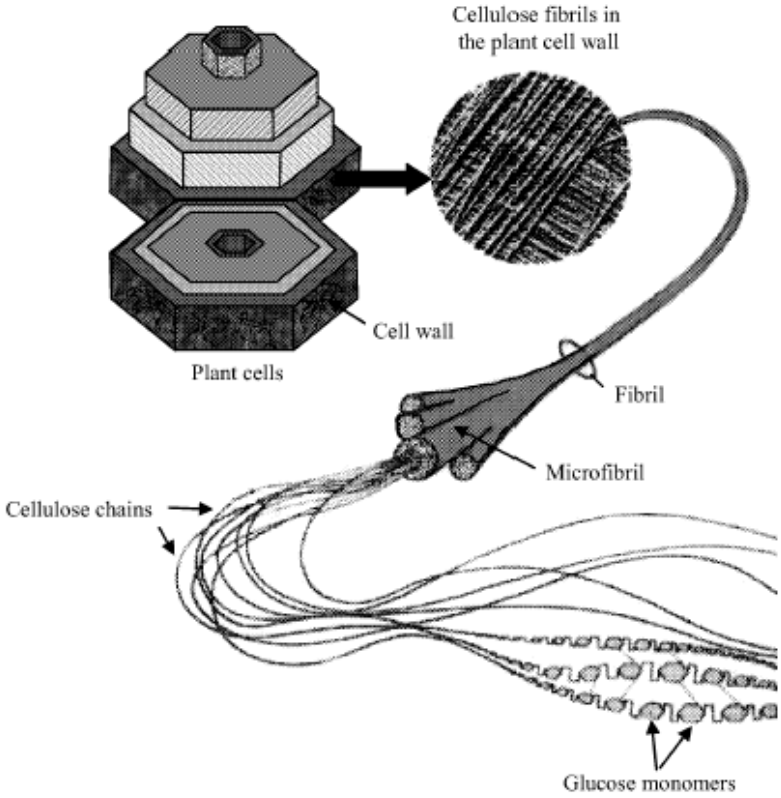

Figure 2. Structural hierarchy of cellulose fibers (Djerbi, 2005)

Of these components cellulose is the main strength delivering component. It is a long linear polymer and has a strong tendency for intra- and intermolecular hydrogen bonding, which leads to formation of microfibrils. These have excellent mechanical properties due to ordered structure. Microfibrils further aggregate into fibrils or fibril aggregates. These fibrils are wound at an angle called microfibrillar angle around fiber axis, and can be thought to form several distinct layers. It can be identified a primary wall and secondary wall, which consist

of three separate sub-layers (S1, S2 and S3). Middle lamella is the material between fibers. Fiber layers have different chemical compositions and microfibrillar angles. In addition to defects in fibers, the microfibrillar angle of the thickest secondary wall layer, the S2-layer, has been shown to have the most significant effect on fiber strength (Page *et al.*, 1985; Page *et al.*, 1977).

2.1 Cellulose

Cellulose is the main load bearing component in fibers. It is a linear polymer composed of glucose units joined together by ß-1,4 glycosidic bonds. The degree of polymerization, DP, or the number of glucose units in a cellulose chain of a native softwood fiber is above 10000, dropping in chemical pulping to around 500-2000 (Fengel and Wegner, 1989).

There are two different crystalline forms of native cellulose, cellulose I, designated as Iα and Iß (Fengel and Wegner, 1989). The proportion of Iα and Iß forms depends on the cellulose origin. Primary walls of conifer tissue contain more cellulose Iα, secondary walls more cellulose Iß. There are other crystalline forms of cellulose, such as cellulose II, but also other forms have been characterized.

The next larger structural unit from single cellulose chains is elementary fibril or microfibril, which consists of 30-40 parallel cellulose chains. As an example, a microfibril with 36 chains would have dimension of around 3.5 x 3.2nm, but this dimensions can vary (Wägberg and Annergren, 1997) Recently, for *Eucalyptus globulus* fibers, Atomic Force Microscopy has been used to measure the microfibril diameter, and a value of 4-5 nm has been obtained (Paiva et al, 2007). Microfibrils again aggregate into what are called fibrils or fibril aggregates, with the size of around 20nm. Usually it is considered that microfibrils consist of crystalline structure but some disorder is present and some cellulose in fibrils exists in amorphous or less ordered form.

2.2 Hemicelluloses

Hemicelluloses constitute about 25-40% of wood material. Hemicelluloses are polysaccharides with a DP of 50-300 (Fengel and Wegner, 1989). Hemicelluloses found in hardwoods are different from those found in softwoods. The major hardwood hemicellulose is a partially acetylated 4-O-methylglucurono xylan with a minor proportion of glucomannan also present. Partially acetylated galactoglucomannans are the most common softwood hemicelluloses. Xylan is also present in softwood, where it is substituted by furanosidically linked arabinose units in addition to 4-O-methylglucuronic acid groups (Fengel and Wegner, 1989).

High hemicellulose content in fibers may in some cases be beneficial for the recycling purposes, since it may lead to lower tendency to hornify in drying.

There are evidences that hemicelluloses affect fiber structure and strength but the mechanisms involved are not completely understood. Hemicelluloses affect the strength of the final fiber network formed, due to the hydroxyl groups in hemicelluloses that are responsible for to the swelling of wet fibers. Besides internal organization that occurs with swelling, the main effect comes when a wet fiber network is dried. Swollen fibers shrink in drying, and while doing so, they activate segments in other fibers, that are connected via inter-fiber bonds (Alava and Niskanen, 2006). This is a favorable effect on the fiber network strength properties, and the more swollen the fibers are, the more favorable the effect. This phenomena can be associated with the Jentzen-effect (Sirvio, 2008 cit. Jentzen, 1964), the improvement of single fiber strength properties when dried under tension.

2.3 Lignin

Around 15-30% of wood fibers are composed of lignin. Its role is to act as cement between fibers and to protect against the enzymatic degradation of the cell wall.
Lignins consist of phenylpropane units and forms cross linked structures. Softwood and hardwood lignins differ in methoxyl content and in the degree of cross linking. Lignin is largely removed in chemical pulping, making wet fibers porous and flexible. When delignification occurs the tensile stiffness of fibers is affected (Paavilainen, 1994; Paavilainen, 1990). Many factors play a role in the final web structure and strength properties (Paavilainen, 1998; Paavilainen, 1993a; Paavilainen, 1993b; Seth and Page, 1988; Page, 1969). The formation of discontinuities, this is, dislocations and pores in cooking and papermaking operations also affect the final web resistance.

2.4 Morphology

Morphological properties include fiber length, fiber width and cell wall thickness. These vary between wood species, within annual growth rings, different stem parts and are also affected by the growing conditions (Paavilainen, 1994).
Fiber length affects the tensile strength, breaking strain and fracture toughness of dry paper, and is especially important for wet web strength (Seth and Chang, 1999a; Seth and Page, 1988).

Chapter 3 3D Network Materials Modeling

Meaningful work has been done in the modeling of fiber materials, the greatest part focusing on two dimensional geometry. Professors C.T.J. Dodson and W.W. Sampson from University of Manchester (UK) have dedicated a considerable amount of work to this field of materials modeling (Dodson and Sampson, 2009a; Sampson, 2009a; Sampson, 2009b; Dodson and Sampson, 2008; Sampson, 2008; Sampson and Urquhart, 2008; Dodson and Sampson, 2007; Dodson and Sampson, 2005; Sampson and Sirvio, 2005; Sampson, 2004). A list of previous Dodson and Sampson publications, also including publications with other authors, have been listed in References. Statistical geometry models started with the Kallmes and Corte (1960) model and a pedagogical revision can be found in the Deng and Dodson (1994) revision book. Studies with three-dimensional network models constitute the latest innovation. In this approach the third dimension is introduced, considering the variations in the z direction, this is, along the thickness of the material, where fibers are allowed to bend out-of-plane to account for the interwoven geometry of paper. This 3D approach has been introduced by Niskanen and Alava (1994) with the KCL-Pakka model. We can find in the literature examples of other structures called 3D, where there is no fiber bending in the z direction. These structures should have a different name, because they are built from the pilling of 2D structures; in fact there is only a change of position in the plane, and third dimension is obtained by the layering of several 2D planes. Several examples can be presented, like the one proposed in the statistical geometry theory by Kallmes and Cortes (1962) consisting of several 2D layers forming a multi-planar structure made from rigid fibers. Other example with rigid fibers is the case of the simulation model by Wang and Shaler (1998), where an artificial fiber sobreposition has to be considered, meaning that it is accepted that two different fibers are occupying the same space, fact that is physically impossible but necessary to obtain the simulated structure. And recently, for the case of nonwoven materials the presented models are either 2D, or 3D but with rigid fibers (Hosseini and Tafreshi, 2010; Maze *et al.*, 2007; Pourdeyhimi *et al.*, 2006; Wang *et al.*, 2006; Kim *et al.*, 2005). In the effective 3D structures there is a variation of the fiber position not only in the plane, but also in the third dimension; the fiber is bending in the z dimension, so a different name should be adopted to distinguish them from the other so called 3D structures. In the following years, some modifications of the initial KCL-Pakka model have been presented. Originally fibers only had two possible directions and were only crossing perpendicularly (figure 3.1), but in the most recent presented structures, fibers were already randomly deposited (Hellén *et al.*, 2002). A three-dimensional model for fibrous fluff materials has been proposed by Heyden and Gustafsson (1998). In this model, every fiber is represented by a single circle arc and placed in a box forming a periodic network. The advantage of the arc model is that it is relatively straightforward to work with it, mathematically, but at the same time it presents a physical limitation because it is not describing the fiber bending that occurs when fibers adjust to the

already formed structure. Another 3D implementation based on SEM images has been done in France (Vincent, Rueff and Voillot, 2009). In this case the fiber bending is defined using an angle that is fixed for each material. An important review of three-dimensional structural analysis has been done by Bloch and Roscoat (2009).

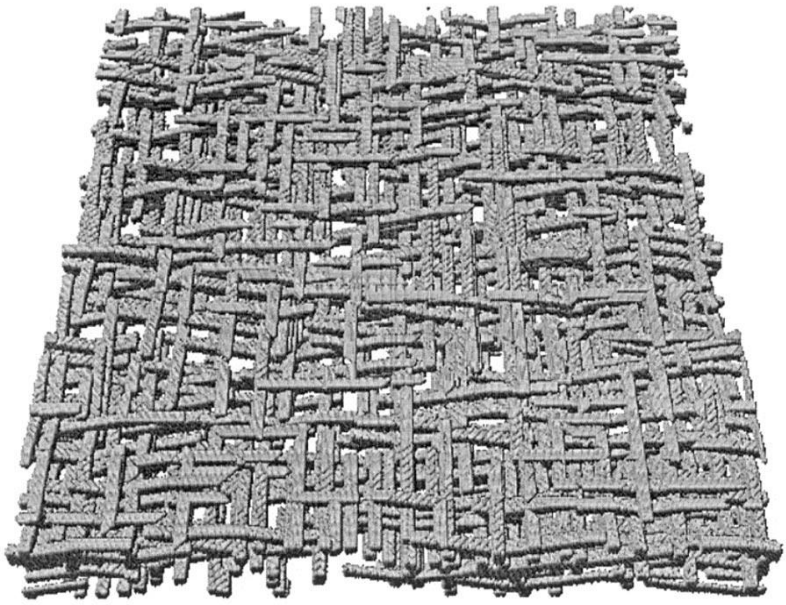

Figure 3.1 – An example of a fiber network structure simulated by the Niskanen and Alava model (Alava and Niskanen, 2006). Reproduced respecting the Journal Permission copyright.

The model implemented in this work is based on the KCL-Pakka model proposed by Niskanen and Alava (1994) but has several innovations. In our work the fiber model includes the fiber internal structure and the possibility to change it and have it collapsing in the z direction. Also two major extensions have been developed: an extension that incorporates other fiber sedimention possibilities, and an extension to other fibrous materials. In this type of model, the three-dimensional structure of paper is simulated using a sedimentation-like or growth process. The sedimentation model of paper assumes that the sheet is formed from a dilute suspension under the influence of an uniform flow field. In its initial assumption all fiber interactions are ignored. The model proposed by Niskanen and Alava was the first to include fiber flexibility. Besides the standard KCL-PAKKA model an extension of this model which incorporates a formation control parameter is implemented by us (Curto *et al.*, 2011; Conceição, 2010). This modification is based on the sedimentation rule developed by Provatas and Useaka (2003).

In our model the lumen of the fiber is introduced in the fiber model for the first time, allowing the study of fiber collapse and intrafiber porosity (Curto *et al.*, 2011c; Curto *et al.*,

2009). At the present stage, the network model is able to predict structural paper properties (Curto *et al.*, 2011c; Curto *et al.*, 2010a). Figure 3.2 shows an example of a fiber network structure simulated by the presented model.

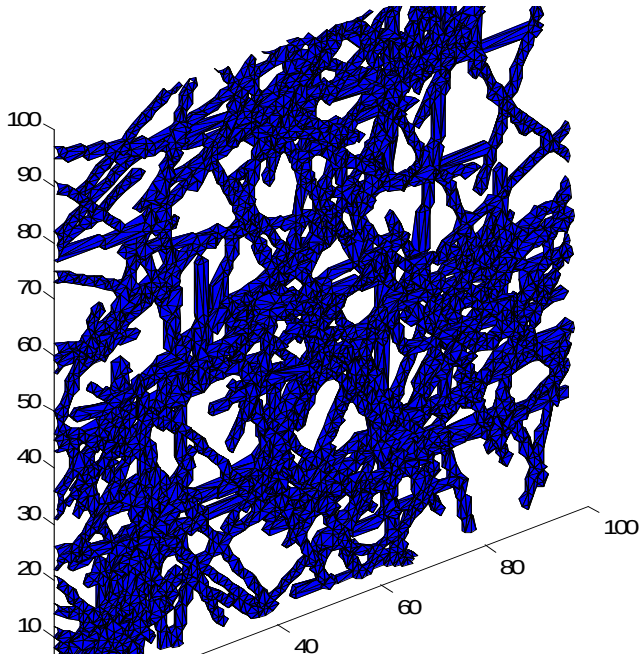

Figure 3.2 – An example of a fiber network structure simulated by the presented model.

Regarding the paper model it is important to remark that the fiber and paper structure is defined using a voxel approach, where each elemental structure is three dimensional. Each voxel can be filled with material, in the case of the being a fiber cell wall, or empty, for a void fraction of the paper or the fiber lumen. To implement the model, the fiber physical quantities should be, in some way, converted into the corresponding computational quantities. In the simplest original version, the fiber width corresponded to the voxel width, but in the latest version this limitation was overcome. In the fiber thickness, or z direction, the fiber is represented by a chosen number of layers, for example 12, resulting in a detailed fiber structure in z direction, with a voxel definition of fiber lumen and fiber collapse. The computational fiber flexibility is obtained using cellular automata, in an innovative computational implementation (figure 3.3).

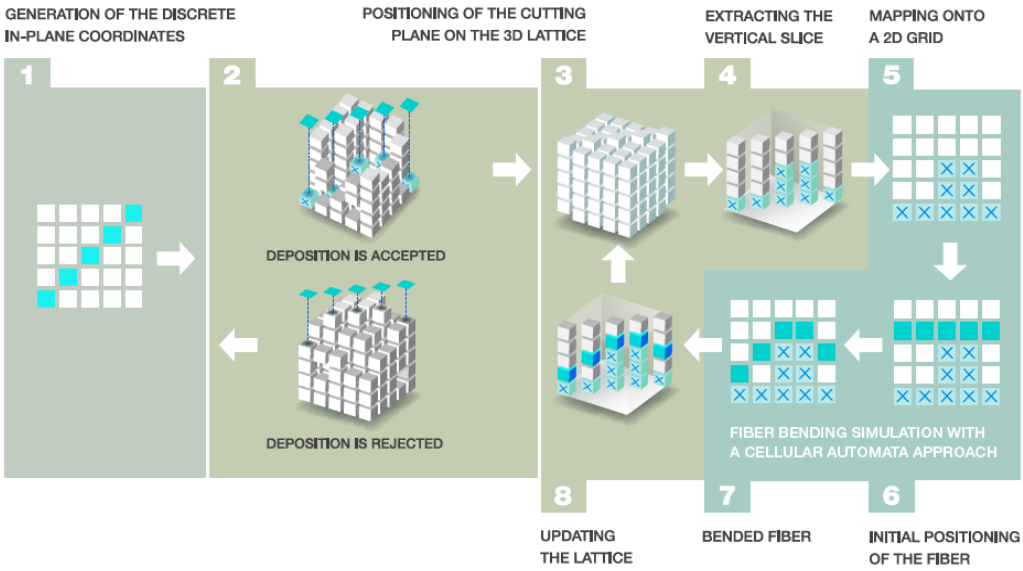

Figure (3.3). Fiber deposition in the 3D matrix followed by plane extraction and fiber bending to conform to the underlying structure.

The computational simulation can be described as follows (figure 3.3):

- Generation of a fiber in the in-plane direction.
- Testing particle deposition rule. If the fiber is not accepted, the generation trial is repeated.
- Extraction of the out-of-plane slice from the 3D network where the bending procedure occurs.
- Fiber deposition according to fiber flexibility and conformation to the underlying surface.
- Updating of the 3D network.

Fibers are modeled according to their dimensions, flexibility, and collapsibility. The input parameters are: length, width, wall thickness, lumen thickness, fiber flexibility, and number of layers in the thickness direction. Length values can be averages or distributions. Fines and fillers can also be introduced.

The computational fiber flexibility is based on the Niskanen approach (Niskanen *et al.*,1997) but has a novel implementation using cellular automata (Curto *et al.*, 2011; Conceição, 2010). The space is discretized into a Cartesian uniform grid of cells so that each fiber in the model is represented by a sequence of cells. A "bending" flexibility or dimensionless computational flexibility gives the largest allowed vertical deflection for the fiber (Niskanen *et al.*, 1997). So, any two nearest neighboring cells on the fiber can make, at most, the maximum fiber flexibility.

The paper is formed by the deposition of single fibers, one at a time. Depending on its position, dimensions, and flexibility, the fiber conforms to the underlying structure. In the present work, fibers are randomly positioned and oriented in the x-y plane to simulate the

formation of isotropic handsheets (the ones used to validate the model). The paper machine orientation can be simulated by using an appropriate spatial distribution.

The model output is a 3D structure formed with occupied voxels and empty voxels, where the information concerning each fiber is kept. From this formed structure several model outputs are calculated: paper thickness (local and average), porosity (interfiber and global), relative bonded area, coverage and number of crossings per fiber.

In addition, the model was implemented with an accessible programming language (MatLab) and is based on cellular automata. These model features enable its easy upgrade, in the future. The model application to nanofibrous materials constitutes, also, an important advantage (Curto *et al.*, 2011a; Curto *et al.*, 2011b).

Chapter 4 List of Publications

1. CURTO, J.M.R., CONCEIÇÃO, E.L.T., PORTUGAL, A.T.G. and SIMÕES, R.M.S., 2011d. The Influence of *Eucalyptus* and reinforcement fibers flexibility on paper properties: experimental and 3D paper model evaluation. In Proceedings of the 5th ICEP International Colloquium on *Eucalyptus* Pulp held in May 9-12, Porto Seguro, Brazil (2011).

2. CURTO, J.M.R, CONCEIÇÃO, E.L.T., PORTUGAL, A.T.G. and SIMÕES, R.M.S., 2010a. Comparative study of fibers for *Eucalyptus globulus* based paper using experimental characterization and 3D paper modeling. In Proceedings of the 2nd "Simpósio de Materiais Têxteis e Papeleiros", Universidade da Beira Interior, Covilhã, Portugal (2010). ISBN: 978-989-654-074-6.

3. CURTO, J.M.R, GIL, C., CONCEIÇÃO, E.L.T., PORTUGAL, A.T.G. and SIMÕES, R.M.S., 2009a. "Estudo comparativo de incorporação de fibra de *Pinus pinaster* branqueada no papel de *Eucalyptus globulus*". *Revista Pasta e Papel* (2009): pp. 52-57.

4. CURTO, J.M.R, CONCEIÇÃO, E.L.T., PORTUGAL, A.T.G. and SIMÕES, R.M.S., 2011c. Three dimensional modeling of fibrous materials and experimental validation. Materialwissenschaft und Werstofftechnik, *Materials Science and Engineering Technology*, Wiley-vch, Germany, Wiley-Blackwell, USA, vol.42 no.5 (2011): pp. 370-374. ISSN: 0933-5137 (Print). ISSN 1521-4052 (Online). ISI IDS no.: 762EM.

5. CONCEIÇÃO, E.L.T., CURTO, J.M.R, SIMÕES, R.M.S and PORTUGAL, A.T.G., 2010. Coding a simulation model of the 3D structure of paper. In Proceedings of the 2nd International Symposium on Computational Modeling of Objects represented in Images, CompIMAGE 2010, USA. *Lecture Notes in Computer Science*, Barneva; R.P. *et al*. (Eds.), Springer-Verlag Berlin, vol.60 no.26 (2010): pp. 299–310. ISBN: 978-3-642-12711-3. ISI Document Delivery No.: BPJ99.

6. CONCEIÇÃO, E.L.T., CURTO, J.M.R., SIMÕES, R.M.S. and PORTUGAL, A.T.G, Parallelization of a parameter estimation problem in a 3D model of paper. In Proceedings of the "Congresso de Métodos Numéricos de Engenharia", CMNE, APMATC, Coimbra, Portugal, 14-17 July, vol.1 (2011).

7. CURTO, J. M. R., HEKMATI, A.H., DREAN, J.Y, CONCEIÇÃO, E.L.T., PORTUGAL, A.T.G., SIMÕES, R.M.S. and SANTOS SILVA, M.J., 2011b. Three dimensional polyamide-6 nanowebs modeling and simulation. In Proceedings of the 11th World Textile Conference AUTEX 2011 (Association of Universities for Textiles), Mulhouse, ENSISA (École Nationale Supérieure d'Ingénieurs Sud Alsace), France, June, vol.2 (2011): pp. 639-643. ISNB: 978-2-7466-2858-8.

8. CURTO, J.M.R, CONCEIÇÃO, E.L.T., PORTUGAL, A.T.G. and SIMÕES, R.M.S., 2011a. The fiber properties influence on a three dimensional web model: reinforced office paper and cellulose nanowebs case studies. In Proceedings of the 5th International Conference on Advanced Computational Engineering and Experimenting, ACE-X2011, Algarve, Portugal (2011). Abstract.
   Best Paper Young Scientist Award, Springer.

The Influence of Eucalyptus and Reinforcement Fibers Flexibility on Paper properties: Experimental and 3D Paper Model evaluation

Curto, J.M.R. [1], Conceição, E. L.T.[2], Portugal, A.T.G.[2] and Simões, R.M.S.[1]
[1]Textile and Paper Materials Research Unit,
Chemistry Department, University of Beira Interior (UBI)
[2] Research Centre for Chemical Processes Engineering and Forest Products,
Chemical Engineering Department, University of Coimbra (UC)

Abstract

There is a lack of information about fiber flexibility and its evolution along the pulping process and stock preparation. Among the many factors that influence final paper properties, fiber flexibility is considered a key factor. Fiber flexibility depends on wood species and pulp treatment. The aim of this study was to quantify the change of fiber flexibility inflicted by the most relevant fiber process operations, these being, bleaching, beating and drying, and its influence on paper properties. The quantification of fiber flexibility, as well as the range of variation for fiber and paper properties constitutes valuable experimental data that will be used as input in a paper model developed to simulate paper structures. To achieve this goal, experimental work was carried out, using pulp fibres with markedly different morphological and mechanical properties (*Eucalyptus globulus, Pinus pinaster* and *Pinus sylvestris*).

This study uses *Eucalyptus globulus* fiber as a representative hardwood fiber and two extremes of representative softwood fibers used on *Eucalyptus* based office paper as reinforcement fibers (*Pinus pinaster* and *Pinus sylvestris*). To evaluate the papermaking potential, the wood chips were screened and Kraft cooked in a pilot controlled reactor. The resulting pulps were bleached, using a chlorine free sequence, beaten in PFI mill, ISO standard handsheets were made and dried under controlled temperature and humidity conditions. Structural, mechanical, and optical paper properties were measured (ISO standards).

Pinus pinaster reinforcement fibers presented thicker fiber walls with higher coarseness (47%) and length (9%) when compared with *Pinus sylvestris* fibers. Results indicated that beating had a major effect on fiber flexibility. *Pinus pinaster* having the thickest fiber wall presents the major change with a rise of $14x10^{11}N^{-1}m^{-2}$, while increasing $4x10^{11}N^{-1}m^{-2}$ with bleaching and diminishing $3x10^{11}N^{-1}m^{-2}$ with drying.

The influence of fiber flexibility on structural and strength paper properties was determined for the two reinforcement fibers under analysis. These fibers correspond to the two extremes of fibers available as reinforcement fibers, regarding wall thickness, beatability and flexibility

values. *Pinus pinaster* has the thickest fiber wall, with a fiber wall near to the double of the Pinus sylvestris fiber wall, and consequently presents less flexible fibers. This work presents experimental results for the evolutions of paper properties, like paper apparent density, air permeability, tensile and tear strength, with fiber flexibility, for the two reinforcement fibers under study. These data constitute valuable information, also applicable for other reinforcement fibers, with fiber wall thickness in between, and also as reference input values for the development of the 3D paper model.

The article will finish with an example of the use of 3D Paper Model to study the influence of fiber flexibility on paper densification, for *Eucalyptus* fibers. The used innovating 3D paper model, was developed and implemented by this research team, and is explained in detail in other publications. The influence of computational fiber flexibility was investigated for Eucalyptus fibers. Experimental results were compared with simulation results and similar evolutions were observed.

Keywords: Fiber Flexibility, *Eucalyptus globulus*, Reinforcement Fibers, Kraft Pulp, 3D Paper Model

Introduction

When producing and optimizing an *Eucalyptus* based office paper it is an important to understand how to choose or to adapt to the reinforcement fibers used in its production. Long fibers from softwood pulps are expensive, and if used in excess, can damage formation and printability. However, its use is necessary to make the paper strong enough for processing. For the sake of competitiveness, it is important to have experimental data to optimize the type and a quantity of reinforcement fiber in paper furnish.

The general difference between softwood and hardwood pulps, and also softwood pulps from different species and proveniences, arises from multifactor causes, being difficult do reduce them to simple relationships. Ultimately, paper strength depends on the competition between fiber failure and bond failure. It is known, but not fully understood, that fiber length affects the fiber behavior in the web forming, because the contact number between fibers increase width this dimension. Other biometry values are also important, for instance, fiber wall thickness has an impact on fiber ability to bend, impacting the degree of bonding between fibers and paper cohesiveness. In spite of its importance, there is not, till today, a clear relation between fiber properties and paper properties. Many factors contribute to the final paper properties and some fiber properties don't change separately, what makes it difficult to interpret traditional laboratory pulp studies. Our three dimensional paper model simulator can constitute useful tool to separate the influence of different fiber properties and to study a broader input range. The 3D paper model is presented in more detail in

previous publications [1-3]. In this 3D paper model fiber flexibility has a major importance. This kind of model was considered, for the first time, by Niskanen and Alava [4]. The definition of computational fiber flexibility allowed paper representation to upgrade from the two dimensional to the, more realistic, three dimensional configurations. Our model not only uses fiber computational flexibility but, for the first time, includes fiber microstructure. The more detailed fiber model, with the inclusion of fiber lumen, can be used to study the influence of fiber collapse and intra fiber porosity [5].

Fiber flexibility plays an important role on paper properties. Fiber flexibility influences apparent sheet density, strength, porosity as well as smoothness and optical properties [6-8]. Several different methods to measure fiber flexibility have been developed [9-15]. All these methods demanded single fibers evaluation and were time consuming if no automated device was present. For example, Samuelson used an hydro-dynamic method in a viscometer where fibers were suspended in a liquid and subjected to laminar shear fields. Then, he studied their rotational orbits and bending using a microscope [9]. Mohlin proposed a conformability method [10], further developed by Steadman and Luner [12] with a successful automatization implemented by Cresson [14] that is the one used in the present study. Recently Yan and Li used the same method with a confocal laser scanning microscope [15].

Definition of Wet Fiber Flexibility (WFF) and experimental methodology

The flexibility of a fiber is physically defined by the inverse of the product of the modulus of axial elasticity (E) by the inertia moment (I) of the fiber section:

$$Flexibility = \frac{1}{EI}$$

Considering the fiber as a solid beam exposed to an uniform load (see Figure 1), the Wet Fiber Flexibility (WFF) is determined using the length of the fiber segment not supported by the glass, as well as the operation conditions, in accordance with the expression deduced from the flexibility definition [8,12].

$$Flexibility = \frac{72d}{Pes^4}$$

Where *d* is the diameter of the support wire, *P* the pressure made in the act of pressing, *e* the projected width of the fiber and *s* the bending fiber segment.

The goal is to submit the wet fibers to the same type of mechanical deformations that occur in the formation of paper. Thus, the fibers are deposited in glass slides that have metallic wires in a way that is possible to quantify its deformation or flexibility. Figure 1 shows a fiber placed on a metallic wire on a glass slide. A more flexible fiber will be better adjusted to the wire.

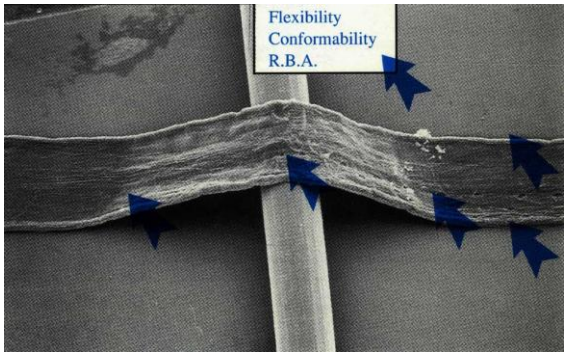

Figure 1. Electronic microscope photography of a fiber supported in a metallic wire as used in our sample preparation. Reproduced with permission (Cresson, 1995).

The goal of the present work is to study the fiber flexibility influence on paper structure and mechanical properties, for relevant *Eucalyptus* based office paper fibers, and to investigate the corresponding influence using a computational 3D paper model.

Experimental

Industrial wood chips were used to produce the following pulps:

- *Eucalyptus globulus* bleached Kraft pulp,
- *Pinus sylvestris* bleached Kraft pulp, North Europe reinforcement pulp,
- *Pinus pinaster* bleached Kraft pulp, South Europe reinforcement pulp.

Roundwood softwood chips were screened and Kraft cooked with an active alkali charge of 20%, sulfidity 30% and H factor equals to 1800. For *Eucalyptus globulus* chips the cooking conditions were milder. The obtained kraft pulps were bleached using a $D_0E_1D_1E_2D_2$ bleaching sequence. The morphological properties of pulp fibers were determined automatically by image analysis of a diluted suspension (20mg/L) in a flow chamber from Morfi® equipment (measurement device developed by TECHPAP, Grenoble, France). The reinforcement pulps were beaten in a PFI mill at 4000, 6000 and 8000 revolutions under a refining intensity of 3.33 N/mm. The *Eucalyptus globulus* unbleached and bleached pulps were beaten in a PFI mill at 1000, 3000 and 4000 revolutions. Wet fiber flexibility (WFF) was determined according to the Steadman and Luner procedure [8,12], using CyberFlex® from CyberMetrics. The experimental method includes the formation of thin oriented fiber network on top of a glass slide with parallel wires. The fiber suspension is deposited on a textile wire using a paper machine head-box, simulating the paper formation. Thereafter, the fibers are transferred from the textile wire to a glass slide, with metal wires, under controlled pressure conditions. An image analysis software is used to determinate fiber flexibility. To complete the

characterization, paper handsheets were prepared according to ISO Standards, and tested regarding structural, mechanical and optical properties.

Results and Discussion

Fiber morphology and coarseness

Table 1 presents the main biometric characteristics for the three pulp fibers analyzed, important for the production of office paper. For the two reinforcement fibers under study, *Pinus pinaster* reinforcement fibers presented the thickest fiber wall, with higher coarseness (47%) and length (9%) when compared with *Pinus sylvestris* fibers. *Eucalyptus globulus* pulp has short fibers with relatively high coarseness, which impart bulk to the paper and constitute a major advantage of the *Eucalyptus* fibers.

Table 1.Fiber length and coarseness measured using Morfi® equipment

	Eucalyptus globulus	*Pinus pinaster*	*Pinus sylvestris*
Fiber length weighted in length (mm)	0.80	2.5	2.3
Coarseness (mg/m)	0.07	0.22	0.15

Bleaching, beating and drying influence on Fiber Flexibility

Reinforcement pulps

Bleaching increases the average flexibility of a pulp. Table 2 presents an example of the bleaching effect ($D_0E_1D_1E_2D_2$) on never dried pine pulps, all PFI beaten at 4000 revolutions. The extraction of some polyssacharides of low molecular weight and the residual lignin has a marked effect on the pulps response to beating.

Table 2. Bleaching effect

	Unbleached pulp WFF ($10^{11}N^{-1}m^{-2}$)	Bleached pulp WFF ($10^{11}N^{-1}m^{-2}$)	WFF variation ($10^{11}N^{-1}m^{-2}$)	Variation (%)
Pinus pinaster	7.2	11.5	4.3	60
Pinus sylvestris	9.1	13.4	4.3	47

Figure 2 shows the evolution of fiber flexibility with beating for the two pine species under analysis. It is verified that *Pinus sylvestris* fibers are more flexible presenting a maximum difference around 4000 PFI revolutions (°SR of 18). Experimental information about fiber ability to bend and adjust to the structure at different levels of beating is relevant to optimize de development of fiber properties during beating for each raw material.

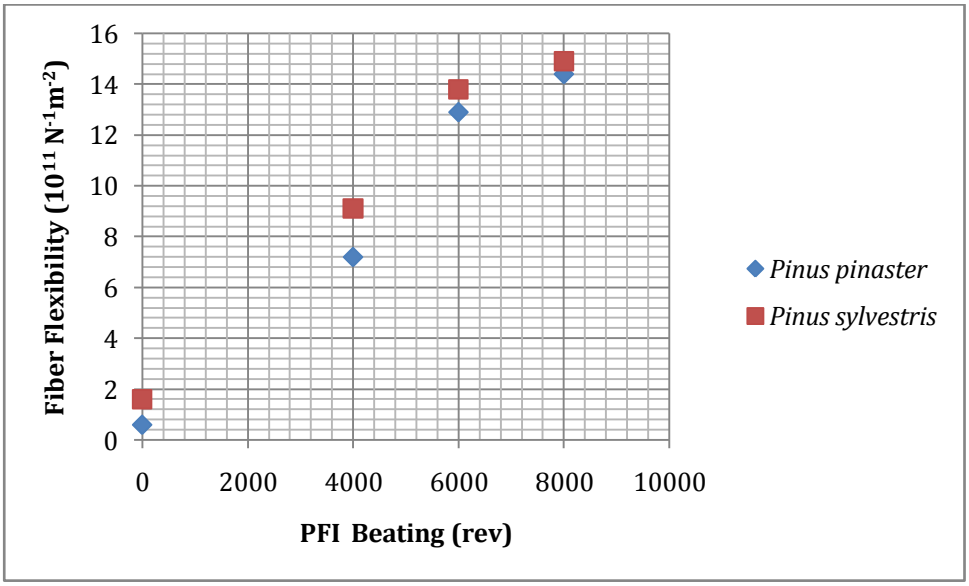

Figure 2. Effect of beating on Fiber Flexibility for the two reinforcement pulps

Drying Effect

Drying reduces the average flexibility of a pulp. Table 3 presents an example of the drying effect in a never dry PFI beaten pulp at 4000 revolutions.

Table 3 – Drying effect

	Never dried pulp WFF ($10^{11}N^{-1}m^{-2}$)	Dried pulp WFF ($10^{11}N^{-1}m^{-2}$)	WFF Variation ($10^{11}N^{-1}m^{-2}$)	Variation (%)
Pinus pinaster	7.2	3.9	3.3	46%

Eucalyptus pulps

In the case of fibers, these fibers develop fiber properties with beating sooner, consequently the experimental plan was designed to obtain more information in the initial part of the curve (Figure 3).

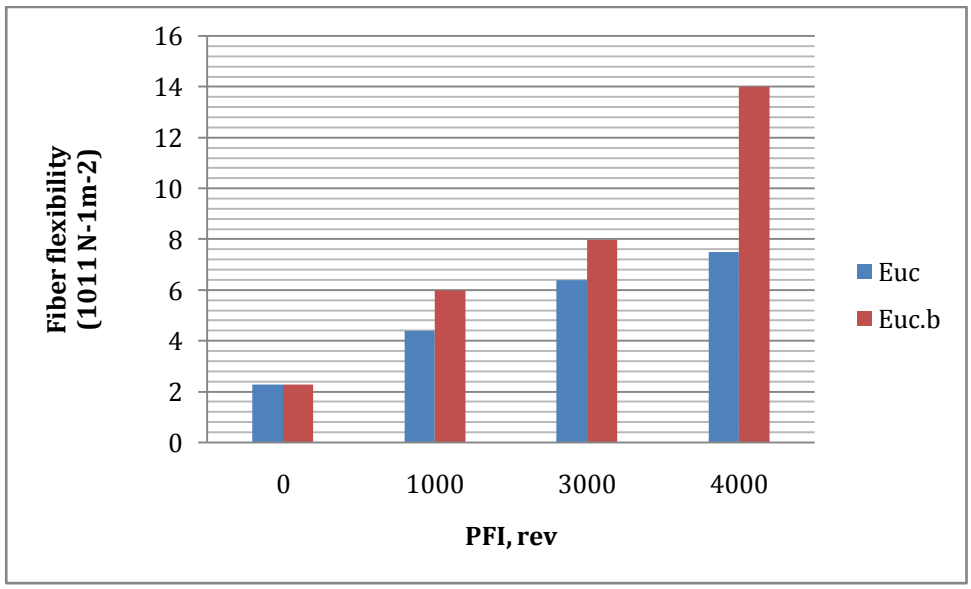

Figure 3. Effect of beating and bleaching on fiber flexibility for Eucalyptus globules (Euc – unbleached; Euc.b –bleached)

Figure 3 illustrates the importance of beating and bleaching in changing fiber flexibility for *Euclyptus* fibers. Beating is the process operation that has a major impact on fiber flexibility and the bleaching has a major effect when fiber properties are already fully developed (note that at 4000 PFI rev the ^{0}SR is 50)

The Fiber Flexibility influence on Pulp and Paper Properties

The influence of fiber flexibility on structural and strength paper properties was determined for the two reinforcement fibers under analyses (Figures 4, 5, 6 and 7) for the unbleached pulps.

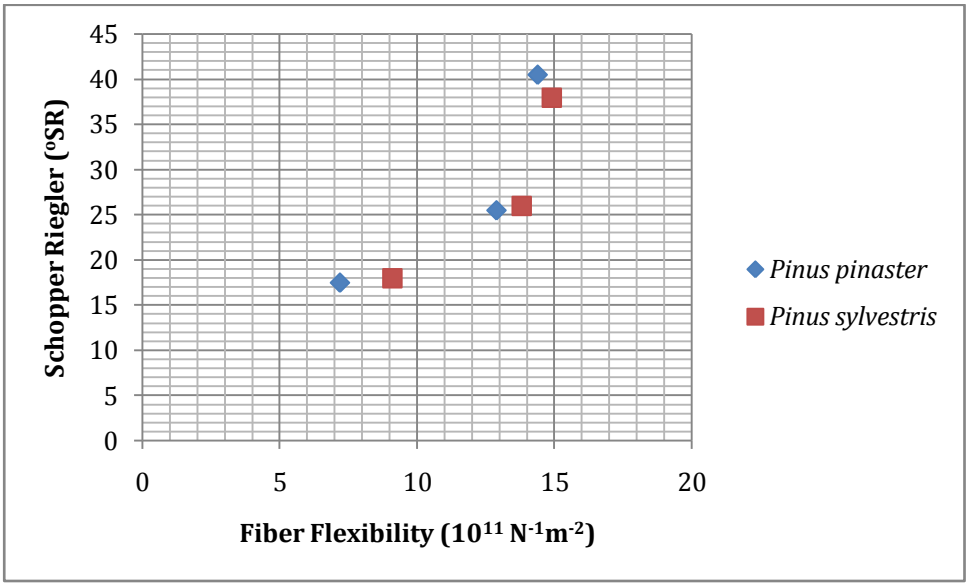

Figure 4. Variation of Schopper Riegler degree with fiber flexibility

These fibers correspond to the two extremes of fibers available as reinforcement fibers, regarding to fiber wall thickness. *Pinus pinaster* is the thickest fiber wall, and consequently less flexible. Analysing the experimental results for the evolution of paper apparent density and air permeability we can conclude that *Pinus pinaster* fibers originates a structure that is more porous and permeable. The evolution of ºSR indicates that the drainability resistance is similar for both pulps, being slightly better for the *Pinus pinaster* fibers.

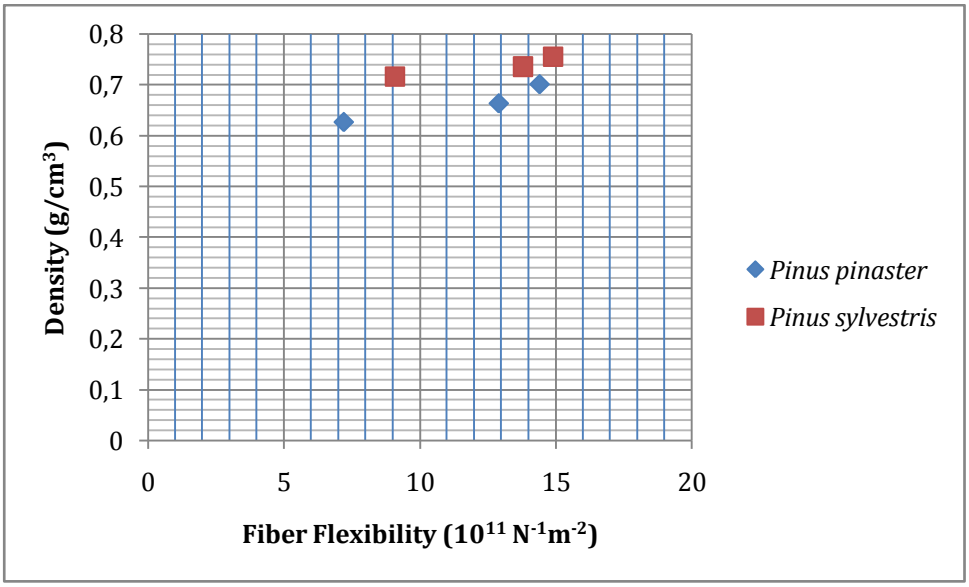

Figure 5. Variation of paper density with fiber flexibility

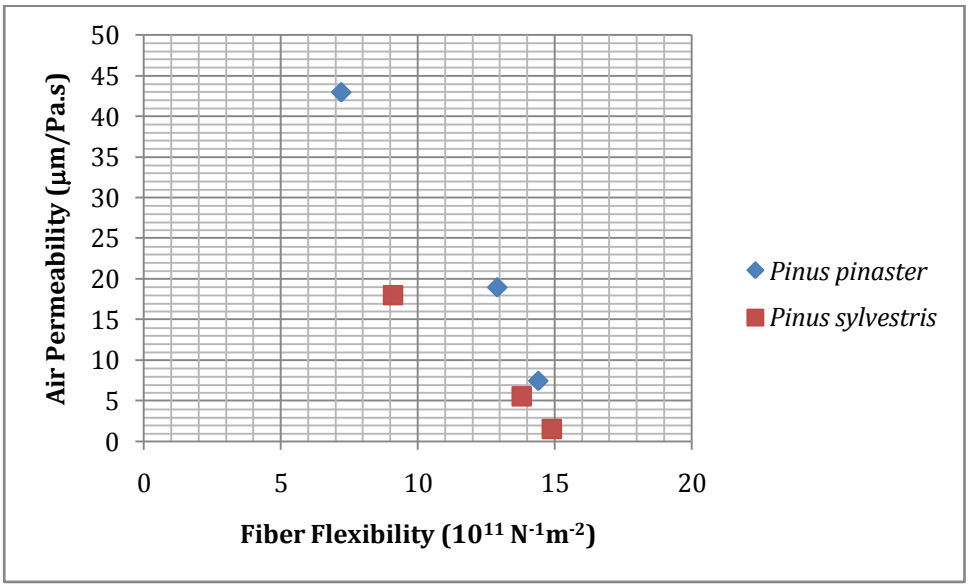

Figure 6. Variation of paper air permeability with fiber flexibility.

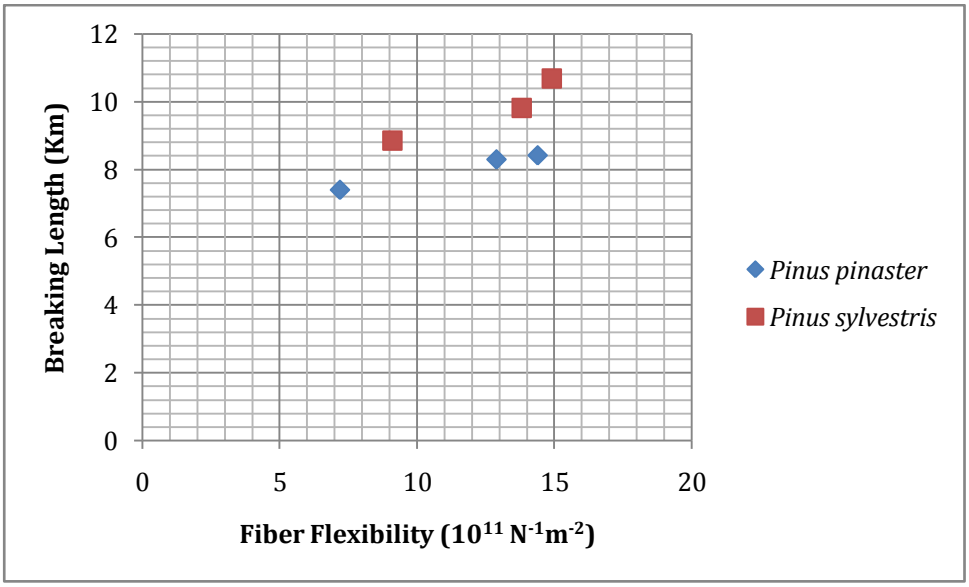

Figure 7. Variation of breaking length with fiber flexibility

Figure 7 shows that *Pinus sylvestris* fibers have the potential to procuce slightly stonger papers, at a given fiber flexibility. This fact is in good agreement with the higher density of the paper structure. Considering the lower coarsenenss of these fibers, it is probable that both, higher fiber collapsibility and higher fiber specific surface area, play a role in obtaining a more dense structure.

For the Eucalyptus fibers, the influence of fiber flexibility on the structure of paper was done both experimentally (table 4) and using a 3D Paper Model (figure 8). The good agreement between the two approaches is revealed in figure 8.

Table 4 – Effect of *Eucalyptus globulus* fiber flexibility on paper density

PFI (revolutions)	0	1000	3000
Fiber flexibility ($10^{11}N^{-1}m^{-2}$)	2.3	6.0	8.0
Paper density, (g/cm^3)	0.56	0.68	0.85

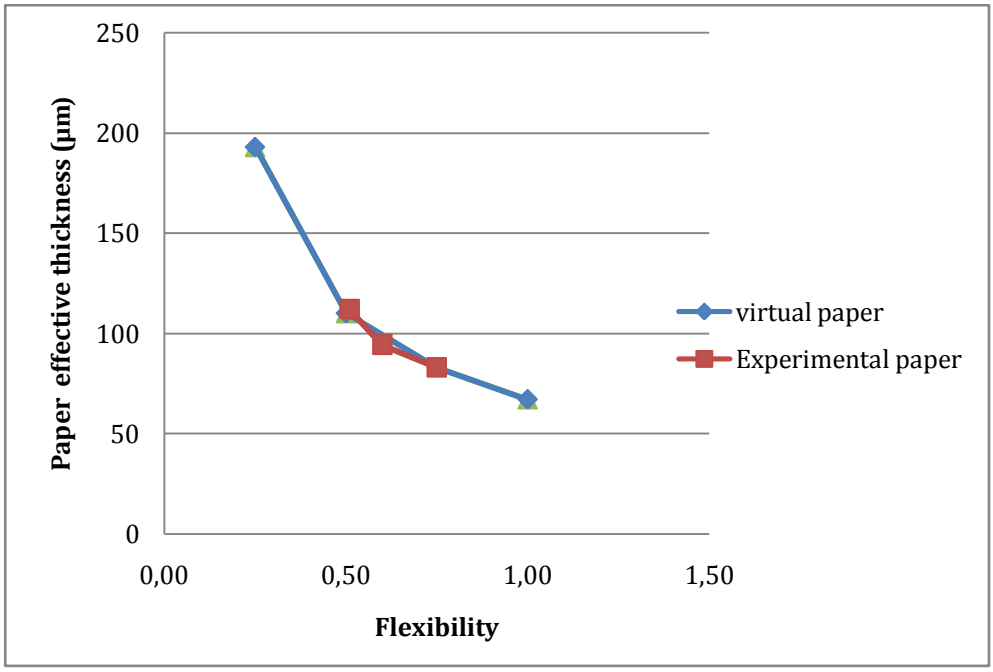

Figure 8. Evolution of paper thickness versus fiber flexibility for real and computational *Eucalyptus* paper. Reprinted from (Curto *et al.*, 2011c) *Materialwissenschaft und Werstofftechnik, Materials Science and Engineering Technology*, Wiley-Vch, vol.42 no.5 (2011): pp. 370-374 [1].

The 3D paper model that we developed and implemented [1-3] includes relevant fiber properties, like fiber flexibility and morphology, and proved to be a useful tool to study several structural paper aspects.

Conclusions

Pinus pinaster reinforcement fibers presented thicker fiber walls with higher coarseness (47%) and length (9%), when compared with *Pinus sylvestris* fibers.

Experimental results indicated that beating had a major effect on fiber flexibility. *Pinus Pinaster* having the thickest fiber wall presents the major change with a rise of $14x10^{11}N^{-1}m^{-2}$, while increasing $4x10^{11}N^{-1}m^{-2}$ with bleaching and diminishing $3x10^{11}N^{-1}m^{-2}$ with drying.

The influence of fiber flexibility on structural and strength paper properties was quantified for the two reinforcement fibers under analyses. These fibers correspond to the two extremes of fibers available as reinforcement fibers, regarding to fiber wall thickness, beatability and flexibility values. *Pinus pinaster* is the thickest fiber wall, and consequently less flexible, and *Pinus sylvestris* is the thinnest fiber wall. Experimental results for the evolution of paper properties, such as paper apparent density, air permeability, and breaking length, with fiber

flexibility, for the two reinforcement fibers, constitute valuable information, also applicable for other reinforcement fibers, with fiber wall thickness or flexibility in between.

For *Eucalyptus globulus* the experimental data for paper density was compared with simulation results and the same evolutions were observed, which shows the potential of the paper model.

References

[1] CURTO, J.M.R, CONCEIÇÃO, E.L.T., PORTUGAL, A.T.G. and SIMÕES, R.M.S., 2011. Three dimensional modeling of fibrous materials and experimental validation. *Materialwissenschaft und Werstofftechnik, Materials Science and Engineering Technology*, Wiley-Vch, Germany, Wiley-Blackwell, USA, vol. 42 no.5 (2011): pp. 370-374.

[2] CONCEIÇÃO, E.L.T., CURTO, J.M.R, SIMÕES, R.M.S and PORTUGAL, A.T.G., 2010. Coding a simulation model of the 3D structure of paper. In Proceedings of the 2th international symposium on computational modeling of objects represented in images, Comp Image 2010, USA. Springer-Berlin, Lecture Notes in Computer Science, Barneva; R.P. *et al.* (Eds.), Springer-Verlag Berlin, vol.60 no.20 (2010): pp. 299–310. ISBN: 978-3-642-12711-3. ISI Document Delivery No.: BPJ99.

[3] CURTO, J.M.R, CONCEIÇÃO, E.L.T., PORTUGAL, A.T.G. and SIMÕES, R.M.S., 2009. The fiber coarseness and collapsibility influence on a three dimension paper model. In Proceedings of the 63rd Appita annual Conference and Exhibition, Melbourne, Australia, 19-22 April (2009): pp. 303-310. ISBN:9780975746952.

[4] NISKANEN, K. AND ALAVA, M., 1994. Planar random networks with flexible fibers *Phys. Rev. Lett.*, vol.73 no.25, (1994): pp. 3475-3478.

[5] CURTO, J.M.R, CONCEIÇÃO, E.L.T., PORTUGAL, A.T.G. and SIMÕES, R.M.S., 2010. The fiber properties influence on a three dimensional paper model. In Proceedings of the XXIII Tecnicelpa conference and exhibition / VI CIADICYP, vol.1 (2010): pp. 123.

[6] PAAVILAINEN, L., 1993b. Conformability – flexibility and collapsibility – of sulphate pulp fibers. *Paperi ja Puu – Paper and Timber*, vol.75 no.9-10 (1993): pp. 689-702.

[7] PAAVILAINEN, L., 1992. The possibility of fractionating softwood sulphate pulp according to cell wall thickness. *Appita Journal* vol.45 no.5 (1992): pp. 319-326.

[8] STEADMAN, R.K. and LUNER, P., 1986. Wet Fiber Flexibility as an Index of Pulp and Paper properties, PIRA International Conference on Advances in Refining Technologies, Birmingham, England, vol.1, Session 1, Paper 3, 23 pages (1986).

[9] SAMUELSON, L.G., 1963. Measurement of the stiffness of fibers, *Svensk Papperstidning*, vol. 66 no.15 (1963): pp. 541-546 (1963).

[10]MOHLIN, U.-B., 1975. Cellulose fiber bonding: Part 5. Conformability of pulp fibers. *Svensk Papperstidning*, vol.78 no.11 (1975): pp. 412-416.

[11]TAM DOO, *P.A. and R.J. KEREKES, 1981. A method to measure wet fiber flexibility. TAPPI Journal*, vol.63 no.3 (1981): pp. 113-116.

[12]STEADMAN, R.K. and LUNER, P., 1992. An Improved Test to Measure the Wet Fiber Flexibility of Pulp Fibers. Empire State Paper Research Institute Report 79, Chapter V (1992): pp. 69-85.

[13]KUHN, D., *et al.*, 1995. A dynamic wet fiber flexibility measurement device. *Journal of Pulp and Paper Science*, vol.21 no.10 (1995): pp. J337-J342 (1995).

[14]CRESSON, T., 1995. Wet fiber flexibility: a measurement whose time has finally come, World Pulp and Paper Report (1995).

[15]YAN, D. and LI, K., 2008. Measurement of wet fiber flexibility by confocal laser scanning microscopy, J.Mater Sci., vol.43 (2008): pp. 2869-2878.

Comparative study of fibers for *Eucalyptus globulus* based paper using experimental characterization and 3D paper modeling

Curto, J.M.R. [1], Conceição, E. L.T.[2], Portugal, A.T.G.[2] and Simões, R.M.S.[1]

[1] Textile and Paper Materials Research Unit,
Chemistry Department, University of Beira Interior (UBI)

[2] Research Centre for Chemical Processes Engineering and Forest Products,
Chemical Engineering Department, University of Coimbra (UC)

Abstract

We present a comparative study of different fibers that are important to produce and optimize an *Eucalyptus globulus* based office paper. The work includes an experimental characterization of *Eucalyptus glo*bulus fibers and two representative reinforcement fibers in order to quantify the influence of fiber and a process (beating) on paper properties. The resulting porous structure was also characterized in the z direction (along paper thickness) using SEM photographs of laboratory isotropic handsheets. The fiber and web experimental data was used as an input in our paper simulator to study the web structure densification that occurs with beating.

Departing from fiber properties, such as fiber wall thickness, fiber flexibility and fiber collapsibility, it was possible to predict paper thickness. The paper will finish with an example of the use of 3D Paper Model to separate the influence of fiber flexibility and fiber collapsibility on paper densification.

Introduction

Office paper is the principal Portuguese paper industry product. This paper is mainly produced from *Eucalyptus globulus* bleached kraft pulp with a small incorporation of a softwood pulp, called reinforcement pulp, to increase paper strength. It is important to access the contribution of different reinforcement pulp fibers with different biometry and coarseness to the final paper properties. The two extremes of reinforcement pulps can be represented by a *Picea abies* kraft softwood pulp, usually considered the best reinforcement fiber, and the Portuguese *Pinus pinaster* Kraft pulp, recently made commercially available.

Many authors have identified the importance of fiber properties, specially fiber transverse dimensions and mechanical behavior (flexibility and collapsibility), on paper properties. Unfortunately, several of the fiber dimensions change simultaneously when changing a raw material. Also, both mechanisms of fiber flexibility and collapse occur simultaneously in beating. Therefore, it is hard to quantify the effect of each cause individually in experiments. However, this can be easily accomplished with computational simulations.

To characterize the paper structures the experimental plan includes the following steps: evaluation of each pulp separately and its evolution with beating, preparation of isotropic paper handsheets, SEM analysis in z direction, and also testing paper regarding structural, mechanical and optical properties.

Having identified the morphological differences between fibers, as well as the fiber flexibility evolution during beating, paper simulations were obtained using a paper model.

The developed paper model intends to capture key papermaking fiber properties (morphology, flexibility, and collapse) and process operations (fiber deposition, network forming, densification). It is a deposition-like model based on the KCL-PAKKA model, extended to simulate fiber interactions and a novel fiber microstructure model that includes fiber lumen.

The 3D paper structure is formed by individual fibers, deposited one at a time, which conform to the underlying structure, depending on its position, dimensions and flexibility. The model is extended to include fiber interactions, like flocculation and hydrodynamic smoothing. In an original form, the fiber model includes fiber wall thickness, and fiber lumen, with a resolution up to 0.05 μm.

The model implemented is based on the KCL-PAKKA model proposed by Niskanen and Alava in 1994 [1]. In this model, the three-dimensional structure of paper is simulated using a sedimentation-like or growth process. The sedimentation model of paper assumes that the sheet is formed from a dilute suspension under the influence of an uniform flow field. In its initial assumption all fiber interactions are ignored. The model proposed by Niskanen and Alava is the first to include fiber flexibility and capture the truly nature of paper. Departing from fiber dimensions and flexibility a three dimensional structure is formed and various paper properties are predicted. The simulations obtained are consistent with experimental data as presented by Alava and Niskanen in 2006 and Niskanen *et al*. [2-3]. Besides the standard KCL-PAKKA model an extension of this model which incorporates a formation control parameter is implemented. This modification is based on the sedimentation rule developed by Provatas e Useaka in 2003 [4]. Moreover, in our model the lumen is introduced for the first time, allowing the study of the influence of fiber collapse and a more realistic simulated structure.

Materials and Methods

The commercial pulps used in this study are identified as follows:

- *Eucalyptus globulus* bleached Kraft pulp (EUC),
- *Picea abies* bleached Kraft pulp, Nordic reinforcement fibers (FL),
- *Pinus pinaster* Kraft pulp, laboratory bleached Portuguese reinforcement fibers (PB).

Kappa number and pulp viscosity were evaluated according to the ISO 302 and ISO 5351/1 standard methods. The unbleached Portuguese pine pulp was delignified with O_2 in the industrial plant (kappa = 25) and bleached in the laboratory using a $D_1E_2D_2$ sequence. The final pulp viscosity was 830 ml/g. The morphological properties of pulp fibers were determined automatically by image analysis of a diluted suspension (20mg/L) in a flow chamber in Morfi® (TECHPAP, Grenoble). The pulps were beaten in a PFI mill at 1000, 3000 and 6000 revolutions under a refining intensity of 3.33 N/mm. Wet fiber flexibility (WFF) was determined according to the Steadman and Luner procedure [5], using CyberFlex® from CyberMetrics. The experimental method includes the formation of a very thin and oriented fiber network on top of a glass slide with parallel wires. The fiber suspension is deposited on a textile wire using a paper machine head-box, simulating the real paper formation. Thereafter, the oriented fibers on the textile wire are transferred to a glass slide, with metal wires, under controlled pressure conditions. An image analysis software is used to calculate fiber flexibility. Paper handsheets were prepared according to ISO standards, and tested regarding structural, mechanical and optical properties.

Results and Discussion

Pulp Fiber characterization

Table 1 presents the principal morphological properties for the three pulps under investigation. The *Eucalyptus* fibers are considered ideal office paper fibers due to their relatively high coarseness when comparing with other hardwood fibers (short fibers). The Portuguese fiber (PB) exhibits higher coarseness (45%), length (13%) and width (15%) than the corresponding Nordic softwood (FL).

Table 1. Fiber morphology

	Market softwood (FL)	Portuguese Pine (PB)	*Eucalyptus* (EUC)
Fiber length weighted in length (mm)	1.79	2.03	0.80
Fiber width (µm)	29.4	33.8	18.0
Coarseness (mg/m)	0.151	0.219	0.067

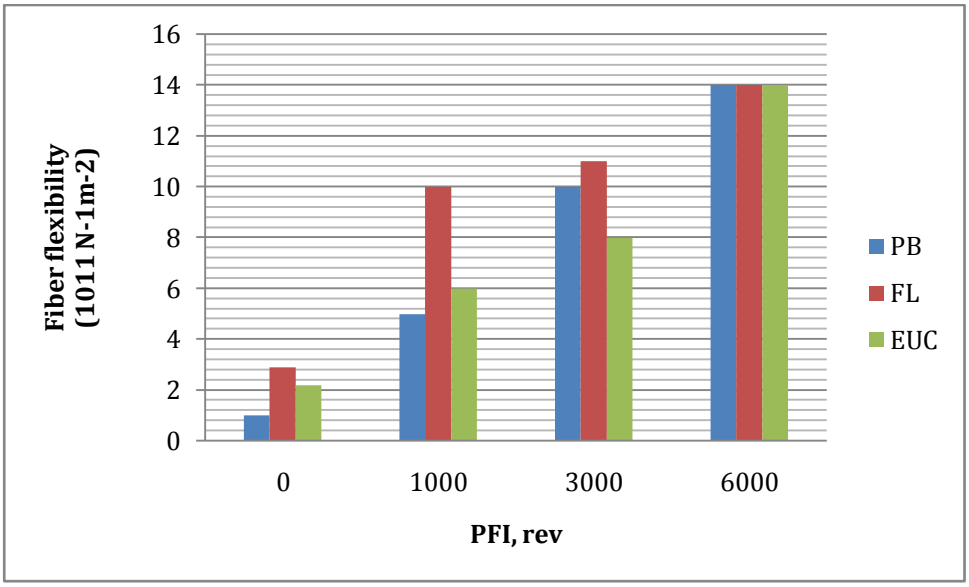

Figure 1. Evolution of Wet Fiber Flexibility with beating

Beating of individual pulps

Figure 1 represents the Wet Fiber Flexibility evolution during beating for the three bleached kraft pulps.

In accordance with the lower coarseness, the *Picea abies* (FL) fibers developed fiber flexibility easier than the *Pinus pinaster* (PB) fibers (Figure 1). The effect is drastic at low beating levels (1000 PFI revolutions) but is progressively attenuated for higher beating levels.

In agreement with the fibers flexibility development with beating, the Schopper Riegler degree evolution is also slower for the *Pinus pinaster* fibers (Figure2). The different specific surface area of the two softwood pulps also played a role on the measured values and on their evolution.

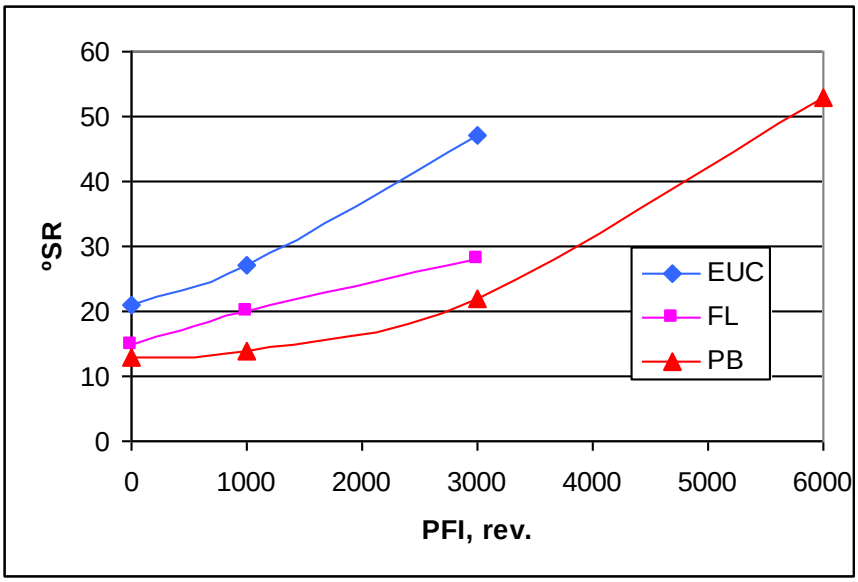

Figure 2. Evolution of Schopper Riegler with beating

The paper structure obtained from coarse fibers (with higher fiber wall thickness) densifies slower, and to a lower final value, than the paper made from thin fibers, with thinner fiber walls (Figure 3).

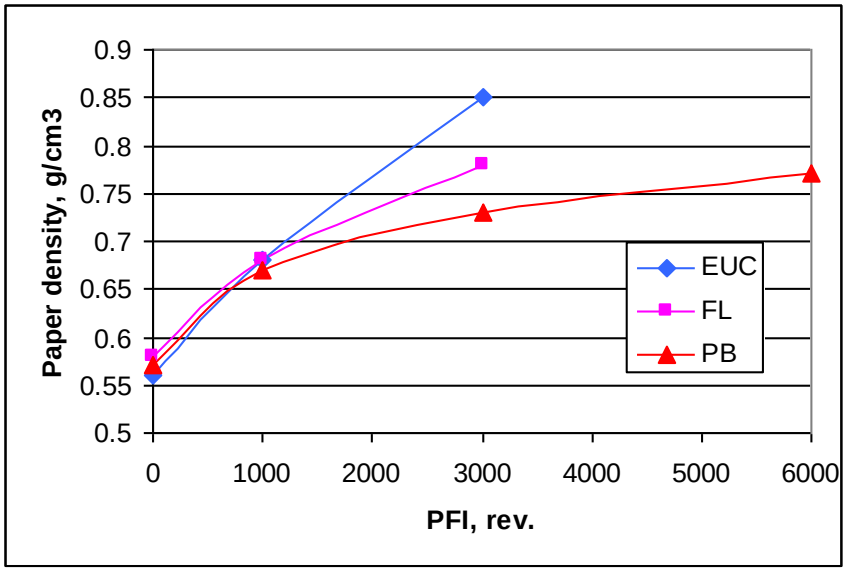

Figure 3. Evolution of paper density with beating

Regarding the mechanical properties and paper structure, the results indicate that the two softwood pulps exhibit similar relationships between tensile index and paper density (Figure 4). At a given tensile, the Portuguese pulp shows a markedly higher tear resistance than the corresponding Nordic pulp (Figure 5), probably due to a combination of higher fiber length and higher fiber coarseness (important to obtain higher paper bulk due to less fiber collapsibility), which are important on tear strength (Clark, 1985).

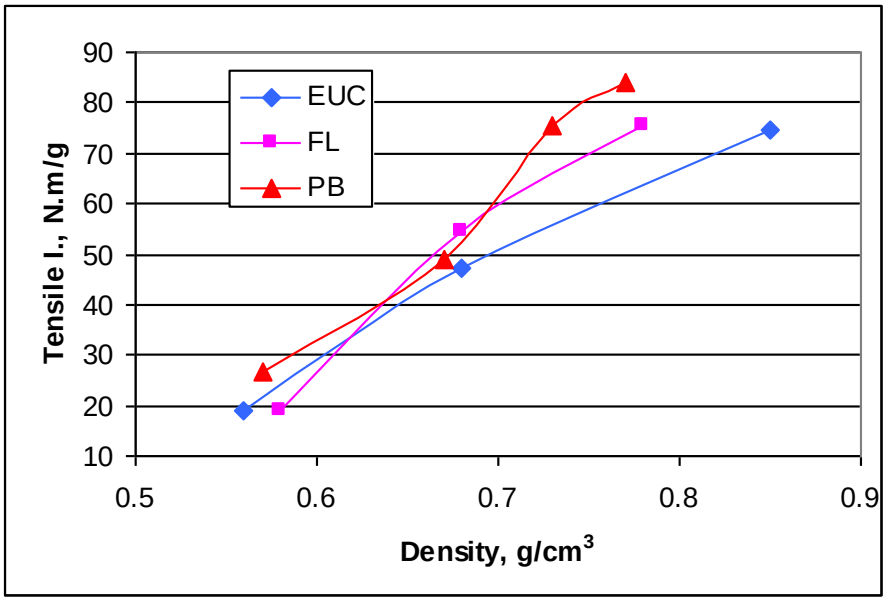

Figure 4. Evolution of paper tensile strength with paper density

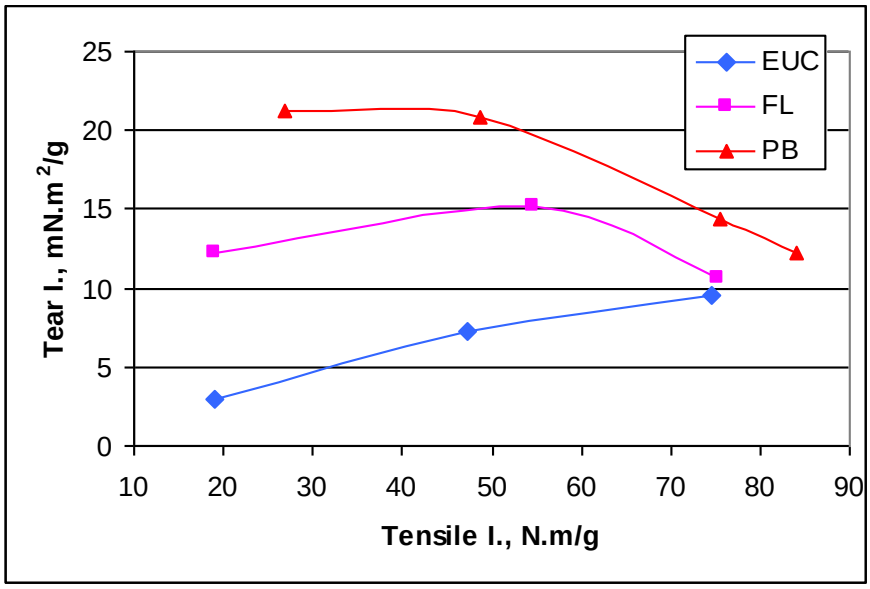

Figure 5. Tear index versus tensile index

The experimental data obtained for fibers with markedly different morphology and corresponding mechanical behavior will certainly play an important role in future model extension to mechanical properties. At the present the paper model is focused on paper structural properties, but the possibility to be extended to mechanical properties remains open.

Comparative study of paper thickness using SEM photographs and model simulations

The visualization of SEM images with different beating degrees puts in evidence different fiber flexibility and collapsibility (Figures 6, 7, 8, 9, 10, and 11). The samples presented are thickness cuts from laboratory handsheets (60 g/m^2) for *Eucalyptus globulus*, *Pinus pinaster* and *Picea abies,* respectively. Tables 2, 3, and 4, 5 summarize the measurement results made from several SEM images using software available at the University of Beira Interior Optical Centre. The corresponding simulation values were determined using our simulator with suitable values for fiber morphology and flexibility, based on experimental data coming from SEM photographs, fiber Morphy analyzer and experimental fiber flexibility information. The experimental quantification was done with statistical representative samples that are available for consultation. To be included in this communication only exemplificative SEM photographs were chosen, for unbeaten and beaten pulps.

Table 2. SEM Paper thickness versus model thickness for *Eucalyptus globulus* fibers

	EUC (0 rev)	EUC (3000 rev)
Paper thickness (µm)	95	62
Model thickness (µm)	94	62

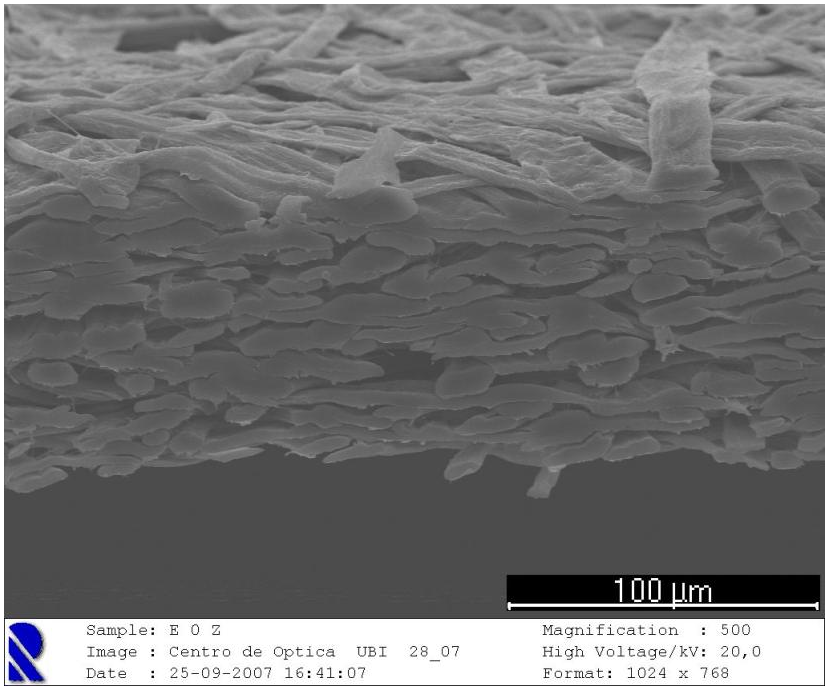

Figure 6. SEM photography of *Eucalyptus globulus* paper thickness without beating (zero PFI revolutions)

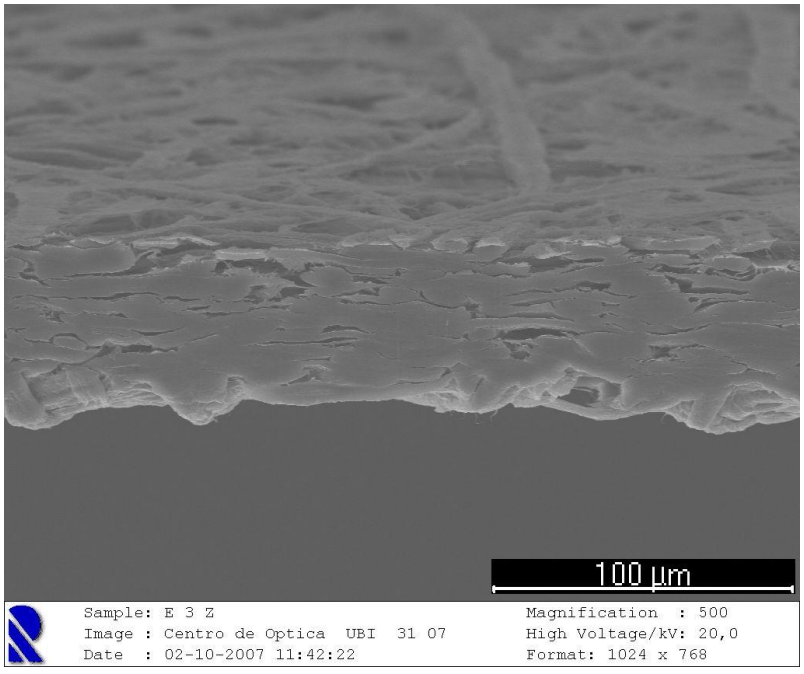

Figure 7. SEM photography of *Eucalyptus globulus* paper thickness with beating (3000 PFI revolutions)

Table 3. SEM paper thickness versus model thickness for *Pinus pinaster* fibers (PB)

	Pinus pinaster (0 rev)	*Pinus pinaster* (6000 rev)
Paper thickness (µm)	95	76
Model thickness (µm)	94	77

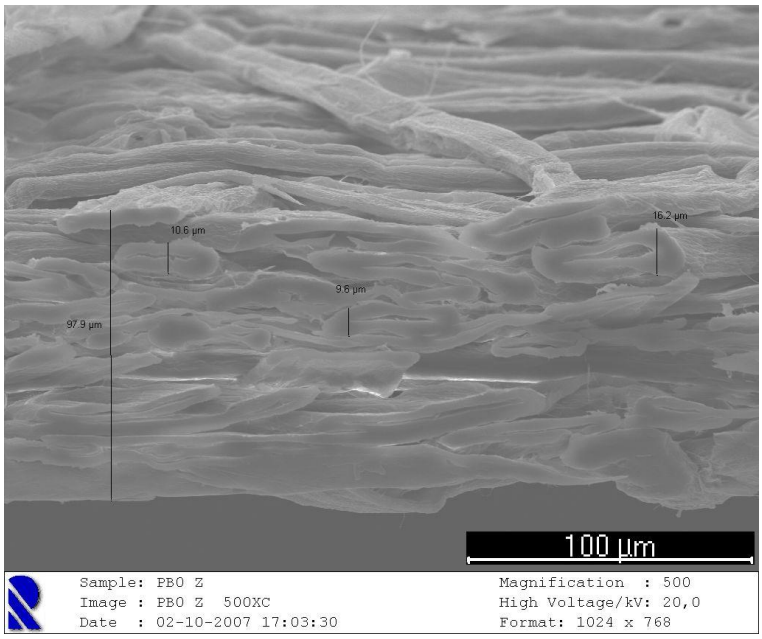

Figure 8. SEM photography of unbeaten *Pinus pinaster* paper thickness (zero PFI revolutions)

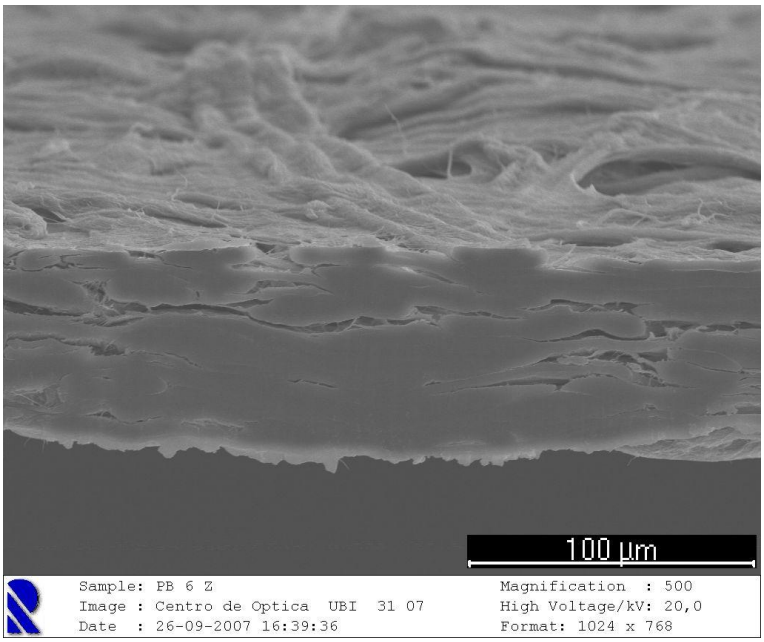

Figure 9. SEM photography of beaten *Pinus pinaster* paper thickness (6000 PFI revolutions)

Table 4. SEM paper thickness versus model thickness for *Picea abies* fibers (FL)

	Picea abies (0 rev)	*Picea abies* (3000 rev)
Paper thickness (µm)	80	67
Model thickness (µm)	80	69

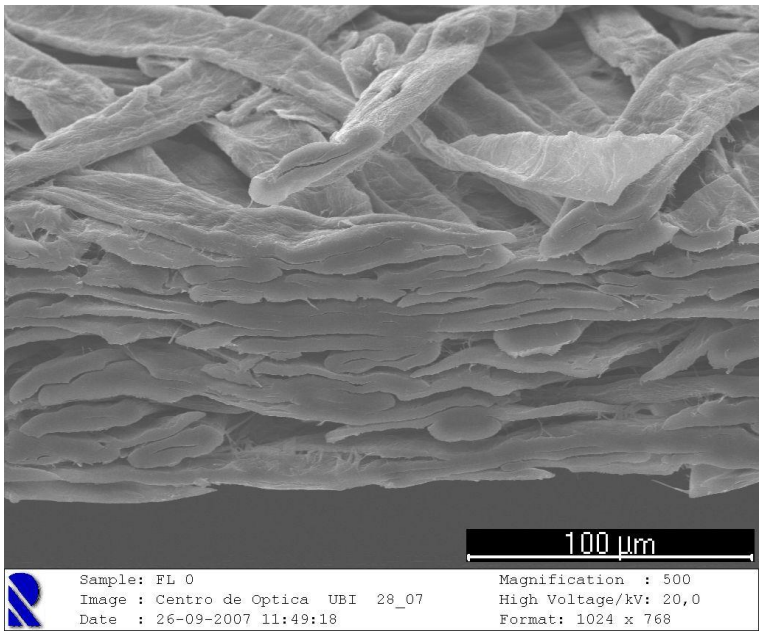

Figure 10. SEM photography of unbeaten *Picea abies* paper thickness (zero PFI revolutions)

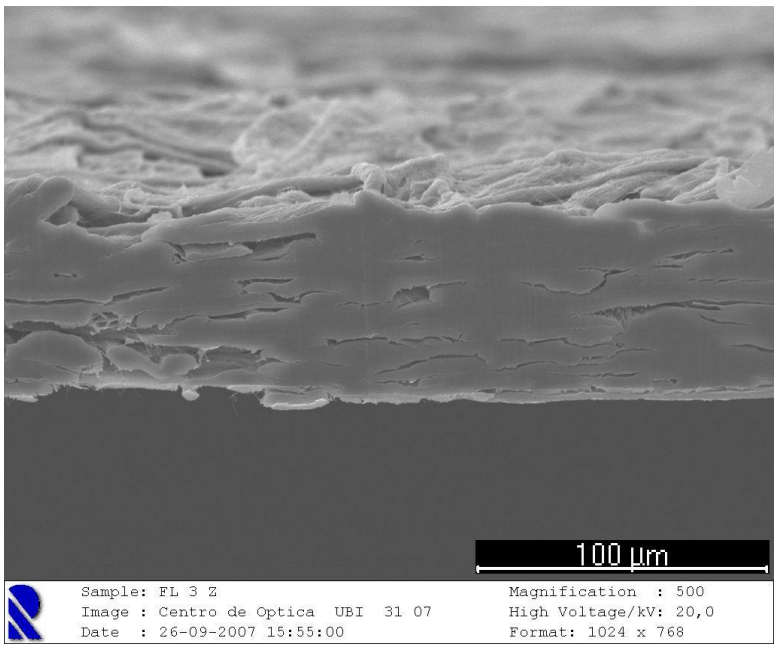

Figure 11. SEM photography of beaten *Picea abies* paper thickness (3000 PFI revolutions)

The analysis made from SEM images points out that fiber wall thickness and collapse degree are key parameters.

A novel paper model, which is an extension of the Niskanen model that includes fiber collapse, was developed and implemented. Table 5 presents the range of fiber collapse parameters based on SEM information (table 5) used on model simulations. As values in table 2, 3 and 4 shows, the paper thickness simulated values agree with experimental determinations.

Table 5. Degree of fiber collapse (fiber thickness/2xfiber wall) for unbeaten and beaten pulps

Beating	EUC	PB	FL
Unbeaten pulps	3/2-6/4	13/10-16/12	6/6-7/6
Beaten pulps	2/2-5/4	11/10-13/12	5/5-6/6

Finally, figure 12 illustrates a simulation study that was done to study the influence of fiber flexibility and fiber collapse on the simulated paper thickness. Fiber length and width corresponds to a typical *Eucalyptus globulus* fiber but a broader range was used for fiber computational flexibility and fiber collapse, including fiber collapses and fiber flexibilities not found in real papers.

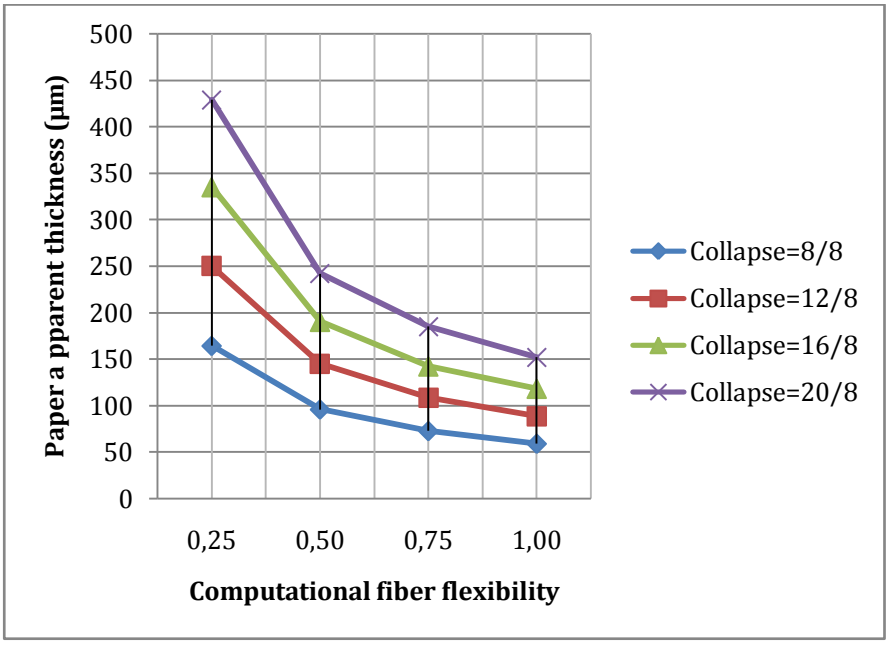

Figure 12. Simulation study of fiber collapse influence on the variation of virtual paper apparent thickness with computational fiber flexibility.

(Note that the fiber collaspse=fiber thickness/2xfiber wall and the computational fiber flexibility is defined according to Niskanen approach [1] and is dimensionless.)

Conclusions

The strong influence of raw material and beating degree on the pulp fibers properties and corresponding paper structural and mechanical properties was confirmed and quantified for *Eucalyptus globulus* and two reinforcement fibers, *Pinus pinaster* and *Picea abies*, using laboratory isotropic handsheets. The structure was characterized on the z dimension using SEM photographs. Different levels of fiber collapse were identified and used to predict paper thickness. The innovative paper model was used to study independently the influence of fiber flexibility and fiber collapse and predict paper thickness.

References

[1] Niskanen, K. and Alava, M., "Planar random networks with flexible fibers", Phys. Rev. Lett., 73(25): 3478 (1994).

[2] Alava, M. and Niskanen, K., "The physics of paper", Reports on Progress in Physics, 69(3): 669 (2006).

[3] Niskanen, K., Nilsen, N., Hellen, E. and Alava, M., "KCL-PAKKA: simulation of 3D structure of paper", 11th FRS, September, 2: 1273 (1997).

[4] Provatas, N. and Uesaka, T., "Modeling paper structure and paper press interactions", J. Pulp Paper Sci., 29(10): 332 (2003).

[5] Steadman and Luner, P., "Wet Fiber Flexibility as a Index of Pulp and Paper properties", PIRA International Conference on "Advances in Refining Technologies", Birmingham, England, vol.1, Session 1, Paper 3, 23 pages (1986).

[6] Curto, J.M.R, Conceição, E.L.T., Portugal, A.T.G. and Simões, R.M.S., "Three dimensional modeling of fibrous materials and experimental validation", *Materialwissenschaft und Werstofftechnik, Materials Science and Engineering Technology*, Wiley-Vch, 5(42):370 (2011).

Estudo Comparativo de Incorporação de Fibra de *Pinus Pinaster* branqueada no Papel de *Eucalyptus Globulus*

CURTO, J.M.R. [1], GIL, C.[1], CONCEIÇÃO, E. L.T.[2], PORTUGAL, A.T.G.[2] and SIMÕES, R.M.S.[1]

[1] Textile and Paper Materials Research Unit,

Chemistry Department, University Of Beira Interior (UBI)

[2] Research Centre for Chemical Processes Engineering and Forest Products,

Chemical Engineering Department, University Of Coimbra (UC)

Abstract

Office paper is the principal Portuguese paper industry product. This paper is mainly produced from *Eucalyptus globulus* bleached kraft pulp with a small incorporation of a softwood pulp, called reinforcement pulp to increase paper strength. Despite *Pinus pinaster* being one of the most important species with the major forest area, Portugal does not bleach this pulp and imports it. To evaluate the Portuguese Pine reinforcement papermaking potential, the pulp was bleached in the laboratory and compared with a reference softwood market pulp. The Portuguese fiber exhibits higher coarseness (45%), length (13%) and width (15%) than the market softwood. In this study the goal is to quantify the influence of beating degree and long fiber incorporation level on the reinforcement *Eucalyptus globulus* based paper. The contribution of different reinforcement pulp fibers with different biometry and coarsenesses to the final paper properties is done with an experimental plan design that includes the following steps: evaluation of each raw material separately, incorporation of long fibers using the same beating revolution number, incorporation using approximately the same beating degree measured as ºSR and evaluation of wet strength. Paper properties have been found to be non linear in relation to pulp mixture proportions. The conclusions pointed out that, with the optimal beating, the Portuguese Pine improves tearing and tensile strength of the Eucalyptus based paper being possible to obtain equivalent or greatest performance than using the market pulp.

Introdução

Na produção de papel de escritório a função principal da fibra de reforço é aumentar a "runnability" do processo de produção de papel, minimizando a ocorrência de quebras. Sendo esta uma variável de processo, uma das questões que tem que ser analisada é qual das propriedades de resistência melhor se correlaciona com a frequência de quebras. Esta questão foi discutida em várias publicações (Uesaka *et al*. 2001, Niskanen *et al*. 1998), tendo-se utilizado, de uma forma geral, os testes de rasgamento fora do plano para avaliar a capacidade de resistência às quebras. Ultimamente verifica-se que alguns autores têm evidenciado também a importância de testes de fractura no plano (Niskanen *et al*., 1998; Page e Seth 1982; van den Akker *et al*., 1967). Os trabalhos publicados indicam que a maior parte das quebras têm origem em pequenas imperfeições do material e em picos de tensão (Moilanen e Linqdvist, 1996; Roisu, 1990; Page e Seth 1982; Sears *et al*. 1965). Neste caso, os factores reológicos são determinantes e a evolução da força exercida versus alongamento traduz o comportamento do papel húmido. Assim, para caracterizar a resistência pode utilizar-se o índice de tracção e o "elastic strech", i.e. a resistência à tracção sobre o módulo de elasticidade, como defende Uesaka num estudo da zona de prensagem (Uesaka *et al*., 2001). Vários autores concluem que as propriedades do papel obtido pela mistura de fibras não são linearmente aditivas em relação às proporções mássicas das matérias-primas que as constituem (Retulainen, 1997; Mohlin e 1984; Parsons, 1969). De entre as teorias explicativas do comportamento das misturas podem referir-se a de Mohlin (Mohlin e Wennberg, 1984), que propõe que na mistura se formam duas redes distintas e outra que evidencia o papel da activação das fibras (Niskanen *et al*., 1998).

Recentemente, Portugal passou a produzir fibra longa branqueada. Uma vez que a fibra longa portuguesa apresenta características morfológicas diferentes da importada, com comprimento e espessura de parede superiores, a viabilidade da sua utilização depende do conhecimento do seu comportamento nas diferentes etapas do processo de produção de papel. Com este trabalho pretende-se contribuir para quantificação da influência relativa de variáveis de entrada, como o grau de refinação e a percentagem da incorporação, na resistência do papel.

Materiais e Métodos

Matéria-prima

Procedeu-se ao branqueamento laboratorial da fibra de Pinheiro Bravo nacional (*Pinus pinaster*). Para o efeito utilizou-se uma pasta comercial, gentilmente cedida pela Celtejo, sem secagem industrial e com um tratamento suave com oxigénio (índice kappa=25) que se sujeitou a uma sequência de dois estágios de dióxido de cloro com uma extracção intermédia,

obtendo-se uma pasta com um valor de viscosidade de 830 ml/g. Utilizou-se pasta comercial de Eucalipto kraft branqueada proveniente de um só lote e pasta comercial de fibra longa kraft branqueada também proveniente de um só lote.

Planeamento experimental

Na primeira fase, com vista a analisar o desempenho individual de cada matéria-prima, refinaram-se as pastas no PFI (1000, 3000 e 6000 rotações), determinando-se o ºSR e o tempo de drenagem no formador laboratorial. Mediram-se as dimensões e a massa linear das fibras, utilizando o Morphi. Produziram-se conjuntos de 14 folhas isotrópicas no formador laboratorial, prensaram-se, secaram-se e determinaram-se as propriedades estruturais e mecânicas em ambiente condicionado de acordo com as normas padrão.
Na segunda fase o objectivo consistiu em estudar o efeito de incorporação em pastas com o mesmo número de rotações no PFI e na terceira fase em pastas com níveis de refinação semelhantes medidos como ºSR. Para tal determinou-se o ºSR e o tempo de drenagem no formador e produziram-se e testaram-se folhas com níveis de incorporação de 10 e 20% de fibra de reforço.
Na quarta fase pretendeu-se testar o desempenho das folhas em estado húmido. Para o efeito, produziram-se conjuntos de 14 folhas laboratoriais isotrópicas que se condicionaram com a humidade pós prensagem. Fazendo variar o teor de humidade, avaliou-se o seu comportamento reológico à tracção. Após cada ensaio em húmido determinou-se o teor de sólidos de cada provete individual.

Resultados

Biometria

Na tabela 1 encontram-se os valores médios para o comprimento das fibras, largura e massa linear. Verifica-se que o Pinheiro Bravo nacional apresenta um comprimento médio 13,4 % superior ao da fibra longa comercial e uma largura 15% superior. Contudo, a maior variação ocorre para a massa linear, com o Pinheiro Bravo nacional a apresentar um valor 45% superior ao da fibra longa comercial. Estes valores indicam que as fibras de Pinheiro Bravo nacional têm paredes mais espessas.

Tabela 1. Principais dados morfológicos das pastas em estudo.

	Fibra longa comercial	**Pinheiro Bravo**	**Eucalipto**
Comprimento médio pesado em comprimento (mm)	1.79	2.03	0.80
Largura (μm)	29.4	33.8	18.00
Massa linear (mg/m)	0.151	0.219	0.067

Evolução com a refinação do Eucalipto e das fibras de reforço

Refinaram-se as pastas no PFI a diferentes níveis de refinação e acompanhou-se a sua evolução com o ºSR, o tempo de drenagem e as propriedades das folhas laboratoriais. Na tabela 2 encontram-se os valores obtidos para a resistência à drenagem das diferentes pastas e para as propriedades estruturais e mecânicas das folhas laboratoriais isotrópicas das fibras em estudo: Eucalipto (Euc), fibra longa comercial (FL) e Pinheiro Bravo nacional (PB).

Tabela 2. Valores médios de resistência à drenagem e propriedades das folhas do Eucalipto (Euc), da fibra longa comercial (FL) e do Pinheiro Bravo nacional (PB).

Matéria-prima Rotações no PFI	**Euc 0**	**Euc 1000**	**Euc 3000**	**FL 0**	**FL 1000**	**FL 3000**	**PB 0**	**PB 1000**	**PB 3000**	**PB 6000**
ºSR	21	27	47	15	20	28	13	14	22	53
Tempo de drenagem (s)	3.8	4.3	9.0	3.2	3.8	4.6	2.9	3.0	3.4	5.4
Massa volúmica (g/cm^3)	0.56	0.68	0.85	0.58	0.68	0.78	0.57	0.67	0.73	0.77
Permeabilidade ao ar Bendtsen (µm/Pa.s)	36.7	20.2	2.5	30.0	12.8	2.2	45.7	28.4	5.2	0.3
Índice de tracção (Nm/g)	19.0	47.2	74.5	19.1	54.6	75.4	26.8	48.8	75.6	84.0
Alongamento (%)	1.2	2.4	4.0	2.3	3.7	3.9	2.5	3.2	3.8	4.0
Índ. Rasgamento ($mN.m^2/g$)	3.0	7.2	9.6	12.2	15.2	10.6	21.3	20.8	14.4	12.2
Lisura Bekk (s)	13	37	137	13	45	132	11	34	105	72

Ao fornecer energia mecânica à pasta com a refinação as fibras tornam-se mais flexíveis, a parede externa desenvolve fibrilação e ocorre produção de finos o que permite aumentar as ligações interfibras e aumentar a resistência do papel. No entanto com o decorrer da refinação aumentam também os efeitos indesejáveis, como por exemplo o corte das fibras e o aumento da resistência à drenagem. Assim a evolução das pastas com a refinação deve ser acompanhada da medição da resistência do papel, onde se verifica um impacto positivo, e da resistência à drenagem onde o impacto é negativo.

Da tabela 2, as observações mais relevantes para o presente estudo dizem respeito ao rasgamento pois as fibras longas apresentam um desempenho muito superior ao Eucalipto e que o Pinheiro Bravo nacional se destaca com um valor 7,2 vezes superior ao do Eucalipto e a fibra longa comercial apresenta um valo 4,1 vezes superior nas pastas não refinadas. O comportamento das pastas na drenagem foi avaliado utilizando o tempo de drenagem no formador e com a medição do Grau Schopper Riegler. Este fornece indicação da dificuldade de drenagem em que os valores superiores correspondem a pastas que drenam pior e utiliza uma escala que vai de 0ºSR a 100ºSR. Pode constatar-se que o Eucalipto refina mais

rapidamente que as fibras longas e entre estas o Pinheiro Bravo nacional refina mais lentamente.

Incorporação de fibra longa com o mesmo número de rotações no PFI

Para estudar o efeito da incorporação de fibras longas no papel de Eucalipto começou por efectuar-se um conjunto de experiências em que as pastas de Eucalipto (Euc) se misturam com pastas de fibra longa (FL) refinadas com o mesmo número rotações no PFI usando uma proporção de 80% de Eucalipto e 10% de fibra longa. Na tabela 3 incluem-se, também, os valores das pastas 100% Eucalipto e 100% fibra longa, para efeito de comparação.

Tabela 3. Valores de resistência à drenagem e de folhas laboratoriais de pastas de Eucalipto com 10% de incorporação de fibra longa refinada com o mesmo número de rotações

Matéria-prima Rotações no PFI	**100%Euc 1000**	**!00%FL 1000**	**90%Euc 1000 10%FL 1000**	**100%Euc 3000**	**100%FL 3000**	**90%Euc 3000 10%FL 3000**	**90%Euc 6000 10%FL 6000**
ºSR	27	20	27	47	28	47	85
T.Drenagem (s)	4.3	3.8	5.0	9.0	4.6	9	65
M.volúmica (g/cm^3)	0.68	0.68	0.69	0.85	0.78	0.79	0.91
Perm.Bendtsen (µm/Pa.s)	20.2	12.8	19.0	2.5	2.2	1.5	0.03
Í.Tracção (Nm/g)	47.2	54.6	48.0	74.5	75.4	78.4	80.5
Alongamento (%)	2.4	3.7	2.6	4	3.9	4.3	4.7
Í.Rasgamento ($mN.m^2/g$)	7.1	15.2	9.2	9.5	10.6	9.3	9.1
Lisura Bekk (s)	37	45	34	137	132	131	285

Pode constatar-se que o Eucalipto refina mais rapidamente que a fibra longa apresentando um valor de ºSR 68% superior ao da fibra longa para as 3000rv e que é indicativo de um desenvolvimento significativo da flexibilidade das fibras e da sua fibrilação. Assim, o Eucalipto, para o mesmo número de revoluções, drena pior que a fibra longa, pois as fibras curtas formam um bolo mais compacto. Com o aumento de refinação a diferença entre Eucalipto e fibra longa acentua-se. A pasta de Eucalipto apresenta um incremento na dificuldade de drenagem de 35% relativamente à fibra longa para 1000 rotações e de 68% para

3000 rotações, o que representa uma duplicação do incremento da dificuldade de drenagem com o aumento da refinação. A pasta de mistura drena com as mesmas características do Eucalipto não se notando a influência da adição da fibra longa no valor do Grau Schopper Riegler e no tempo de drenagem. Para 1000 rotações verifica-se que as folhas de fibra longa são mais resistentes e a sua incorporação em 10% faz aumentar a resistência das folhas de Eucalipto em 2% para a tracção e 33% para o rasgamento. Para 1000 rotações obtêm-se folhas com a mesma massa volúmica para a fibra longa e curta e ligeiramente superior para a mistura, o que pode indicar algum efeito de empacotamento. Nas 3000 rotações a fibra longa prejudica a densificação o que se pode justificar pelo facto de as fibras longas ainda não terem desenvolvido significativamente as propriedades com a refinação, ao contrário das fibras curtas, que apresentam já um aumento na flexibilidade e fibrilação externa compatível com um valor de ºSR de 47 para o Eucalipto em oposição ao valor de 28 para a fibra longa. Apesar do ºSR ser mais elevado para a fibra curta, o que significa que a água tem mais dificuldade em sair no bolo húmido, pois aqui o comprimento das fibras é determinante, a permeabilidade das folhas é superior, indicando uma estrutura mais aberta em seco e que pode ser justificada pela menor colapsibilidade das fibras de Eucalipto, que têm uma parede com um valor de espessura importante, quando comparado com o diâmetro. Esta explicação pode estender-se à lisura, onde também se verifica que a fibra longa dá origem a papéis mais lisos para as 1000 rotações. Neste caso o papel de mistura é menos liso que o 100% Eucalipto e 100 % fibra longa o que pode indicar um ajuste ou acomodação mais difícil na superfície com a presença de fibras de tamanhos diferentes. Com a refinação a permeabilidade das folhas decresce acentuadamente parecendo apresentar valores mais baixos na mistura o que se pode dever a um empacotamento mais eficiente dessa estrutura. Não existe contradição com a lisura que é uma propriedade de superfície enquanto a permeabilidade traduz a distribuição de porosidade no seio da estrutura. Na opacidade influi tanto a superfície como o todo da estrutura ou "bulk". As folhas mais opacas são as da mistura verificando-se, neste caso um efeito sinérgico positivo que está em sintonia com maior rugosidade da superfície que favorece a dispersão da luz. As folhas de Eucalipto são mais opacas e menos lisas que as de fibra longa, o que mais uma vez é indicativo da menor colapsibilidade das suas fibras

Incorporação de fibra longa e Pinheiro Bravo nacional com o mesmo nível de refinação

Tendo-se escolhido como pasta de base a pasta de Eucalipto refinada a 1000 rotações no PFI com um ºSR de 27 incorpora-se pasta de fibra longa a 3000 rotações com um ºSR de 28 e pasta de Pinheiro Bravo Na 3000 rotações com um ºSR de 22 e 6000 rotações com um ºSR de 53. Testaram-se dois níveis de incorporação, 10 e 20%, tendo-se verificado que o ºSR é semelhante para todas as suspensões.

Tabela 4. Valores de resistência à drenagem e de folhas laboratoriais de pastas de Eucalipto com 10% e 20% de incorporação de fibra longa e Pinheiro Bravo nacional.

Matéria-prima Rotações no PFI	**Euc 0**	**Euc 1000**	**90%Euc 1000 10%FL 3000**	**80%Euc 1000 20%FL 3000**	**90%Euc 1000 10%PB 3000**	**80%Euc 1000 20%PB 3000**	**90%Euc 1000 10%PB 6000**	**80%Euc 1000 20%PB 6000**
ºSR	21	27	27	28	27	28	29	32
T.Drenagem (s)	3.8	4.3	4.6	4.8	4.4	4.4	4.6	4.9
M.volúmica (g/cm^3)	0.56	0.68	0.72	0.73	0.71	0.73	0.73	0.73
Perm.Bendtsen (µm/Pa.s)	36.7	20.2	12.2	6.7	17.4	8.3	7.9	5.0
Í.tracção (Nm/g)	19.8	47.2	55.0	56.5	54.0	57.0	56.8	60.6
Alongamento (%)	1.2	2.4	3.2	3.9	3.0	3.1	3.3	3.5
Í.Rasgamento ($mN.m^2/g$)	3.00	7.16	9.36	9.71	9.68	10.20	9.16	10.73
Lisura Bekk (s)	13	137	52	56	43	60	56	59

Na tabela 5 quantifica-se o efeito da incorporação da fibra de reforço nas propriedades mais relevantes do papel. Em primeiro lugar, é de realçar o impacto muito significativo das fibras de reforço na resistência à tracção, no alongamento ena resistência ao rasgamento. Verifica-se que o maior aumento na resistência à tracção (28%) e rasgamento (50%) ocorre com a incorporação de 20% de Pinheiro Bravo e o maior aumento de alongamento (62%) para a fibra longa comercial também a 20% de incorporação. De realçar, ainda, que globalmente não há diferenças significativas entre as duas fibras de reforço objecto deste estudo.

Tabela 5. Percentagem de variação das propriedades de resistência do papel de Eucalipto reforçado relativamente ao não reforçado

Variação em relação a Euc 1000 (%)	**90%Euc 1000 10%FL 3000**	**80%Euc 1000 20%FL 3000**	**90%Euc 1000 10%PB 3000**	**80%Euc 1000 20%PB 3000**	**90%Euc 1000 10%PB 6000**	**80%Euc 1000 20%PB 6000**
Í.tracção (Nm/g)	16.5	19.7	14.4	20.8	20.3	28.4
Alongamento (%)	32.1	62.5	25.0	29.2	37.5	45.8
Í.Rasgamento ($mN.m^2/g$)	30.7	35.6	35.2	42.45	27.9	49.9

Na Tabela 6 encontra-se o efeito dos principais factores (refinação do Eucalipto, refinação da fibra de reforço e da % de incorporação) na variação das propriedades de drenagem, de resistência em seco, etc. A refinação do Eucalipto de 1000 para 3000 rotações no PFI é o factor que mais faz variar a resistência ao rasgamento e à tracção, embora à custa de um aumento impraticável da resistência à drenagem. Para as pastas incorporadas verifica-se que para as pastas reforçadas com fibra longa comercial o aumento da refinação de 1000 para 3000 é o factor com maior percentagem de variação da resistência à tracção (14,6%) enquanto a mudança de percentagem de incorporação de 10 para 20% apenas faz aumentar essa resistência em 2,7%. Quando a fibra de reforço é o Pinheiro Bravo nacional tanto a refinação como a percentagem de incorporação contribuem para o aumento da resistência à tracção com valores próximos, entre os 5 e os 7%.

Tabela 6. Efeito dos principais factores (refinação do Eucalipto, refinação da fibra de reforço e da percentagem de incorporação) na variação das propriedades de drenagem, de resistência em seco, etc.

Factores	**Refin. do Euc.**	**Refin. da Fibra Longa**	**Incorp. Fibra Longa (%)**	**Refin. Pinho Nac. (10% inc.)**	**Refin. Pinho Nac. (20% inc.)**	**Incorp. Pinho Nac. 3000 (%)**	**Incorp. Pinho Nac 6000 (%)**
Pasta de referência	Euc 1000	90%Euc 1000 10%FL 1000	90%Euc 1000 10%FL 3000	90%Euc 1000 10%PN 3000	80%Euc 1000 10%PN 3000	90%Euc 1000 10%PN 3000	90%Euc 1000 10%PN 6000
Pasta que varia	Euc 3000	90%Euc 1000 10%FL 3000	80%Euc 1000 20%FL 3000	90%Euc 1000 10%PN 6000	80%Euc 1000 10%PN 6000	80%Euc 1000 10%PN 3000	80%Euc 1000 10%PN 6000
	Variações (%)	Variações (%)	Variações (%)	Variações (%)	Variações (%)	Variações (%)	Variações (%)
ºSR	74	0	3.7	9.4	14.3	5.7	1.03
T.Drenagem (s)	1.2	7.7	3.0	2.9	11.1	0	7.9
M.volúmica (g/cm^3)	25	4.3	1.4	2.8	0	2.8	0
Perm. Bendtsen (µm/Pa.s)	-87.6	-35.8	49.9	-54.6	-39.3	-52.4	-36.4
Índice tracção (Nm/g)	57.8	14.6	2.7	5.2	6.3	5.6	6.7
Alongamento (%)	66.7	21.9	23.0	3.3	12.9	3.3	6
Ind. Rasgamento ($mN.m^2/g$)	33.3	-1.6	3.7	-5.4	5.2	-5.4	17.4
Lisura Bekk (s)	270	52.9	7.6	30.2	-1.7	30.2	5.3

Resistência em húmido

Considerando que uma das áreas críticas para as quebras é a secção de prensas, onde o teor de sólidos pode estar entre 30 e 50% analisou-se o desempenho das folhas em estado húmido.

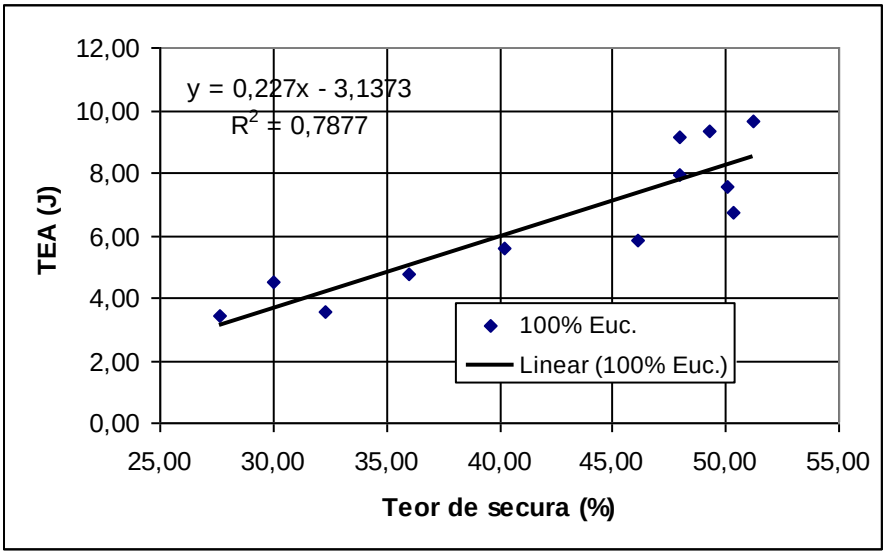

Figura 1 – TEA versus TS para o Eucalipto

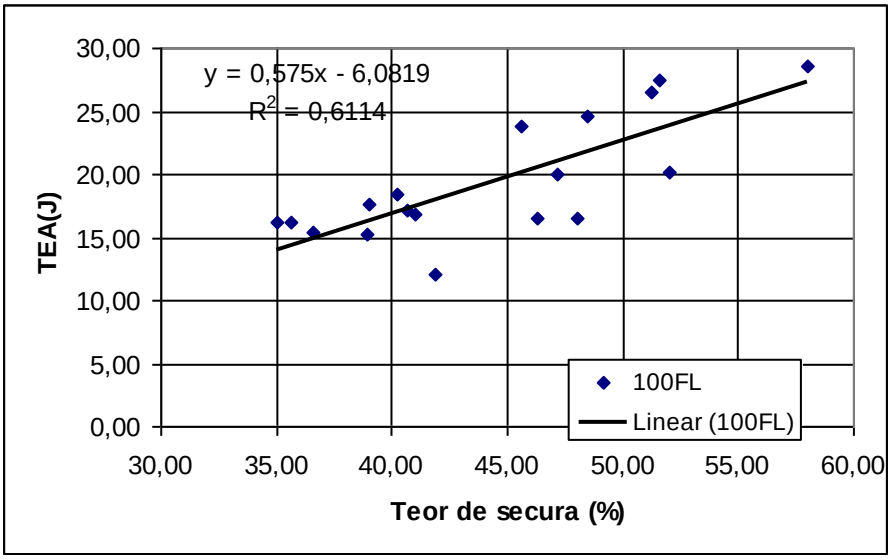

Figura 2. TEA versus TS para a fibra longa comercial

Nas figuras 1 e 2 representa-se o valor da energia absorvida por um provete de 25mm até ao ponto de ruptura, quando traccionado a uma velocidade de 10mm/min, para diferentes teores de secura dos provetes.

Para um intervalo de teor de secura de 40 a 45% o Eucalipto apresenta um TEA (Tensile Energy Absorption) de 6 a 7%, o Pinheiro Bravo de 17a 21% e a fibra longa comercial de 16 a

20%. Estes dados experimentais evidenciam desde logo a grande debilidade das estruturas fibrosas húmidas de Eucalipto face às correspondentes estruturas de fibras longas.

Nas pastas com incorporação utilizou-se Eucalipto refinado a 1000 rotações com 27 ºSR, fibra longa comercial refinada a 3000 rotações com 28 ºSR e Pinheiro Bravo nacional refinado a 4000rv com 25 ºSR

Testaram-se dois níveis de incorporação podendo concluir-se que no intervalo de teor de secura de 40 a 45% o Eucalipto reforçado com 20% de Pinheiro Bravo apresenta um TEA de 9.5 a 12% e reforçado com fibra longa comercial de 10 a 11.5% (ver figuras 3 e 4). Para 90% de incorporação e mesma gama de teor de sólidos obtém-se um TEA de 8 a 9.5 % para o Pinheiro Bravo e 8 a 9% para a fibra longa comercial.

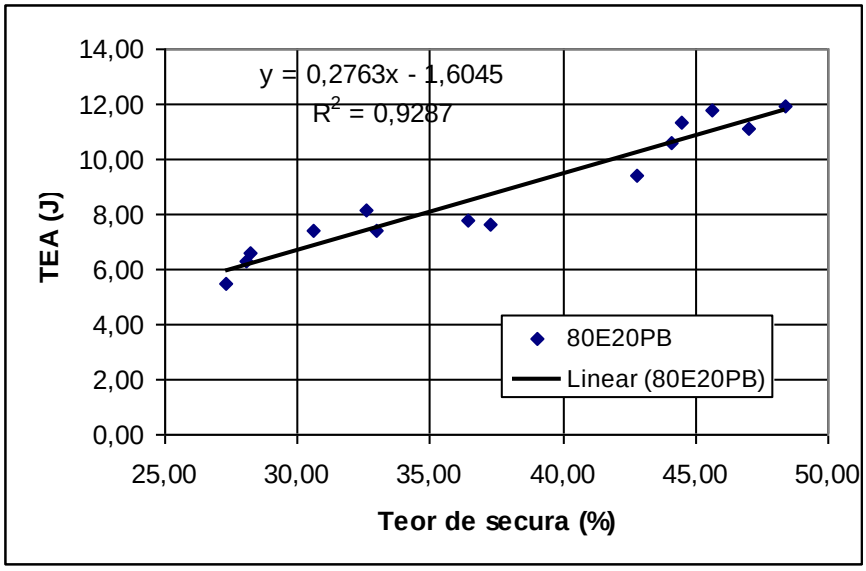

Figura 3. TEA versus Teor de secura para 20% de Pinheiro Bravo

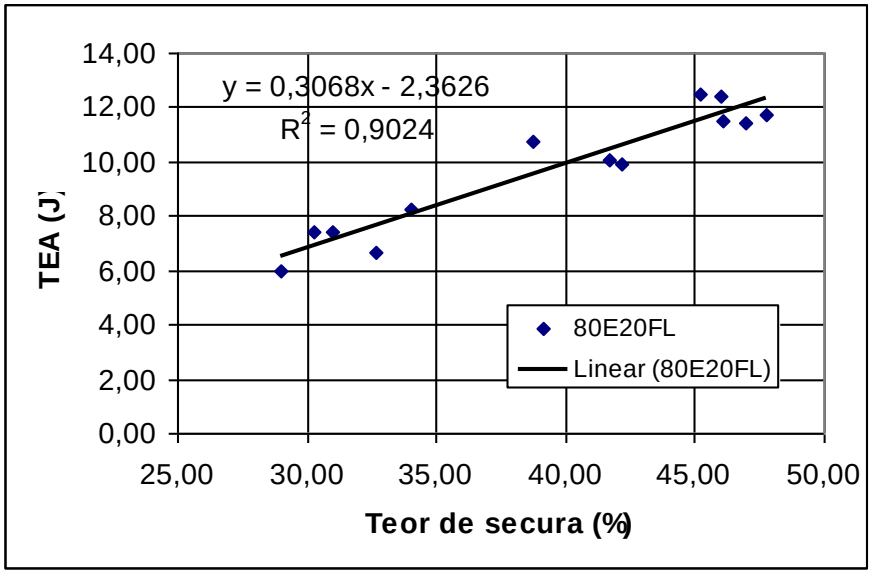

Figura 4. TEA versus Teor de secura para 20% de Pinheiro Bravo

Bibliografia

Mohlin, U-B., Wennberg, K., Tappi Journal 67, 1984, 1, 90-93.

Moilanen, P., Linqdvist, U., Tappi J. 79, 1996, 9, 88-94.

Niskanen, K., Kärenlampi, P., Paper Physics. Ed. K. Niskanen, Finnish Paper Engineers' Ass. TAPPI, Jyväskylä, Finland, 1998a, 139-191.

Niskanen, K., Kajanto, I., Pakarinen, P., Paper structure. Paper Physics. Ed. K. Niskanen, Finnish Paper Engineers' Ass. TAPPI, Jyväskylä, Finland, 1998, 14-53.

Page, D.H., Seth, R.S., Tappi 65, 1982, 8, 92-95.

Parsons, S.R., Tappi 52, 1969, 7, 1262-1266.

Retulainen, E., D.Sc. (Tech) thesis. HUT, Lab. of Paper Technology, Reports Series A7, Espoo, Finland, 1997.

Roisum, D.R., Tappi Journal 73, 1990, 2, 101-106.

Sears, G.R., Tyler, R.F., Denzer, C.W., Pulp and Paper Magazine of Canada 66, 1965, 7, T351-T360.

Uesaka, T., Ferahi, M., Hristopulos, D., Deng, N., Moss, C., The Science of Papermaking, Transactions of the 12th, FRS, Oxford, England, 2001.

van den Akker, J.A., Wink, W.A., Van Eperen, R.H., Instumentation studies LXXXIX, Tappi 50, 1967, 9, 466-470.

Three dimensional modeling of fibrous materials and experimental validation

Curto, J.M.R. [1], Conceição, E. L.T.[2], Portugal, A.T.G.[2] and Simões, R.M.S.[1]
[1]Textile and Paper Materials Research Unit,
Chemistry Department, University of Beira Interior (UBI)
[2] Research Centre for Chemical Processes Engineering and Forest Products,
Chemical Engineering Department, University of Coimbra (UC)

Abstract

This article presents a computational model and some simulation results for fibrous materials such as paper. To obtain a better understanding of the influence of fiber properties on the paper structure a novel paper model was developed. This is a physically based model where paper is formed by the sequential deposition of individual fibers. The model intends to capture key papermaking fiber properties like morphology, flexibility, and collapsibility, and also process operations such as fiber deposition, network forming or densification.
This model is a step forward in transverse paper modeling. In fact, it is a three dimensional model that includes the fiber microstructure, that is, lumen and fiber wall thickness, with a resolution up to 0.05 μm.
To test the model validity and predictive capability, laboratory handsheets were used to study the network formation of an office paper, mainly produced from *Eucalyptus globulus* bleached Kraft pulp. This paper was characterized via an experimental design that included factors such as raw material and beating degree. The resulting porous structure was characterized and the mechanical performance was assessed.
The computational simulation was used to investigate the relative influence of fiber properties such as fiber flexibility, dimensions and collapsibility. The developed multiscale model gave realistic predictions and enabled us to link fiber microstructure and paper properties.

Keywords: Three dimension modeling, fiber modeling, cellulosic fiber materials modeling, fiber flexibility and collapsibility, office paper case study
Corresponding author: jmrc@ubi.pt, Fax: +351 275 319730, Phone: +351 96 6485662

1 Introduction

Paper is a complex material built from wood fibers. Many authors have identified the importance of fiber properties, especially fiber transverse dimensions and mechanical behavior (flexibility and collapsibility), on paper properties [1-3]. Due to the variability and complexity of fibers, it is difficult to separate the individual effects when trying to establish relationships based on experimental data. This is because when changing a raw material, several, if not all, of the fiber dimensions change. Also, when studying paper densification two mechanisms (fiber flexibility and collapse) occur simultaneously. For these reasons, mathematical paper models can be useful tools to overcome experimental limitations.

The papermaking process consists on handling fibers and building a network to obtain the desirable end use specifications. Although chemical and mineral additives are present in most papermaking furnishes, this work focuses on the fiber network structure and on the influence of fiber properties.

In the papermaking process, a fiber network of say 60 g/m2, built with approximately 0.1 µg fibers, has around 60 000 fibers per square centimeter. To treat so many fibers, the first attempt to establish relationships and model paper structure was done using statistical geometry by Kallmes and Corte [4, 5]. Since then, many researchers have considered an idealized two dimensional random network when modeling paper structure. In this framework it is worth mentioning the publications by Sampson, Dodson and Deng [6-8]. In 1998 Wang and Shaler [9] proposed a three dimensional structure made from rigid cylindrical fibers. The major breakthrough came with the introduction of the fiber flexibility in the work of Niskanen and Alava [10]. This model is called KCL-PAKKA and the three-dimensional structure of paper is simulated by means of a sedimentation-like or growth process which assumes that the sheet is formed from a dilute suspension under the influence of a uniform flow field and ignores fiber interactions. Departing from fiber dimensions and flexibility, a three dimensional structure is formed and various paper properties are predicted. The simulations obtained are consistent with experimental data as presented by Alava and Niskanen, in 2006, and Niskanen et al. in 2006 and 1997 [11, 12].

The first part of this article presents a novel paper model developed to include key fiber parameters including fiber collapsibility, and the second part demonstrates its utility by applying it to a concrete paper.

2 Computer Model

A summary of the model is presented, step by step, explaining how different physical operations are mathematically described. To obtain a realistic model, it is very important to choose the determinant processes steps and parameters.

2.1 Fiber Modeling

Fibers are modeled according to their dimensions, flexibility, and collapsibility. The input parameters are: length/width ratio, wall thickness, lumen thickness, fiber flexibility, and resolution (number of layers in the thickness direction). Length values can be averages or distributions. Fines and filler can also be introduced.

The computational fiber flexibility is based on the Niskanen approach [10] but has a novel implementation using cellular automata (see Fig. 1) [13, 14]. The space is discretized into a Cartesian uniform grid of cells so that each fiber in the model is represented by a sequence of cells. A "bending" flexibility or dimensionless computational flexibility gives the largest allowed vertical deflection for the fiber [10]. So, any two nearest neighboring cells on the fiber can make, at most, the maximum fiber flexibility.

The new model is detailed up to the point to include fiber morphology and the behavior in the z-direction. Both fiber wall thickness and fiber lumen can be changed independently, which allows the implementation of different degrees of fiber collapse.

2.2 Fiber Deposition

The paper is formed by the deposition of single fibers, one at a time. Depending on its position, dimensions, and flexibility, the fiber conforms to the underlying structure. In the present work, fibers are randomly positioned and oriented in the x-y plane to simulate the formation of isotropic handsheets (the ones used to validate the model). The paper machine orientation can be simulated by using an appropriate spatial distribution.

2.3 Fiber Interactions

Several modifications to the original KCL-PAKKA model are proposed and implemented, resulting in a model that goes further simulating the fiber suspension micro hydrodynamics. To better simulate the papermaking process physics, a formation control parameter is introduced to the model fiber flocculation. Furthermore, the tendency of the fibers on suspension to concentrate around drainage sinks, leading to a smoothing mechanism of the paper sheet is also modeled. These effects are simulated by the particle deposition rule of Provatas and Uesaka [15], which works over the rejection model introduced by Provatas *et al*. in 2000 [16].

The computational simulation can be described as follows (see also figure 1):

- Generation of a fiber in the in-plane direction.
- Testing particle deposition rule. If the fiber is not accepted, the generation trial is repeated.

- Extraction of the out-of-plane slice from the 3D network where the bending procedure occurs.
- Fiber deposition according to fiber flexibility and conformation to the underlying surface.
- Updating of the 3D network.

The paper model is developed and implemented using MATLAB from MathWorks, a numeric computation environment and programming language.

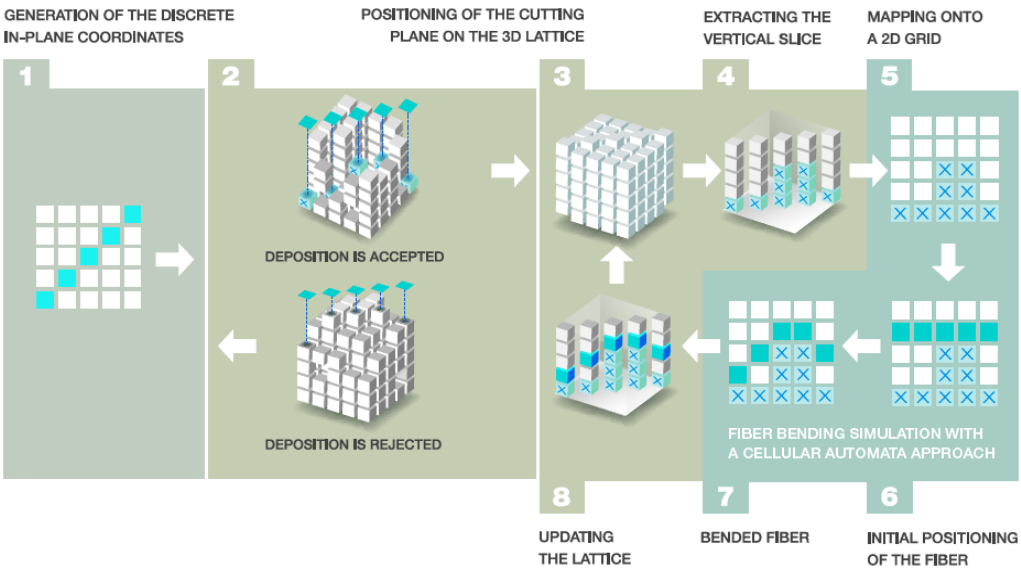

Figure 1. Fiber deposition in the 3D matrix followed by plane extraction and fiber bending to conform to the underlying structure.

3 Case Study

3.1 Materials and Methods

The model is applied to study a concrete material: the network structure needed to form an hardwood office paper. Office paper is the principal Portuguese paper industry product. This paper is mainly produced from *Eucalyptus globulus* bleached kraft pulp with a small incorporation of a softwood pulp, called reinforcement pulp, to increase the paper strength. It is important to assess the contribution of different reinforcement pulp fibers with different biometry and coarseness to the final paper properties. The two extremes of reinforcement pulps are represented by a market *Picea abies* kraft softwood pulp, usually incorporated in the paper, and the Portuguese pine *Pinus pinaster* kraft pulp, recently made commercially available.

To evaluate the impact of different fibers on paper properties, isotropic paper handsheets were prepared and tested regarding structural, mechanical, and optical properties.

To characterize this network an experimental design was devised in order to quantify the raw material influence (including two reinforcement pulps) and beating degree. The complete characterization is available in previous publications [17, 18]. Only a summary of this data is presented here.

The morphological properties of pulp fibers were determined automatically by image analysis of a diluted suspension (20 mg/l) in a flow chamber in Morfi (TECHPAP, Grenoble). The pulps were beaten in a PFI mill at 1000, 3000 and 6000 revolutions under a refining intensity of 3.33 N/mm. PFI is an ISO standard mill who provides a pulp mechanical treatment called beating. Wet Fiber Flexibility (WFF) was determined according to the Luner procedure [19], using CyberFlex from CyberMetrics. The experimental method includes the formation of a very thin and oriented fiber network on the wire of a small head-box simulating the paper formation, followed by transfer under controlled pressure conditions to a glass slide with metal wires. The paper handsheets were prepared and tested in regard to their structural, mechanical, and optical properties (ISO and Scan standards).

4 Results and Discussion

4.1 Pulp Fiber Characterization

The three investigated raw materials present different morphology, coarseness and flexibility (table 1 and figure 2).

Table 1. Fiber morphology and coarseness.

	Picea abies (FL)	*Pinus pinaster (PB)*	*Eucalyptus globulus* (EUC)
Fiber length weighted in length (mm)	1.8	2.0	0.8
Fiber width (µm)	29	34	18
Coarseness (mg/m)	0.15	0.22	0.067

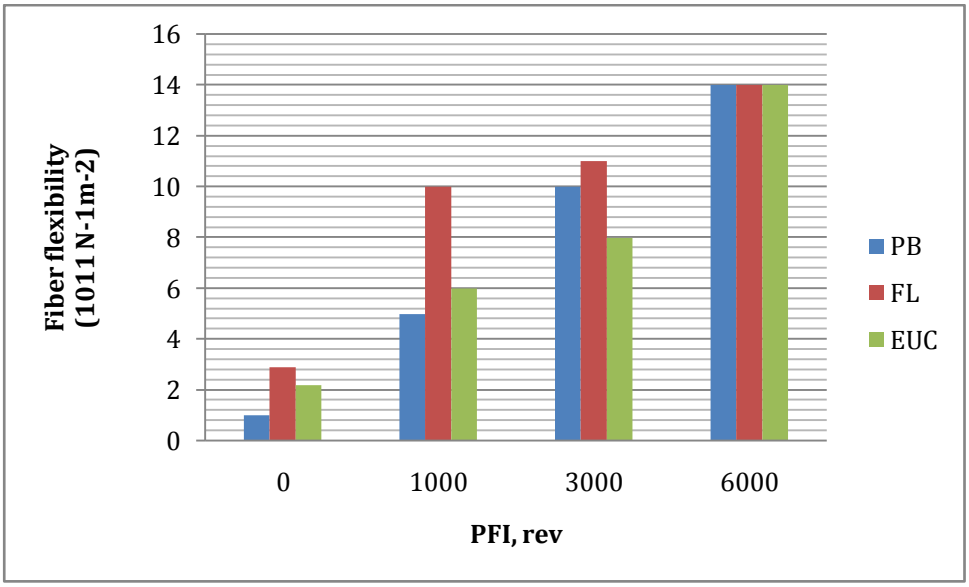

Figure 2. Evolution of Wet Fiber Flexibility (WFF) with beating. PFI is an ISO Standard beater, i.e., a mechanical treatment mill. PB, FL and EUC are raw material identifications, respectively *Pinus pinaster*, *Picea abies* and *Eucalyptus globulus*.

4.2 Structure Characterization

The network structure was characterized in terms of porosity and thickness. In SEM photographs (figures 3 and 4), it is evident the densification that occurs from changing the fiber flexibility and collapse with beating. The samples presented are thickness cuts from laboratory handsheets (60 g/m2).

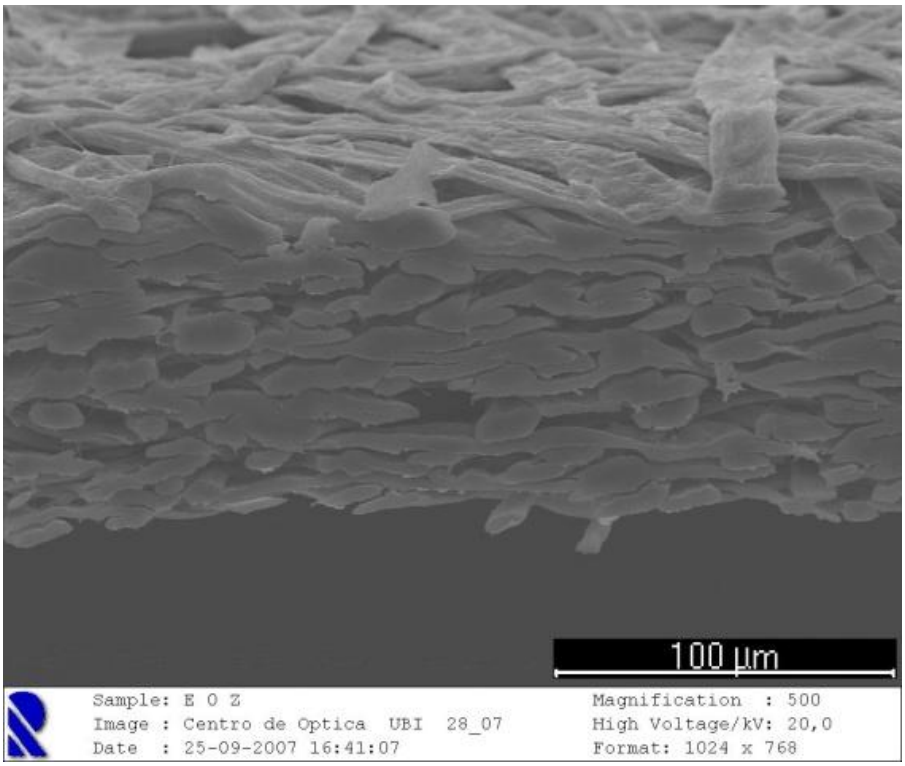

Figure 3. SEM (Scanning Electron Microscopy) photography of *Eucalyptus globulus* paper (zero PFI beater revolutions).

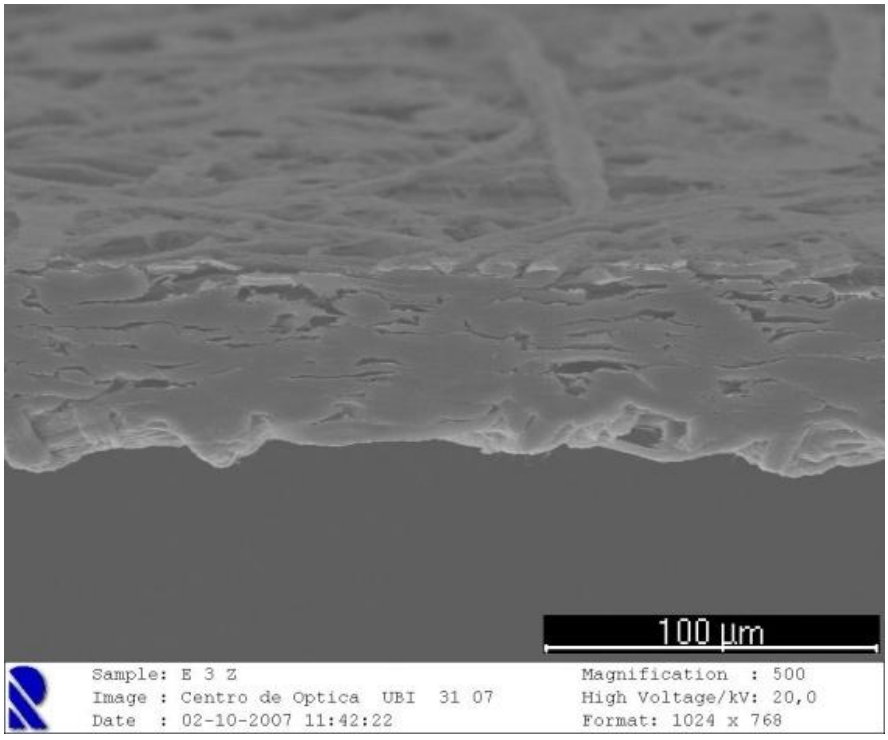

Figure 4. SEM (Scanning Electron Microscopy) photography of *Eucalyptus globulus* paper (3000 PFI beater revolutions).

4.3 Simulation Results

4.3.1 Fiber Flexibility

As figure 2 illustrates the fiber flexibility changes markedly during beating. Therefore, the response of the model to this parameter is very important for the model performance evaluation. Figure 5 represents the fiber flexibility influence on the paper thickness for real and simulated paper (*Eucalyptus globulus* 60 g/m^2). The pulp fibers have been beaten in three beating levels (0 PFI revolutions, 1000 PFI revolutions and 3000 PFI revolutions), and laboratory handmade papers have been made according to standard ISO, corresponding to a paper thickness of 112, 94 e 83 µm, respectively. For the simulated paper, the fiber wall thickness was fixed at 2 µm.

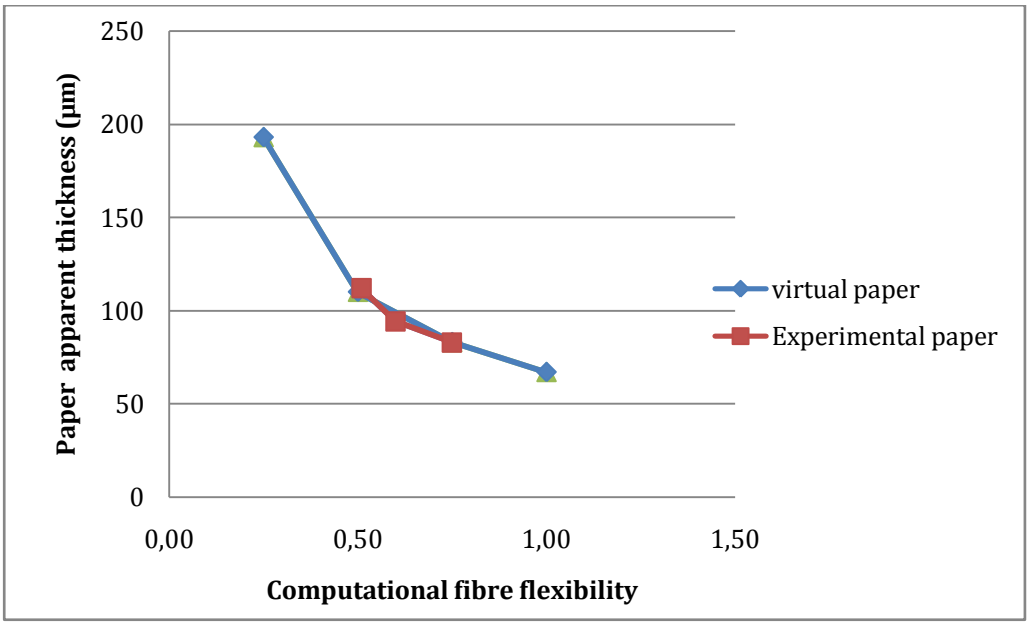

Figure 5. Fiber flexibility influence for real and virtual paper (60 g/m^2 *Eucalyptus globulus* paper). The Computational fiber flexibility is defined according to Niskanen approach [10] and is dimensionless.

In order to relate simulations with experimental data, a computational paper thickness needs to be defined. A possibility is to use the average value of local thickness, often called the effective thickness [20]. To compare with experiments the apparent thickness of the simulated sheets is very useful because it mimics the real thickness measurement with a hard platen, as suggested by Hellen *et al*. [20]. The apparent thickness is defined for the simulated sheets as being the one that corresponds to 80% of local thickness being below this value [20]. In accordance with our experimental verification, the fiber flexibility has a crucial impact on the paper structure. A similar impact for the influence of computational fiber flexibility on

simulated structures was verified. Furthermore, the model proves to adjust to the experimental data.

4.3.2 Fiber Collapse

To study the influence of the fiber collapse on the final paper thickness, a complete design of simulation experiments was implemented. For each fiber wall thickness, different lumen dimensions were tested and the paper properties determined. The computer simulated paper sheets were obtained for a fixed basis weight of 60 g/m2, identical to that of the experimental data. To illustrate the results obtained, one example was selected having a fiber wall thickness represented by four layers (figure 6). For other fiber wall values, the same tendency was observed.

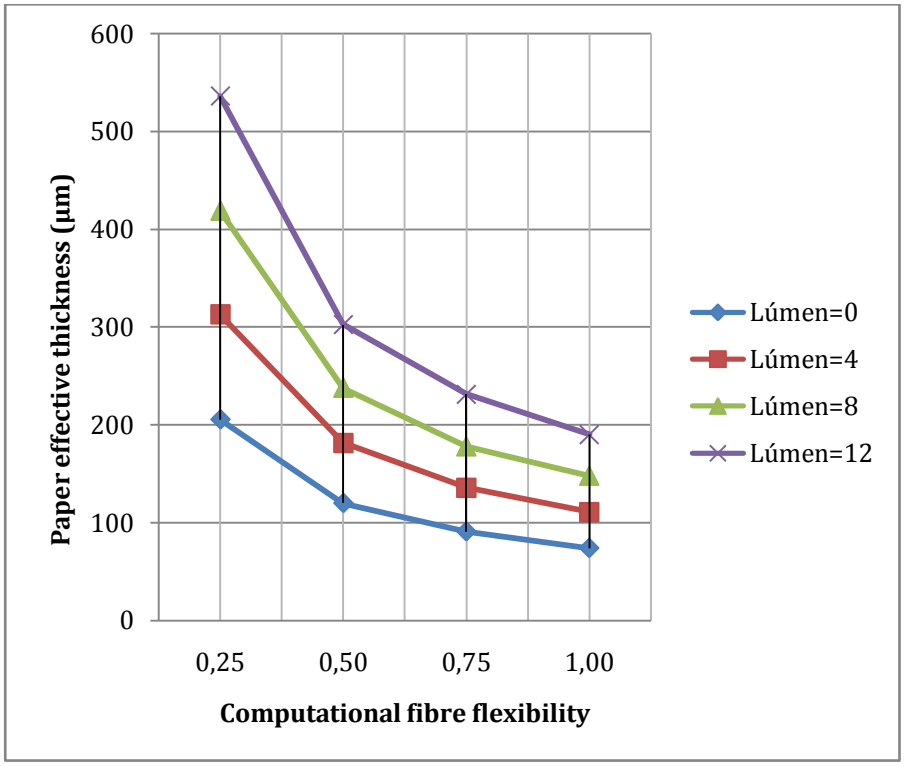

Figure 6. Fiber collapse influence on the variation of virtual paper apparent thickness with computational fiber flexibility. The computational fiber flexibility is defined according to Niskanen approach [10] and is dimensionless.

In the case of paper thickness, it is apparent that different degrees of fiber collapse have major influence on this final property. Notice that lumen equal to zero corresponds to a totally collapsed fiber, and lumen equal to twelve would correspond to a lumen three times the fiber wall thickness, which is an unexpected condition for chemical pulps. However, this can occur for mechanical pulps and in wet end consolidation.

For inter fiber porosity, the differences obtained from fiber collapse are not significant when compared with the variation due to fiber flexibility (figure 7).

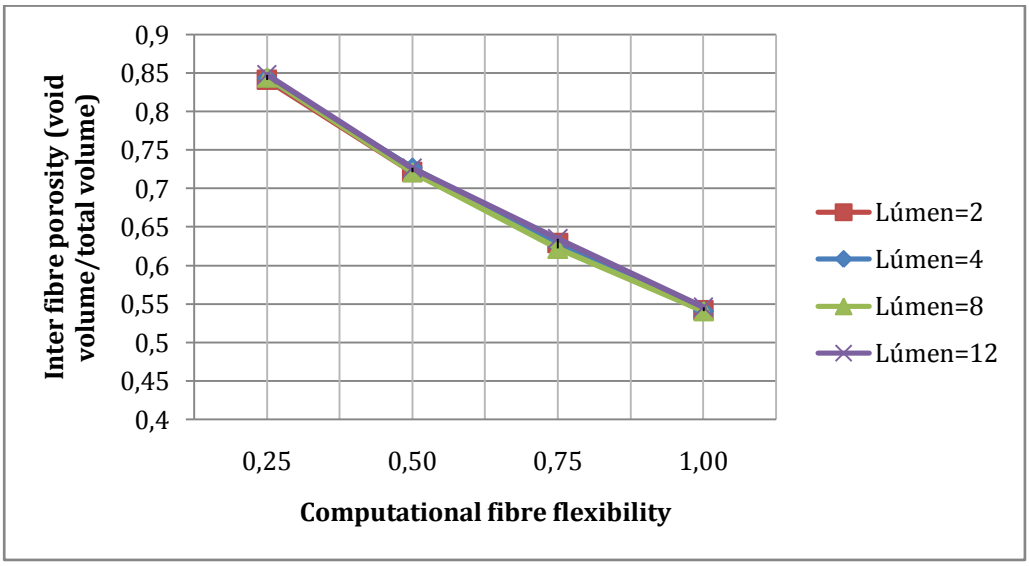

Figure 7. Evolution of virtual paper inter fiber porosity with computational fiber flexibility. The Computational Fiber Flexibility is defined according to Niskanen approach [10] and is dimensionless.

5 Conclusions

The purpose of this article was to present a novel three dimensional paper model developed to include key fiber dimensions and properties. The paper structure was built by the sequential deposition of individual fibers, taking into account determinant process operations that take place to form a network structure. The model is detailed up to the point where it includes fiber morphology and behavior in the z-direction. Both fiber wall thickness and fiber lumen were changed independently in order to allow the implementation of different degrees of fiber collapse. The simulated results represented a good estimative of the real papers network.

The paper model presented proved to be an interesting tool for studying the influence of fiber properties such as fiber flexibility, fiber dimensions, and fiber collapse on paper structure.

6 References

[1] L. Paavilainen, Paper Ja Puu. 1993, 75(5), 324.

[2] L. Paavilainen, PaperJa Puu. 1993, 75(9-10), 689.

[3] Pulkkinen, V. Alopaeus, J. Fiskari, O. Joutsimo, O Papel 2008, 69(10), 71.

[4] O. Kallmes, H. Corte, Tappi J. 1960, 43(9), 737.

[5] O. KallmeS, H. Corte, Tappi J. 1961, 44(7), 519.

[6] M. Deng, C. Dodson, Paper: an engineered stochastic structure, Tappi Press, Atlanta 1994.

[7] C. Dodson, W. Sampson, J. Statist. Phys. 1999, 96(1-2), 447.

[8] W. Sampson, Proc. 12th FRS, Oxford 2001, pp.1205-1288.

[9] H. Wang, S. Shaler, J. Pulp Pap. Sci. 1998, 24(10), 314.

[10]K. Niskanen, M. Alava, Phys. Rev. Lett. 1994, 73(25), 3475.

[11]M. Alava, K. Niskanen, Reports on Progress in Physics, 2006, 69(3), 669.

[12]K. Niskanen, N. Nilsen, E. Hellen, M. Alava, Proc. 11th FRS, Cambridge 1997, pp. 1273-1293.

[13]J. Curto, E. Conceição, A. Portugal, R. Simões, Proceedings Engenharias'07: 4ª Conf. de Eng., UBI, Covilhã, 2007, pp. 8-12.

[14]N. Provatas and T. Uesaka, J. Pulp Pap. Sci. 2003, 29(10), 332.

[15]N. Provatas, M. Haataja, J. Asikainen, J. Majaniemi, M. Alava, T. Ala-Nissila, Fiber, Colloids and Surfaces A: Physicochemical and Eng. Aspects. 2000, 165: 209-229.

[16]E. Conceição, J. Curto, R. Simões, A. Portugal, Procedings CompIMAGE 2010, 2nd International Symposium on Computational Modeling of Objects Represented in Images, vol. 6026 of Lecture Notes in Computer Science, Springer, Berlin 2010, pp. 299–310.

[17]J. Curto, C. Gil, E. Conceição, A. Portugal, R. Simões, Revista Pasta e Papel 2009, pp. 52-57.

[18]J. Curto, E. Conceição, A. Portugal, R. Simões, Proc. 63rd Appita Annual Conference and Exhibition, Melbourne 19-22 April, Australia, 2009, pp. 303-310.ISBN:9780975746952.

[19]P. Luner, PIRA International Conference on "Advances in Refining Technologies", Birmingham, England, vol.1, Session 1, Paper 3, 1986, pp.77-103.

[20]E. Hellen *et al*, Difusion through fiber networks, J. Pulp Pap. Sci. 2002, 28(2), 55.

Coding a simulation model of the 3D structure of Paper

Conceição, E. L.T.[1], Curto, J.M.R.[2], Simões, R.M.S.[2] and Portugal, A.T.G.[1]
[1] Research Centre for Chemical Processes Engineering and Forest Products,
Chemical Engineering Department, University of Coimbra (UC)
[2]Textile and Paper Materials Research Unit,
Chemistry Department, University of Beira Interior (UBI)

Abstract

Almost everyone agrees on the central role that simulation plays in the understanding of complex systems such as the 3D network formed by stacking millions of fibers on top of each other in a paper sheet. Clearly, the computational implementation of the few models which describe the microstructure of paper is far from trivial. Unfortunately, to our knowledge, there is no description in the literature of the methodology used for programming these algorithms. As a contribution towards overcoming this gap, the present article explains the software implementation of key features of a 3D random fiber deposition model into a high-level MATLAB computer code.

Keywords: 3D modeling, paper structure, cellular automata.

1 Introduction

The formation of a paper sheet involves the drainage of a suspension of cellulosic fibers in water leading to a network structure in which the fibers lie roughly horizontal and their agglomeration is stochastic in nature. It turns out that even for a thin material as paper it appears necessary to develop a 3D structure model to be able to predict several of its properties consistent with experimental data [2]. Simulation models which grow networks by random deposition of fibers are traced to the work of [6], which featured a 3D stacking of bendable fibers resembling real paper. Certainly, the KCL-PAKKA simulation model [5] ranks as one of the most successful and mature of these approaches.

Although the fundamentals of the KCL-PAKKA paper model have been published in the literature for over one decade, lack of availability of an open source implementation on

which we could base our studies led to the decision to design and develop a prototype system from scratch.

In this context, this paper serves to illustrate and discuss the concepts and techniques used in translating the KCL-PAKKA model, by describing key building blocks of our MATLAB implementation. Throughout this work we assume the reader to be familiar with the MATLAB language.

In the next section we briefly review the basics for the sedimentation-like process of forming a paper web. Besides the standard KCL-PAKKA we also discuss an extension of this model to incorporate a formation control parameter.

Section 3 is the core of the paper. There we present the prominent design features and discuss its MATLAB-specific implementation. Calculation of physical properties is briefly considered in Section 4. Section 5 gives some conclusions.

2 Brief description of the hand sheet formation model

In order to grow a paper web, flexible straight fibers are laid down, one at a time, onto a flat substrate. Fibers are positioned and oriented at random in the in-plane (x and y) directions and placed parallel to the substrate on top of the underlying network. Thereafter the parts of the fiber that do not touch the network underneath them undergo bending in the vertical (z) direction (or thickness direction) such that they either do contact with previously deposited fibers or the largest deflection allowed by the bending stiffness of fibers is reached. In the latter case, free space arises in the thickness direction between the fiber and the entangled network of fibers located just below because its stiffness prevents it from adjusting to the top surface roughness.

2.1 Flexing rule

Space is discretized into a Cartesian uniform grid of cells so that each fiber in the model is represented by a single vertical planar strip one cell wide and thickness of m vertical cells. Any two nearest neighboring cells in the same layer of the fiber can make at most the maximum F vertical lattice steps allowed. We remark that this depends only on the behavior of the bottom surface layer which may be described mathematically as

$$|zB(j) - zB(j')| \leq F , \qquad (1)$$

where zB(j) and zB(j') are the elevations of two nearest neighbor cells j and j' occupied by the surface bottom of a fiber and F can be any positive integer ≤ m, which is related to fiber flexibility. Figure 1 shows a representation of a deformed fiber in 2D.

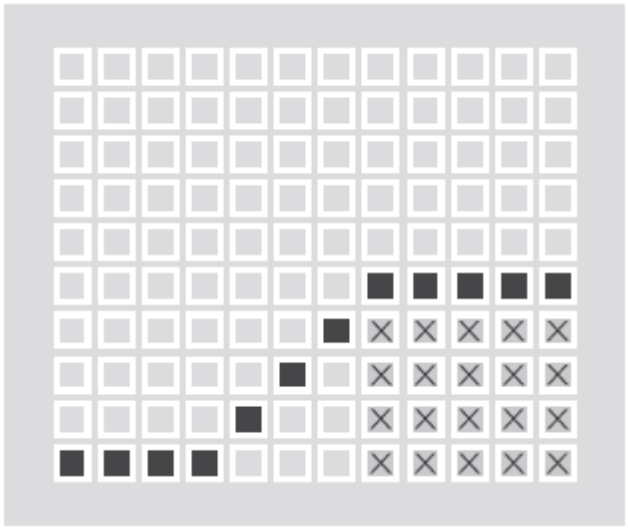

Figure 1. Final configuration of a bended fiber with flexibility F = 1. The crosses represent parts of previously deposited fibers with squares denoting the bottom layer of the fiber.

2.2 Fiber interactions

The tendency of fibers in the suspension to concentrate around drainage sinks (those parts of the deposit that have less fibers per unit area) leads to a smoothing effect in these less dense areas in the paper sheet. This mechanism is simulated by the particle deposition rule of [8] which works over the rejection model introduced by [7]. The operation works as follows: A candidate fiber lands on a section of the web whose mean height is compared with a fraction of its counterpart of the entire paper. If the following condition is fulfilled, the attempt is always accepted:

$$h \leq \alpha H , \qquad (2a)$$

where h is the average thickness of the paper over the projected area of the trial fiber, $0 \leq \alpha \leq 1$ is a constant, and H is the average thickness of the entire paper. Otherwise, the attempt is accepted only with a probability p, called the acceptance probability.

In the limit p = 1 produces uniformly random networks for all values of α. However, for $p \rightarrow 0$ mass density uniformity is enhanced by the rule favoring depositions into the valleys within the web. Two configurations of the fiber network are shown in Figure 2.

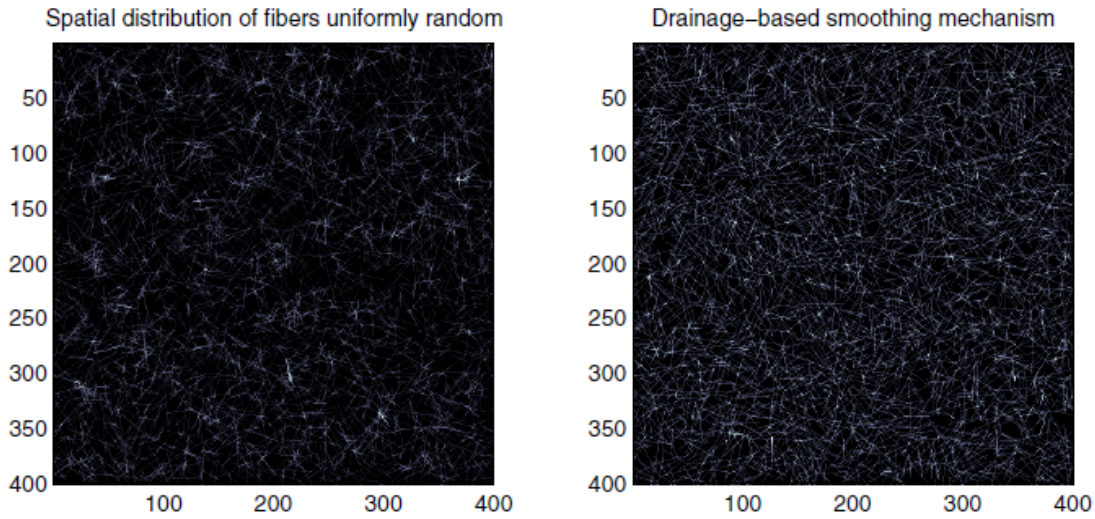

Figure 2. Simulated X-ray image of the (x, y) plane for a paper handsheet as generated from the deposition rule, with formation control parameters set to $p = 1$, $\alpha = 1$ (left) and $p = 0.01$, $\alpha = 0.94$ (right)

We refer the interested reader to [9, Chap. 4] for a clear and simple presentation of the paper formation process.

3 Some implementation aspects

This section outlines the most relevant points of the implementation. For each one we give a sample code fragment and present a brief walkthrough. To focus on the principal ideas, we omit details regarding code optimization. Please note that we restrict ourselves to only one type of fiber for the sake of simplicity.

To summarize, our growth process of a 3D fiber network consists of the following steps (see Figure 3):

1. Generation of a fiber in the in-plane directions.
2. Testing the rule for particle deposition. If the fiber is not accepted, the generation trial is repeated.
3. Extraction of the out-of-plane vertical slice from the 3D network where the bending procedure occurs.
4. Fiber bending simulation for its bottom surface.
5. Filling up the remaining $m - 1$ cell layers.
6. Updating by reinsertion of the modified slice into the 3D network.

3.1 Generation of a fiber

Each straight fiber is built by randomly placing the center within the boundaries of a flat surface represented by the rectangle [0, Lx] × [0, Ly] such that both position and orientation are uniformly distributed. This corresponds to the case of laboratory handsheets. Fiber length is characterized by a Poisson distribution following [8]. After this, the fiber is discretized to a chain of square cells, defined by the Bresenham's line drawing algorithm [1, pp.38–40], onto a discrete lattice [1,Nx] × [1,Ny]. The parts of a fiber that cross the lattice limits are cut. In MATLAB this can be done with

```
XMIN = 1, YMIN = 1, XMAX = Nx, YMAX = Ny,
midpoint = unifrnd([0 0], [Lx Ly], 1, 2),
orientation = unifrnd(−1, 1, 1, 2),
half_fiber_length = poissrnd(mean fiber length) / 2,
orientation = orientation / norm(orientation),
mov = half_fiber_length∗orientation ,
startPt = midpoint − mov % Start point of segment.
endPt = midpoint + mov % End point of segment.

% Transforming from continuous to discrete coordinates.
scales = [(Nx−1)/Lx, (Ny−1)/Ly],
startPt = floor(startPt.∗scales ) + 1,
endPt = floor(endPt.∗scales) + 1,
```

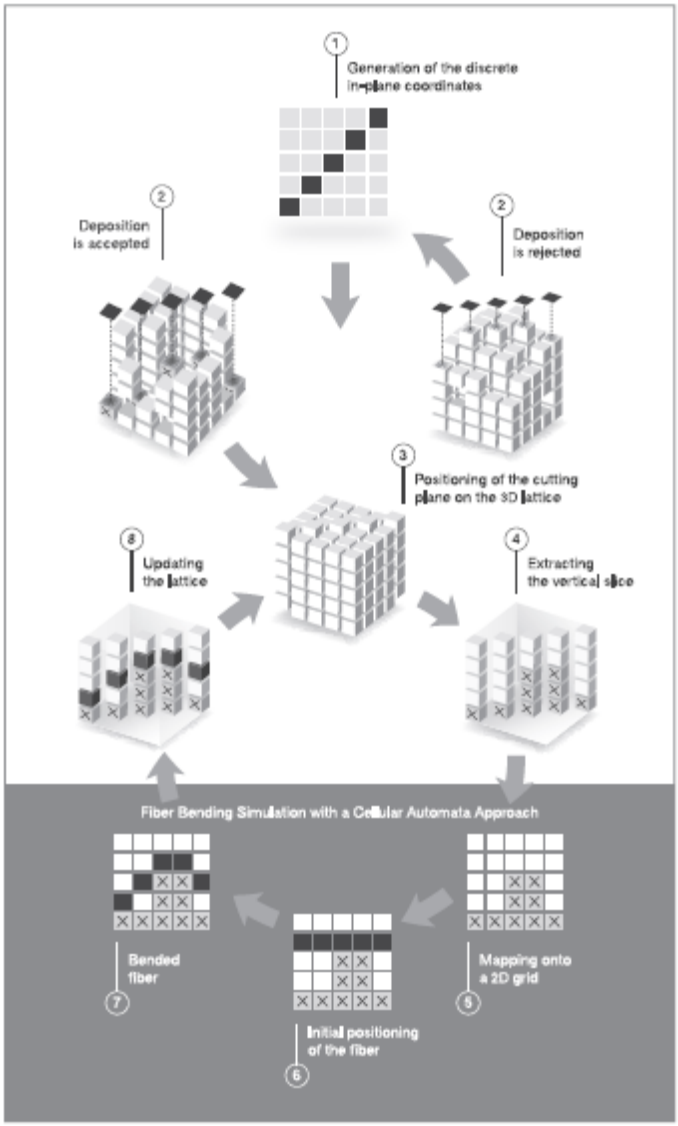

Figure 3. Data flow diagram that illustrates the core of the sequence of computations for the fiber deposition model. Note that the step filling the layers atop the bottom one is not depicted here.

```
% Draw the discrete fiber segment using Bresenham algorithm.
[ fiber_xcoord , fiber_ycoord ] = bresline(startPt , endPt),

% Restrict the fiber segment to the rectangle [1,Nx] x [1,Ny].
clip = fiber x_coord < XMIN | fiber xcoord > XMAX ...
| fiber ycoord < YMIN | fiber ycoord > YMAX,
Fiber_xcoord( clip ) = [],
Fiber_ycoord( clip ) = [],
```

3.2 Rejection model

Notice that the origin of 2D coordinates in the vertical plane is located at the upper left corner. The trivial change of variables h' = Nz − h, H' = Nz − H
allow us to convert (2a) into

$$h' < \alpha H' + (1 - \alpha)Nz \qquad (2b)$$

for the rejection with probability 1 − p of a deposition trial.

This can be done with code like

```
Fiber_mask = sparse(fiber_xcoord, fiber_ycoord, true ),
zPos = E(fiber_mask),
if rand > acceptanceprob && mean(zPos) < alpha∗mean(E(:)) + (1−alpha)∗Nz
continue
end
```

The space is divided into Nx × Ny × Nz cells or voxels in the form of a square parallelepiped into a regular grid of discrete locations. Each entry of the 2D array E contains the elevations of the paper web surface grid cells and those corresponding to the in-plane location of the trial fiber have been selected into zPos.
Because the && operator short-circuits the evaluation of the logical expression, it saves computation time to test Eq. (2b) in the last place.

3.3 Extracting a vertical slice from the 3D lattice

The array web of dimension Nz-by-Nx-by-Ny is used to store information of the discretized volume elements. Once the (x, y) coordinates of an accepted fiber have been obtained in the column vectors fiber xcoord and fiber ycoord, our task is to extract the corresponding 2D vertical slice in the volume web. The sedimenting fiber bends around structures along this strip. The following is one possible way to do this:

```
firstVPos = 1, lastVPos = Nz,
z extent = firstVPos:lastVPos,
height = length(z extent),
width = length(fiber xcoord),
X = repmat(fiber xcoord, height, 1),
Y = repmat(fiber ycoord, height, 1),
Z = repmat(z extent', 1, width),
strip idx = sub2ind([Nz Nx Ny], Z, X, Y),
strip = web(strip idx),
```

Note that here we select all the vertical extension of web, but it is possible to find a tighter confined layer, which results in considerable savings in computing time.
This will compute the (i, j, k) subscripts of web comprising a particular slice. We then use the function sub2ind to convert to one-dimensional subscripting and this can be used to index onto web.

3.4 Simulation of bending using a cellular automata framework

The spatial discretization allow us to exploit the potential of cellular automata (see the book [10]). A cellular automaton (CA) is a spatial discrete time model.
Each cell can exist in different states chosen from a finite set. At each time step each cell changes its state based on a set of rules or transition functions that represent the allowable physics of the phenomena.
The discrete space for the automaton maps identically onto the vertical plane in which bending takes place represented by the 2D array strip. For each cell (i, j) at time t there are three states which represent the presence or absence of fiber particles, namely:
Moving. Deforming particle covers cell.
Idle. Stopped particle covers cell.
Empty. The cell is unoccupied.

As time goes on, the new state of each cell st+1(i, j) is then updated according to the following rules:

$$s_{t+1}(i,j) = \text{idle} \leftarrow s_t(i,j) = \text{moving} \wedge (s_t(i-F, j-1) = \text{idle} \vee s_t(i+1,j) \neq \text{empty} \vee s_t(i-F, j+1) = \text{idle}) \quad (3)$$

$$\left.\begin{matrix} s_{t+1}(i,j) = \text{empty} \\ s_{t+1}(i+1,j) = \text{moving} \end{matrix}\right\} \leftarrow s_t(i,j) = \text{moving} \wedge \neg (s_t(i-F, j-1) = \text{idle} \vee s_t(i+1,j) \neq \text{empty} \vee s_t(i-F, j+1) = \text{idle}) \quad (4)$$

$$s_{t+1}(i,j) = \text{idle} \leftarrow s_t(i,j) = \text{idle} \quad (5)$$

$$s_{t+1}(i,j) = \text{empty} \leftarrow s_t(i,j) = \text{empty} \wedge (s_t(i-1,j) = \text{empty} \vee s_t(i-1,j) = \text{idle}) \quad (6)$$

where i and j are the row and column indices and the negation of a given statement P is denoted by ¬P.

Via the preceding rules, particles can move only in the downward (increasing time) direction at most one cell at each time step t. We have chosen to update the cell states asynchronously by a line-by-line sweep of each row sequentially, so that we can eliminate a substantial amount of spurious reference to the above rules, for instance in the region “above the fiber”. An example of code that would implement this behavior might look like this:

```
strip = [repmat(EMPTY, height, 1) strip repmat(EMPTY, height, 1)],
stop = false (1, width+2),
run = [ false true(1, width) false ],
j = 2:(width+1),
for i = 1:(height−1)
stop(j ) = strip( i−F, j−1) == IDLE ... % Eq. (1)
| strip ( i+1, j) ˜= EMPTY ...
| strip ( i−F, j+1) == IDLE, % Eq. (1)
strip ( i , run & stop) = IDLE, % CA rule (3)
run = run & ˜stop, % CA rule (5)
if all(˜run), break, end % Fiber bending stops.
% CA rule (4)
strip ( i , run) = EMPTY,
strip ( i+1, run) = MOVING,
end
strip ( end, strip(end, :) == MOVING ) = IDLE,
strip (:, [1 end]) = [],
```

In the first part of this code segment the 2D lattice is augmented by a column vector of fictitious cells having the pre-assigned value EMPTY at the extreme left and right sides, so that the corresponding neighborhood is completed. The loop, for i = 1:(height−1), drives the line-by-line sweep. In each iteration the logical vector run & stop picks out those js where the particles stop to move. We can then compute vector run & ˜stop whose components with value true specify the remaining particles still bending downward. Assignment of this value to the variable run implements implicitly rule (5). On leaving the loop we can return to the original dimensions of the lattice with the assignment strip (:, [1 end]) =[].
Finally, notice that in this case rule (6) is not needed anymore.
Figure 4 shows the sequence of discrete steps in bending a fiber.

3.5 Filling up the remaining layers

Now it is time to start filling up the remaining m−1 cell layers by stacking one on top of the other through each point of the fiber. The fiber was modeled as a concentric assembly with lumen in the middle followed by the cellulosic wall.
We distinguish three types of layers: top, bottom, and lumen. For simplicity we make both the top and bottom ones only one cell high.

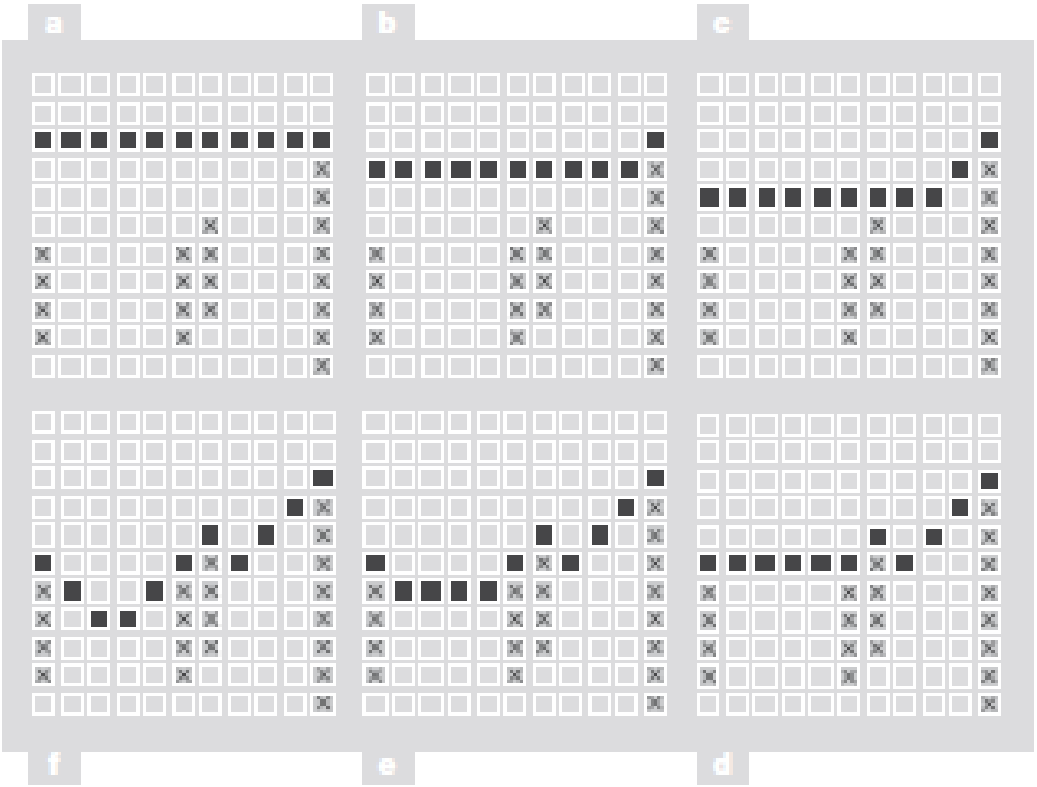

Figure 4. (Clockwise, from top left) The time evolution of a single fiber having flexibility F = 1, from the initial positioning parallel to the substrate until the bending capacity is exhausted. The crosses represent parts of previously deposited fibers with squares denoting the bottom layer of the bending fiber.

After having found the i indices corresponding to the vertical coordinates zj describing the elevation of the bottom layer, all we need is to define those for the other two. Each layer is then tagged with a label. This can be done by

```
zPos = find(strip == IDLE),
bottom_idx = sub2ind([height width], zPos, 1:width),
lumen_idx = bsxfun(@minus, bottom_idx, 1:(m−2)),
top_idx = bottom_idx − (m−1),

strip (bottom_idx) = BOTTOM,
strip (lumen_idx) = LUMEN,
strip (top_idx) = TOP,
```

3.6 Updating the lattice

All we are left is to carry out the updating of the 3D array web as well as matrix E
E(fiber_mask) = zPos − (m−1),
web(strip_idx) = strip ,

3.7 All done

Now we merely have to choose the output format of the simulation
out = struct('web', web, ...
' thickness ' , (Nz+1) − E, ...
'empty', web == EMPTY, ...

'top' , web == TOP, ...
' lumen', web == LUMEN, ...
'bottom', web == BOTTOM),

Figure 5 shows an example of the 3D fiber network constructed with our prototype implementation.

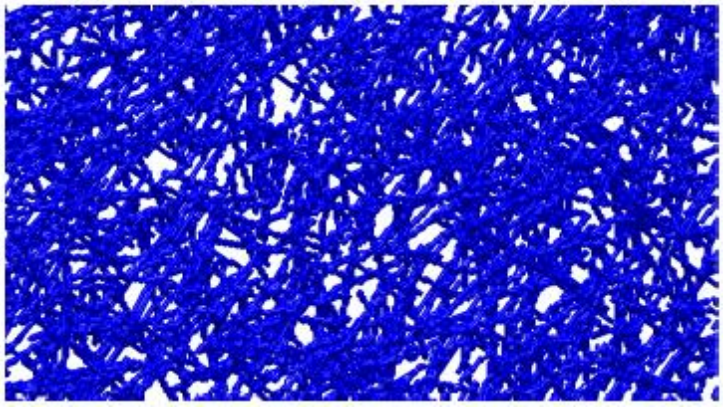

Figure. 5. Simulated 3D fiber network

4 Physical properties of simulated paper

As a voxel-based approach, this has the huge advantage that it allows for easy identification of regions of interest. Furthermore, the basic method for computing many paper properties lies simply on counting the number of appropriate voxels in the appropriate region. Next we present two examples of concrete implementations, one for sheet porosity and one for relative bonded area.

4.1 Porosity

By definition, bulk porosity is the volume fraction not occupied by the fibers within a paper sheet. This is simply obtained by dividing the volume of all the voids by the total volume of the sheet [12, pp. 279 and 280]. The code for the function can be written:

```
function val = porosity(x)
void_space_above_surface = sum(sum( size(x.web, 1) − x.thickness )),
pores_volume = sum(x.empty(:)) – void_space_above_surface,
total_volume = numel(x.web) – void_space_above_surface,
val = pores_volume/total_volume,
```

Note that x.empty is a 3D array with logical 1s when the corresponding position in x.web is not occupied, and their sum is the total number of empty voxels.
To get the correct volume of pores, we have to subtract the contribution of the empty voxels above the sheet surface. The same correction has to be applied to calculate the real number of voxels in the whole paper sheet.
It is curious to note that this is the same as counting the number of blackwhite pixels in binarized images obtained from X-ray microtomography, as done by [4]. For a recent overview of image analysis methods for studying the internal porous structure of paper, see [3].

4.2 Relative Bonded Area

The relative bonded area (RBA) is the fraction of fiber surface in contact with other fibers. Basically, the implementation means to count the number of fiber fiber contacts:

```
function val = rba(x)
[m, n, p] = size(x.top),

% Insure that fibers at the upper and lower sides of the paper sheet
% are not found to be adjacent.
top = cat( 1, x.top, false (1, n, p) ),
bot = cat( 1, x.bottom, false (1, n, p) ),

% Count each pair of adjacent top and bottom layer cells.
Num_cell_contact_area = sum( bot(:) & circshift(top (:), −1) ),

% Calculate RBA.
Num_cell_total_area = sum(top(:)),
val = num_cell_contact_area/num cell total area,
```

Similarly to x.empty, x.top and x.bottom are 3D arrays with logical 1s in the elements belonging, respectively, to the top or bottom layer of a fiber. The basic idea is based on the observation that if we can reach a “bottom” voxel from a “top” one by walking up one position at the same in-plane location, these two are adjacent. To do this, vector top(:) is circularly shifted upwards by one position.

Only those locations in the compound expression bot(:) & circshift (top (:), −1) that evaluate to true indicate fiber-fiber contact points. The resulting logical 1s are summed to obtain the desired number of voxels at the total contact surface.

However, in addition we have to prevent that the top layer of a fiber located at the top face of the sheet is falsely found to be connected to the bottom layer of another fiber at the bottom side. This is accomplished by adding an extra level of falses on top of both x.top and x.bottom.

The procedure just described is akin to the direct determination of RBA using image analysis of sheet cross sections (see [11, pp. 884 and 885] and references therein).

5 Conclusion

We believe that this article will provides a basis for the understanding of a number of practical issues that arise in the implementation of a 3D fiber deposition model. In particular, the CA approach is an attractive paradigm by allowing the high-level bending behavior to emerge as a result of rules fairly straightforward to implement. Not to be overlooked is the simplicity gained in computing physical properties by using a voxel based approach.

References

[1] Agoston, M.K.: Computer Graphics and Geometric Modeling: Implementation and Algorithms. Springer, London (2005).

[2] Alava, M., Niskanen, K.: The physics of paper. Reports on Progress in Physics 69(3), 669–723 (2006).

[3] Axelsson, M., Svensson, S.: 3D pore structure characterization of paper. Pattern Analysis & Applications (2009).

[4] Goel, A., Tzanakakis, M., Huang, S., Ramaswamy, S., Choi, D., Ramarao, B.V.: Characterization of the three-dimensional structure of paper using X-ray microtomography. TAPPI Journal 84(5), 72–80 (2001).

[5] Nilsen, N., Zabihian, M., Niskanen, K.: KCL-PAKKA: a tool for simulating paper properties. TAPPI Journal 81(5), 163–165 (1998).

[6] Niskanen, K.J., Alava, M.J.: Planar random networks with flexible fibers. Physical Review Letters 73(25), 3475–3478 (1994).

[7] Provatas, N., Haataja, M., Asikainen, J., Majaniemi, S., Alava, M., Ala-Nissila, T.: Fiber deposition models in two and three spatial dimensions. Colloids and Surfaces A: Physicochemical and Engineering Aspects 165(1-3), 209–229 (2000).

[8] Provatas, N., Uesaka, T.: Modeling paper structure and paperpress interactions. Journal of Pulp and Paper Science 29(10), 332–340 (2003).

[9] Roberts, J.C.: The Chemistry of Paper. Royal Society of Chemistry, Cambridge (1996).

[10] Schiff, J.L.: Cellular Automata: A Discrete View of the World. Wiley, New Jersey (2008).

[11] Uesaka, T., Retulainen, E., Paavilainen, L., Mark, R.E., Keller, D.S.: Determination of Fiber-Fiber Bond Properties, 2nd edn. Handbook of Physical Testing of Paper, vol. 1. Marcel Dekker, New York (2001).

[12] Yamauchi, T., Murakami, K.: Porosity and Gas Permeability, 2nd ed. Handbook of Physical Testing of Paper, vol. 2. Marcel Dekker, New York (2001).

Parallelization of a Parameter Estimation Problem in a 3D Model of Paper

Conceição, E. L.T.[1], Curto, J.M.R.[2], Simões, R.M.S.[2] and Portugal, A.T.G.[1]
[1] Research Centre for Chemical Processes Engineering and Forest Products,
Chemical Engineering Department, University of Coimbra (UC)
[2]Textile and Paper Materials Research Unit,
Chemistry Department, University of Beira Interior (UBI)

Abstract

The freely available library pMatlab is one of several tools for parallel computing with the MATLAB language. We present the rationale behind our choice of parallelization approach for a nonlinear parameter estimation problem within a 3D simulation model of paper structure. Also, we describe the key features of the computational implementation using this tool.

Keywords: Parallel MATLAB, nonlinear regression, paper, simulation

1 Introduction

The formation of a paper sheet involves the drainage of a suspension of cellulose fibers in water. This leads to a 3D network structure in which millions of fibers are stacked roughly horizontally on top of each other, agglomerated in a random fashion. Clearly, the role of simulation in the understanding of such complex systems would be very useful. Unfortunately, a major obstacle in the practical exploitation of simulation techniques for modeling paper structure is, without doubt, the lack of easily accessible implementations. Motivated by this, we have been developing from scratch a MATLAB program using the framework of cellular automata. Currently, we are able to generate 3D paper webs (the forming stage) by a stochastic fiber deposition process similar to that used by the KCL-PAKKA model [1].
Some of the model parameters, such as those of the hydrodynamic smoothing, should be estimated by nonlinear regression of experimental data. This is a daunting task given the big execution time of just one simulation. Thus, it is quite natural to explore the parallelism available within the parameter estimation process.

It is of primary importance to ease the parallelization task to be able to use high-level abstractions, follow a well defined development process, and remain close to the original sequential code. The pMatlab library [2] addresses all of the above requirements.
This article serves to highlight the use of pMatlab with the parallelization of a based on computationally expensive simulations. We assume a general familiarity with the MATLAB language.
In the next section we provide a succinct overview for the sedimentation-like process of forming a paper web. Section 3 is the core of the paper, explaining the implementation of the parallel approach, and the paper concludes with a summary in Section 4.

2 Some details on the simulated handsheet formation

A paper web is grown by successively laying down *straight* fibers, one after another, onto a flat substrate. Each one is positioned and oriented at random in the in-plane (x and y) directions and placed parallel to the substrate on top of the underlying network.
Since the fibers are flexible they undergo bending in the thickness (z) direction. For this reason, the straight shape is subsequently conformed to the surface topology of the previously deposited fibers located just below. Pores arise from the voids formed because fiber stiffness may prevent a perfect contact everywhere along the web surface. Notice, however filtration leads to a more homogeneous microstructure than that obtained in a random deposition model due to a smoothing effect (see Figure 1). This mechanism is simulated by the particle deposition rule of [3]: a candidate fiber lands on a section of the web whose mean height is compared with a fraction of its counterpart of the entire paper sheet. If the following condition is fulfilled, the attempt is always accepted:

$$h \leq \alpha H,$$

where h is the average thickness of the paper over the projected area of the trial fiber, $0 \leq \alpha \leq 1$ is a constant, and H is the average thickness of the entire paper. Otherwise, the attempt is accepted only with probability p, called the acceptance probability.

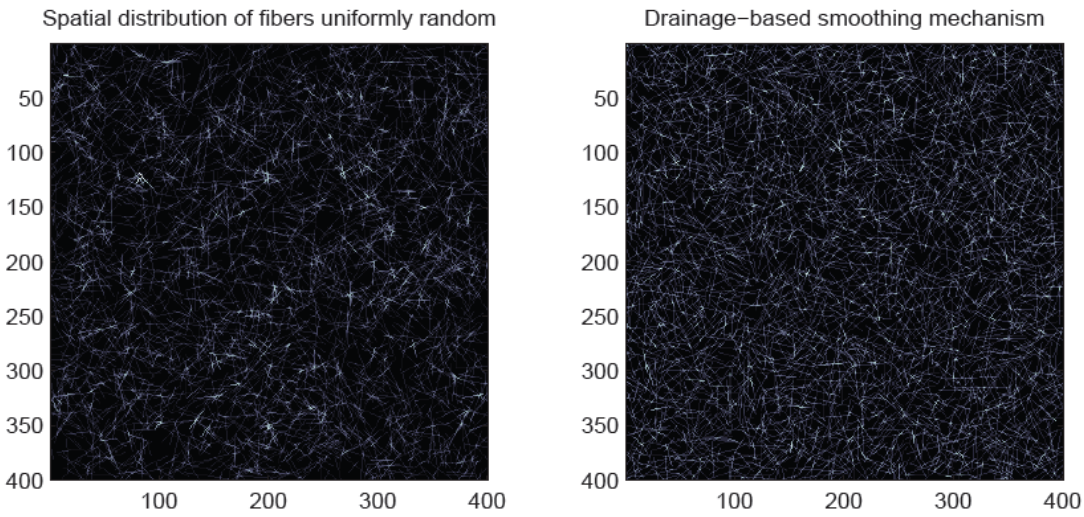

Figure 1. Simulated X-ray-like image of the (x; y) plane for a paper handsheet as generated from the deposition rule, with formation control parameters set to ρ=1, α=1(left) and ρ=0:01, α=0:94(right)

In overview, our growth process of a 3D fiber network consists of the following basic steps (see Figure 2).

1. Generation of a fiber in the in-plane directions.
2. Testing the rule for particle deposition. If the fiber is not accepted, the generation trial is repeated.
3. Extraction of the out-of-plane slice from the 3D network.
4. Fiber bending simulation using a cellular automaton approach.
5. Updating by reinsertion of the modified slice into de 3D network.

3 Parallel Design

3.1 “Pleasingly parallel" data fitting

Recall that regression minimizes an error criterion between experimental data and the computed model response. Here we take α and p as free parameters that are adjusted to fit porosity data. Given the nature of the simulation model, the Differential Evolution (DE) stochastic global search heuristic [4] which uses only function values and does not require derivatives is an appealing choice for that purpose.

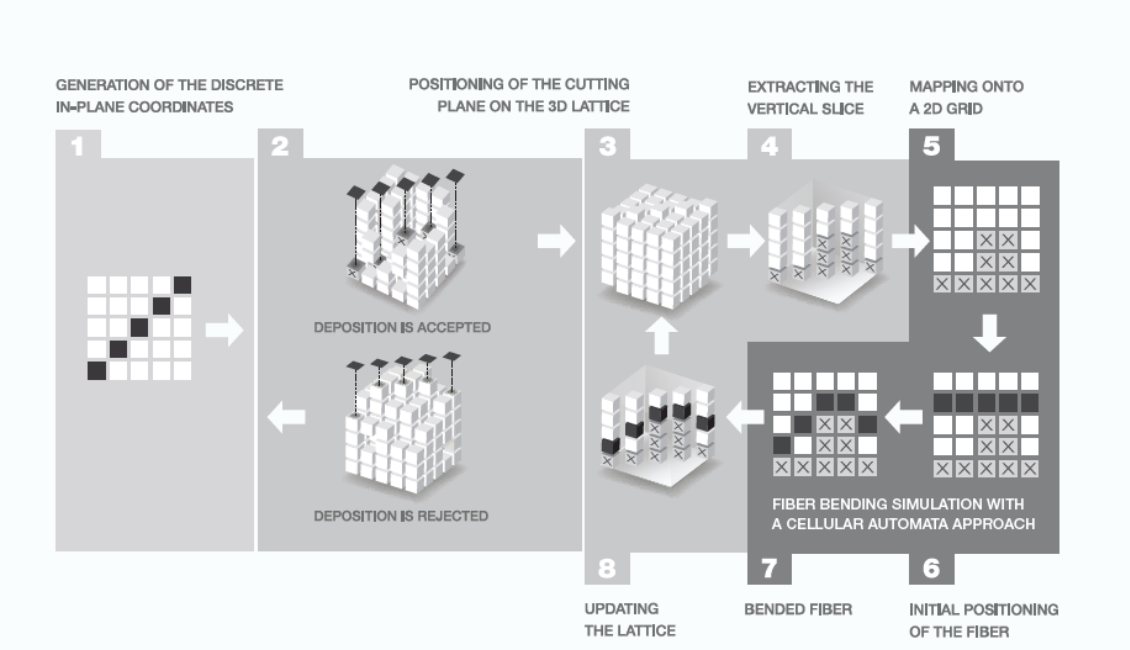

Figure 2. Data flow diagram that illustrates the core of the sequence of computations for the fiber deposition model.

The fiber deposition algorithm is inherently sequential, and hence difficult to parallelize. On the other hand, DE is a population based method. This means that at any one stage DE operates on a set, P_G, of candidate solutions, θ, not just a single solution, namely

$$P_G = \{\boldsymbol{\theta}_{1,G}, \ldots, \boldsymbol{\theta}_{2,G}, \ldots, \boldsymbol{\theta}_{i,G}, \ldots, \boldsymbol{\theta}_{N_{\mathrm{pop}},G}\},$$

where N_{pop} denotes the number of population vectors which remains constant during the optimization process, and G is the generation (iteration) to which the population belongs. After initialization, P_G=0 is subjected to certain evolutionary operators and evolves through several generations.

Consequently, parallelism occurs naturally when the objective function is evaluated over all individuals in the current population. In addition, the evaluation of the objective function also lends itself to parallelization because it is composed of several independent simulations of paper sheets for different experimental runs. Clearly this falls in the category of “embarrassingly parallel" problems.

It follows from the above reasoning that the essence of this parallel computing is running the calculation

$$\mathrm{porosity}(\ \mathrm{forming}(\mathrm{alpha(j)},\ \mathrm{p(j)},\ \mathrm{argA(i)},\ \mathrm{argB(i)},\ \mathrm{argC(i)})\ );$$

Repeatedly over and over again for each experimental point i=1,…,N_{obs} and candidate solution

$$\boldsymbol{\theta}_{j,G} = [\alpha_j, p_j]^T_G, \quad j = 1, \ldots, N_{\mathrm{pop}},$$

which, as stressed before, can be computed independently of each other. Here N_{obs} is the number of experimental runs and argX denotes a vector of input arguments corresponding to the different experimental conditions.

3.2 Implementation specifics

Fragmented distributed arrays is the core parallel programming model of the pMatlab library, which uses a MATLAB implementation (MatlabMPI) [5] of the Message Passing Interface (MPI) protocol to perform communication between processors. Specially, an array is distributed among N_p compute cores with the computations performed on just the local part of the array. When needed, locally computed results can update the global structure. It is thus necessary to map the elements of a distributed array onto a set of cores/processors. This mapping describes the arrays' indices that each processor "owns". Based on these ideas, it is natural to split the elements of a N_{obs} X N_{pop} matrix of objective function values X along both dimensions evenly among the available processors. This is called a *block distribution*. Consider, for illustration, the case N_{obs} = N_{pop} = 6 and N_p = 4. A visual representation of this mapping is shown in Figure 3. The function map() creates the parallel map Xmap

```
m = min(sqrt(Np), Nobs);
n = Np/m;
Xmap = map([m n], {}, 0:Np−1);
```

whereas the overloaded zeros() function uses this map to create the corresponding distributed array

```
X = zeros(Nobs, Npop, Xmap);
```

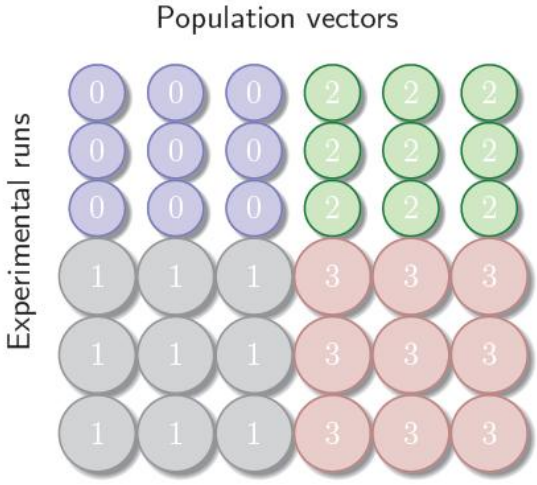

Figure 3. (Block distribution) A map for assigning array indices to processors. The processors are labeled 0 through 3. The big circles represent a greater execution time.

Ideally, the time spent on each processor should be approximately the same, since the total time for the whole computation will be determined by that one which takes longer to complete its subtask. In other words, the work should be distributed evenly across the different processors so that no processor sits idle during the calculation. Since the execution time depends both on the data and on the value of parameters and p, any potential correlation between the sequence position in each dimension and these times will result in a load imbalance. This occurs naturally for any dataset with some kind of structure (row-wise)

as depicted in Figure 3. On the other hand, it is unlikely to occur column-wise due to the stochastic nature of the DE algorithm. A cyclic distribution along rows breaks up the correlations

```
m = min(sqrt(Np), Nobs);
n = Np/m;
dist(1).dist = 'c'; dist(2).dist = 'b';
Xmap = map([m n], dist, 0:Np-1);
```

as illustrated in figure 4.

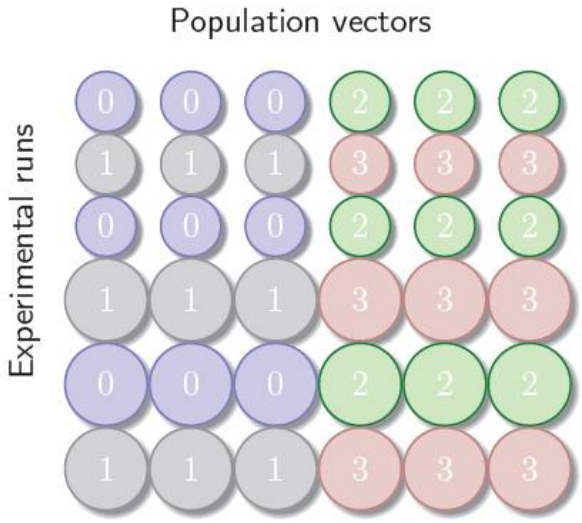

Figure 4. Cyclic rows. The processors are labeled 0 through 3. The big circles represent a greater execution time.

Next, for each processor we get the local part of X as a regular MATLAB array Xloc = local(X), and retrieve the indices I and J of the distributed array X corresponding to its local part, that is, the indices that a particular processor “owns"

I = global_ind(X, 1), J = global_ind(X, 2),

For example, for processor 3 in Figure 4 I = {2, 4, 6} g and J = {3, 4, 5}.
Now each processor will compute the simulated porosity. The local indices (I, J) are used to select the appropriate inputs for computing the results.

```
for i = 1:length(I)
    ii = I(i);
    for j = 1:length(J)
        jj = J(j);
        Xloc(i, j) = porosity( forming(alpha(jj), p(jj), ...
                                       argA(ii), argB(ii), argC(ii)) );
    end
end
```

The local results are passed back to the distributed array X using the function put_local()
X = put_local(X, Xloc),

Finally, the entire contents of X is copied to a regular MATLAB array across all the processors using agg_all

Xagg = agg_all (X);

Having this synchronization point forces all processors to reach this point before they can proceed from the current generation to the next one.

4 Conclusions

In this paper we have presented the following:

- a general and very brief overview of a 3D fiber deposition model for simulation of the structure of paper,
- an embarrassingly parallel approach to estimate unknown parameters of this model,
- some specific features of a software implementation using the pMatlab library.

References

[1] K.J. Niskanen and M.J. Alava. Planar random networks with flexible fibers. Physical Review Letters, Vol. 73, pp. 3475-3478, (1994).

[2] J. Kepner, Parallel MATLAB for Multicore and Multinode Computers, SIAM, Philadelphia, (2009).

[3] N. Provatas and T. Uesaka. Modeling paper structure and paperpress interactions. Journal of Pulp and Paper Science, Vol. 29, pp. 332{340, (2003).

[4] R. Storn and K.V. Price. Differential evolution | a simple and efficient heuristic for global optimization over continuous spaces. Journal of Global Optimization, Vol. 11, pp. 341{359, (1997).

[5] J. Kepner and S. Ahalt. MatlabMPI, Journal of Parallel and Distributed Computing, Vol. 64, pp. 997{1005, (2004).

Three Dimensional (3D) Polyamide-6 Nanowebs Modeling and Simulation

Curto, J.M.R. [1], Hekmati, R.A.H. [2], J. Y. Drean, J.Y. [2], Conceição, E. L.T.[3], Portugal, A.T.G.[3], Simões, R.M.S.[1] and Santos Silva, M.J.[1]

[1] Textile and Paper Materials Research Unit, Chemistry and Textile Departments, University of Beira Interior (UBI), Covilhã, Portugal

[2] Laboratoire de Physique et Mécanique Textiles, École Nationale Supérieure d'Ingénieurs Sud Alsace (ENSISA), Mulhouse, France

[3]Research Centre for Chemical Processes Engineering and Forest Products, Chemical Engineering Department, University of Coimbra (UC), Coimbra, Portugal

Abstract

The importance of modeling and computational simulation to study materials in the nanoscale, where experimental determinations are difficult, is widely recognized. Here, we present the key aspects of a three dimensional (3D) nanoweb model and of its computational implementation to study a Polyamide-6 electrospun network.

The model includes key nanofibers properties like fiber morphology as inputs, as well as the physical mechanisms of fiber bending. With this a fiber model is build and a network is formed respecting the fiber and the physical constrains from the structure that is growing. After the web formation the model returns web structural properties such as coverage, thickness, porosity and relative bonded area (RBA).

A web simulator was developed, from scratch, using the MATLAB platform. Basically, the 3D web structure is formed by the sequential deposition of fibers. The model includes fiber interactions as well as a novel nanofiber model, for the representation of infinite length fibers like the ones obtained by electrospun. The implementation presents several original contributions, namely full discretization of space in both the in-plane and out-of-plane directions, and an approach using cellular automata to drive fiber bending. This framework allows an easy extraction of determinant web structural properties from the simulation output.

The fiber morphological characterization of the obtained nanowebs is performed, using scanning electron microscope (SEM). The information about the range of fiber morphology

dimensions coming from experimental data was used as an input in the computational plan of simulations. A Latin hypercube computer experiments design was implemented for 1000 simulations and the resulting networks structures were organized using regressions trees. Comparing in a qualitative way, the simulation results with the nanowebs, we found that the model is able to reproduce the nanowebs structures.
Moreover, simulations indicate that nanofibers morphology and network formation have a determinant effect on the resulting nanowebs structure and this can be studied using the developed simulator

Keywords: modeling, three dimensional (3D) structure, nanowebs, nanofibers, Polyamide-6.

Introduction

There has been an increasing interest in the use of electrospun fibrous networks for applications such as scaffolds in tissue engineering, filters, protective clothing, reinforcement in composite materials and sensors [1]. The basic principle of electrospinning is that a volume of polymeric solution, in contact with a large electric potential, delivered to a needle tip is deformed and can be ejected towards an earthed or charged target [2].
The materials produced by this process consist on fibrous networks, with typical fiber diameters in the range 10nm-10μm [3]. Circular cross sections are typically produced, although under certain conditions, other geometries such as tube and collapsed ribbon like structures have been reported [4].
There is a lack of information about nanowebs modeling and simulation. We propose a 3D model and simulator, developed with the necessary modifications to nanowebs materials, and its application to a simulation study of Polyamide-6 nanofibrous network

Modeling of Nanofibrous Network Materials

The first approach for modeling disordered fibrous materials was done by Kallmes and Corte [5]: a two dimensional approach, for a very thin material, a material like paper but with only one layer. The fiber network was formed considering that the location of any given fiber is independent and each fiber has equal probability of making all possible angles with any arbitrarily chosen axis. This can be the first approach for materials such as paper, non-woven textiles and fibrous filters, materials where fibers have finite length.

For electrospun networks, fibers can be assumed to have infinite length [6]. Such networks can be modeled as a random network of infinite lines that represent the longitudinal axes of fibers and pass through points distributed according to a point Poisson process, in the plane

[7]. This was proposed, in a two dimensional approach, with uniformly distributed orientation [7]. This modification, that captures the physics of electrospun nanofibers, was implemented in our model. But our approach was to develop a 3D model, to better describe what happens in the Z direction.

The Importance of 3D for Network Modeling

Researchers like Sampson and Dodson have considered an idealized two dimensional random network when modeling network structure [8-9]. In 1998 Wang and Shaler [10] proposed a structure made from rigid cylindrical fibers. The major breakthrough came with the introduction of the fiber flexibility in the work of Niskanen, Alava and coworkers [11-13]. This model is called KCL-PAKKA and was developed for paper. We incorporate this 3D approach, where fibers are flexible and bend in Z direction, but with an original computational implementation.

Our Network Materials Model

Our network materials model was originally developed to study an important network material: paper. For this material, several novelties have been successfully implemented. Since our nanofibrous material model can be considered as a modification of our paper network model we revise some aspects that are important for both models.

In this network model, the fiber model is built departing from fiber dimensions and flexibility. Then, fiber after fiber, a three dimensional structure is formed and various network properties are predicted. The simulations obtained are consistent with experimental data as presented by Curto *et al*. [14]. The 3D paper model is presented in more detail in a previous publication [15].

Two important modifications to the original KCL-PAKKA model are introduced in our model. First, the possibility to model the real paper structural anisotropy, this is, the deviation from purely random distribution of fibers. With this, fiber interactions like the ones that occur in flock formation can be simulated. The flock formation formation control parameter is implemented based on the sedimentation rule presented by Provatas and Uesaka in 2003 [16,17]. Secondly, the fiber model representation of hallow fibers is introduced for the first time, being determinant to capture what happens when fibers collapse.

Fibers are modeled according to their dimensions, flexibility, and collapsibility. The input parameters indicate with detail the fiber morphology, this includes, length, width, wall thickness, and lumen thickness. And also the fiber bending behavior, with several possibilities for flexibility, and the level of resolution, this is, how far in discretization the model goes,

done by the number of layers in the thickness direction. Note that dimension values can be introduced as averages or distributions.

In this model, the computational fiber flexibility is based on the Niskanen approach [11] but has a novel implementation using cellular automata (see Figure 1) [15]. The space is discretized into a Cartesian uniform grid of cells so that each fiber in the model is represented by a sequence of cells. A "bending" flexibility or dimensionless computational flexibility gives the largest allowed vertical deflection for the fiber [11]. This means that any two nearest neighboring cells on the fiber can make at most the maximum fiber flexibility.

Both fiber wall thickness and fiber lumen can be changed independently, which allows the implementation of different degrees of fiber collapse.

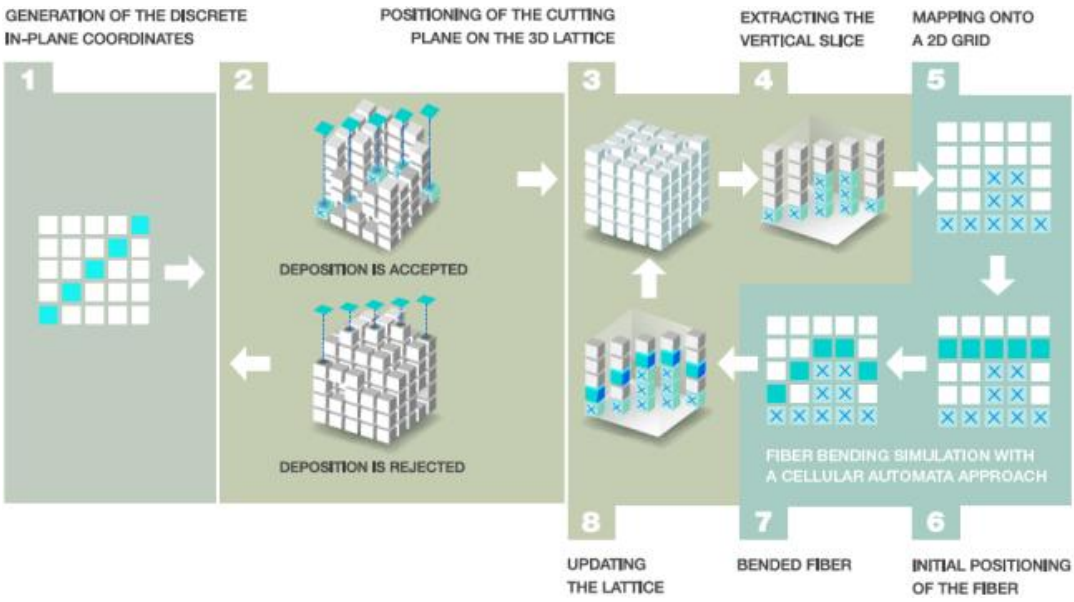

Figure 1. Fiber deposition in the 3D matrix followed by plane extraction and fiber bending to conform to underling structure

The computational simulation can be described as follows (see also Figure 1):

1. Generation of a fiber in the in-plane direction.
2. Testing particle deposition rule. If the fiber is not accepted, the generation trial is repeated.
3. Extraction of the out-of-plane slice from the 3D network where the bending procedure occurs.
4. Fiber deposition according to fiber flexibility and conformation to the underlying surface.
5. Updating of the 3D network.

The web materials model was developed and implemented using MATLAB from MathWorks, a numeric computation environment and programming language.

This numerical simulation model is used to study the structure of nanowebs. The new model is detailed up to the point to include fiber morphology and the behavior in the z-direction. The design of computer experiments was done using a space filling design, namely the Latin hypercube sampling design [18, 19].

Several inputs are changed and the results are treated using decision trees. Decision trees are an exploratory tool for the analysis of large quantities of data because of their unique properties, namely its straightforward interpretation enhanced by a self explanatory graphical representation [20, 21]. Here they are used to organize the simulations, obtained for a range of inputs like fiber properties, and detect, for each final structural property, the most important inputs.

Results and Discussion

Figure 2 is a SEM photography of a Polyamde-6 electrospun web obtained at "Laboratoire de Physique et Mécanique Textiles", in ENSISA, for this work. The range of nanofiber dimensions was obtained from the analysis of SEM photographs.

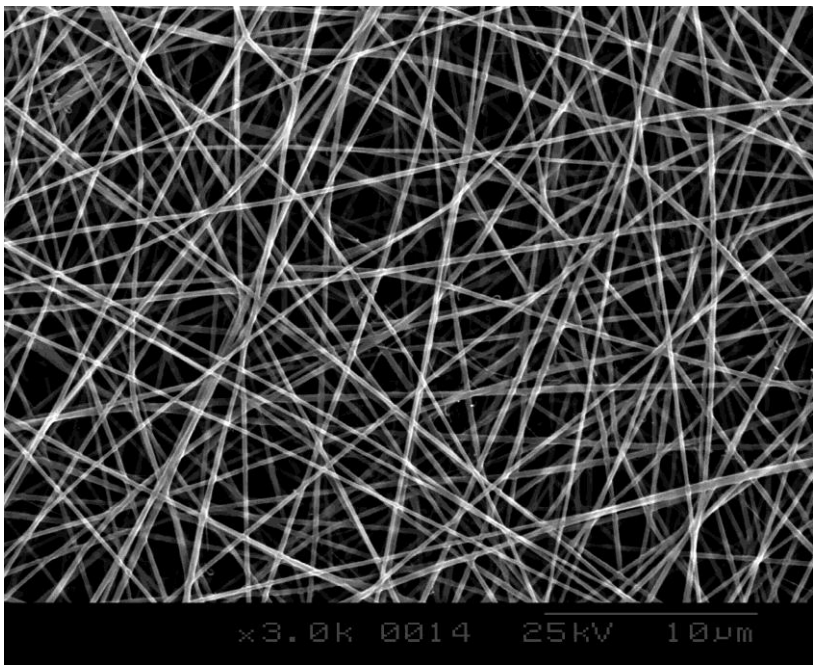

Figure 2. Polyamde-6 nanowebs SEM photography

A simulation study was planned determine the influence of the input values on the final nwnoweb properties. We have defined a realist input range based on experimental data and a preliminary simulation studies. Several factors were considered: fiber dimension; fiber flexibility; lattice dimensions; and a formation control parameter (the accepatance probability parameter). The design of computer experiments was done using a space filling design, namely the Latin hypercube sampling design [18, 19], and the simulations results

were organized and interpreted using regression trees. The design of simulation experiments was implemented for 1000 simulations. The input variables range and limits, as well as the obtained simulation results, are available for consultation.

The simulation results data for thickness, relative bonded area, and porosity were classified using decision trees (see figures 3, 4 and 5).

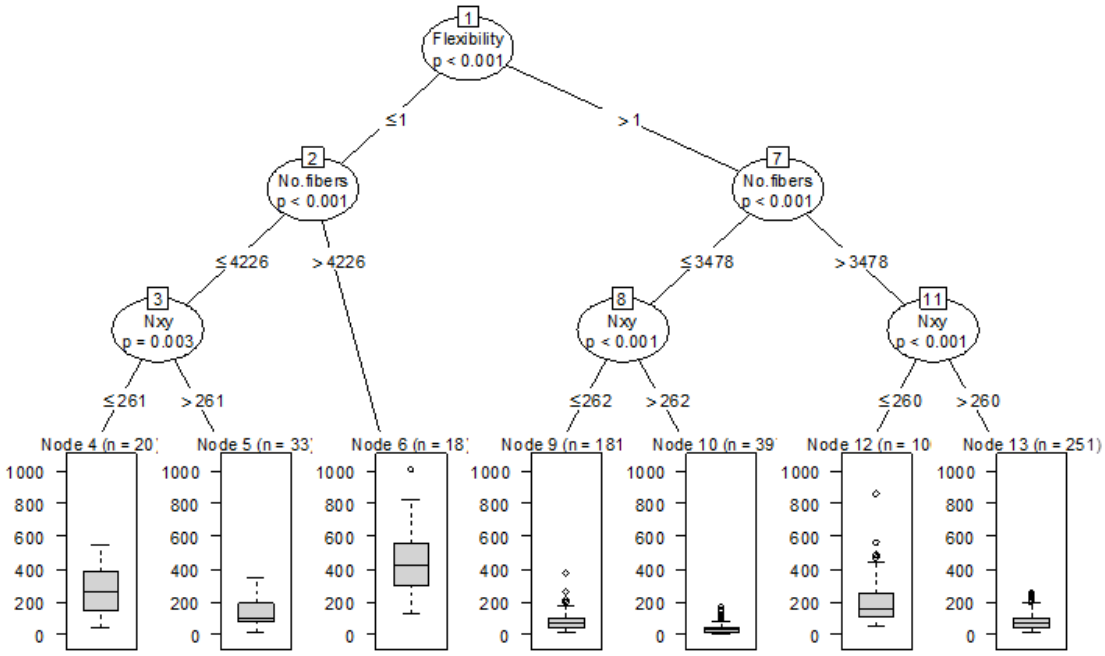

Figure 3. Decision tree for nanowebs thickness. Number of simulations = 1000.

For all the regression trees presented here, namely web thickness, porosity, and relative bonded area (RBA), the first split occurs at fiber flexibility, indicating the important role that this fiber properties has in defining final web structural properties.

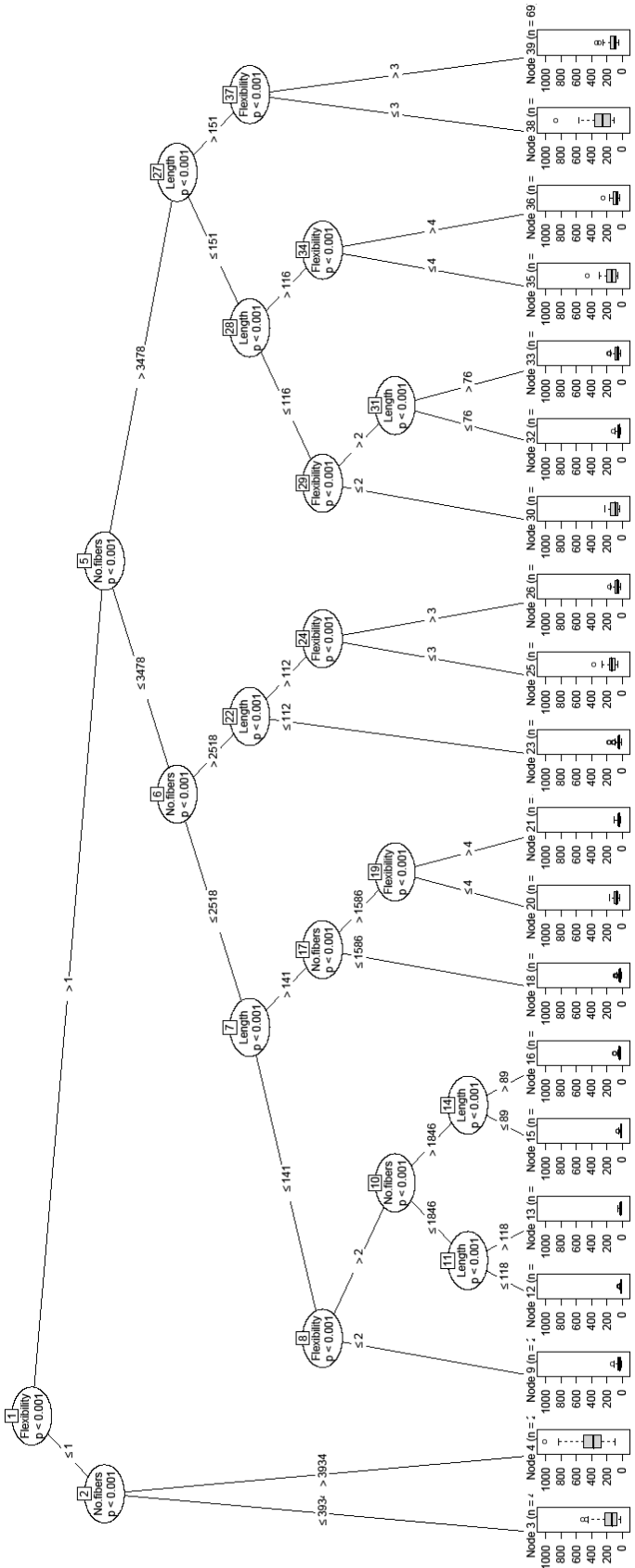

Figure 4. Decision tree for nanowebs RBA. Number of simulations = 1000.

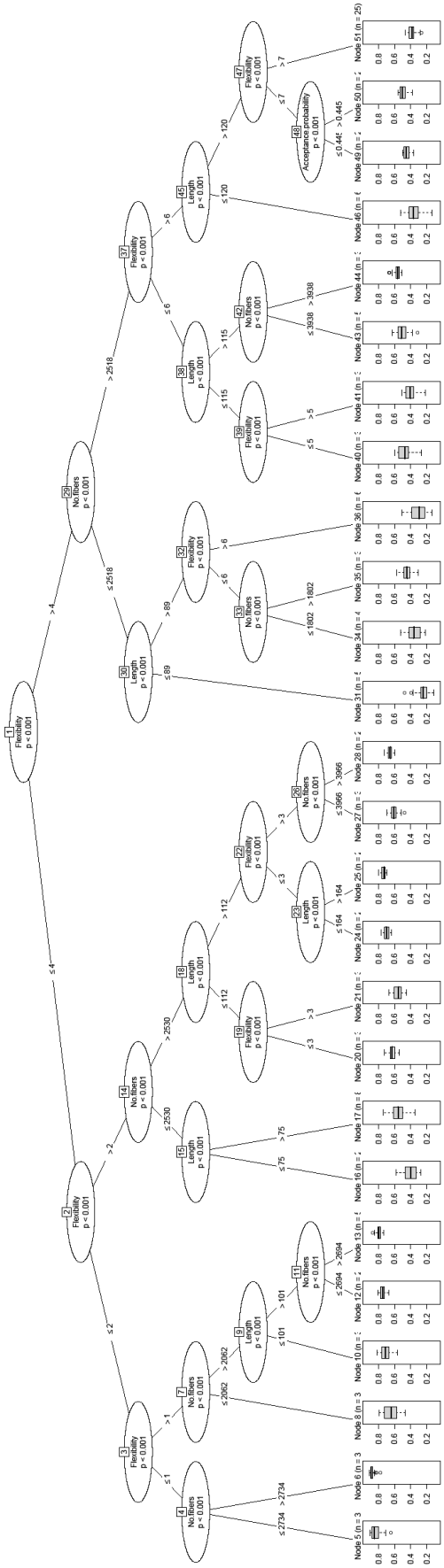

Figure 5. Decision tree for nanowebs porosity. Number of simulations = 1000.

The central idea behind building a decision tree consists of a binary split of the data made according to the value of the single most appropriate predicting variable, so that the observations on each of the two resulting subsets are as similar as possible regarding the response variable of interest. Starting from the root node containing the entire original data, a test is constructed to divide up the data into two mutually exclusive groups, said to be the children nodes, of that parent node. The observations that meet the condition follow the left branch while those that do not go to the right branch. Next, each child node is split in turn and this procedure is repeated downwards in a recursive manner until some termination condition is satisfied. A terminal node which is not subdivided any further is called a leaf node. Note that a multiway split into more than two groups can only be done using the same variable with a different breakpoint at the next level down.

The simulation results were organized using decision trees, provided by the function ctree, in the R package party, using the default settings. The number of simulations chosen was 1000. A range for the input parameters was defined based no experimental SEM information and a preliminary simulation study. Several web properties were accessed: thickness, porosity, relative bonded area, and coverage. To organize the output data we used decision trees and a multivariable graphical representation. Some trends can be identified. For example it is evident that the influence of fiber flexibility overcame the influence of fiber dimensions. Information can be obtained about the influence of other input parameters such as the acceptance probability. This is a formation parameter that is included in the flocculation model, first proposed by Provatas and Useaka in 2003 [16, 17]. The visual representation of the 1000 simulation using multivariable graphics helps to organize the information and the use of regression tree establishes a visual model which contains valuable information about the influence of the different inputs, for each web property.

The simulation results were represented to study the variation of several structural properties (Figures 6, 7, 8 and 9). Using the 3D web model it was possible to separate the influence of different fiber properties, like fiber dimensions and fiber flexibility on the structural web properties.
The SEM photographs of experimental nanowebs samples were compared visually with web simulation structures and the same configurations were observed. Properties, like porosity and relative bonded area (RBA) that are difficult to obtain experimentally, especially at the nanoscale, were accessed.

Figure 6 show that fiber flexibility has a drastic impact on the Relative Bonded Area that represents the contact between fibers, while fiber length and an acceptance probability have practically no impact.

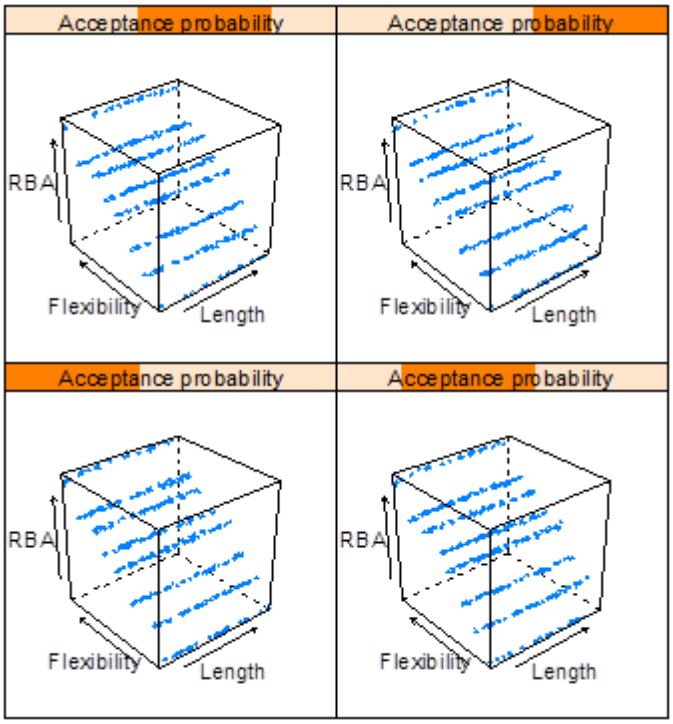

Figure 6. Evolution of RBA (Relative Bonded Area) with fiber flexibility, dimension and formation acceptance probability.

The nanofiber flexibility also influences positively the coverage (see Figure 7), in accordance with its influence on relative bonded area (RBA). However, some interaction between nanofiber flexibility and nanofiber length seems to occur, which deserves further analysis.

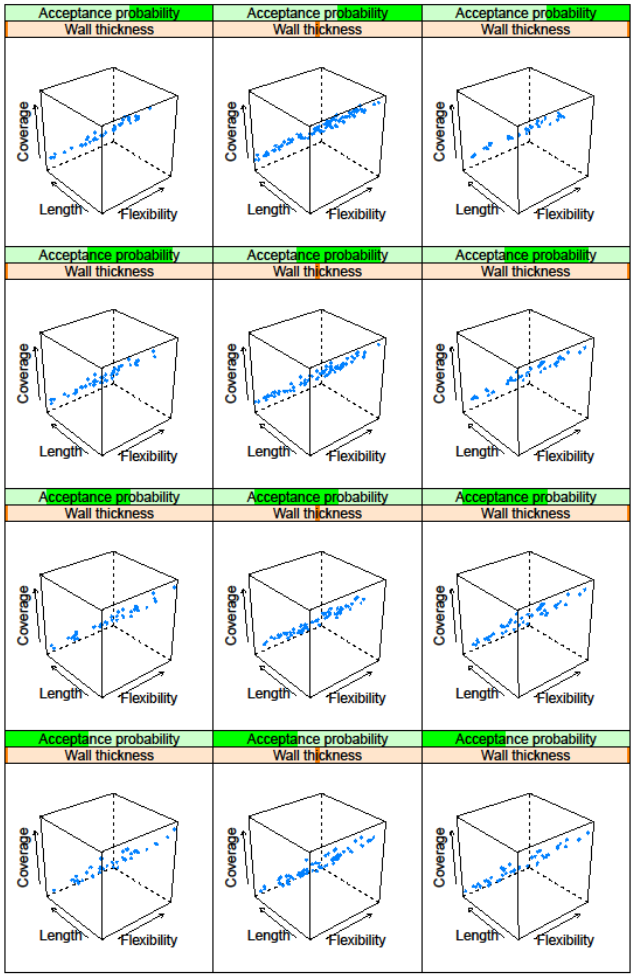

Figure 7. Evolution of coverage with fiber flexibility, dimension and formation acceptance probability.

Figure 8 shows that the nanoweb porosity decreases markedly with increase in nanofiber flexibility and exhibits low sensitivity to length and acceptance probability.

Regarding to nanoweb thickness, higher nanofiber flexibility induces lower apparent thickness, as expected, while increase in nanofiber length can induce lower nanoweb thickness (see Figure 9). Moreover, these trends exhibit some sensitivity to nanofiber wall thickness and acceptance probability.

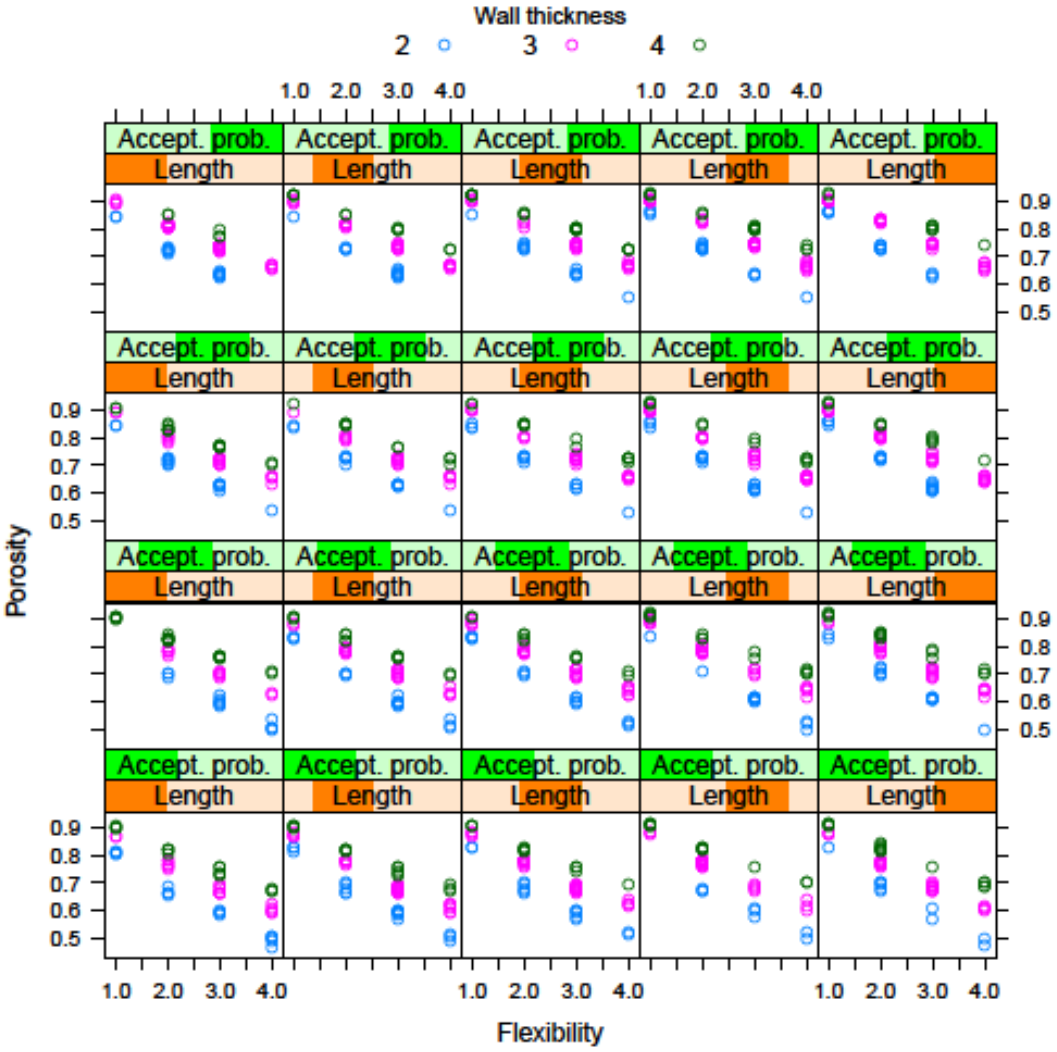

Figure 8. Evolution of porosity with fiber flexibility, dimension and formation acceptance probability.

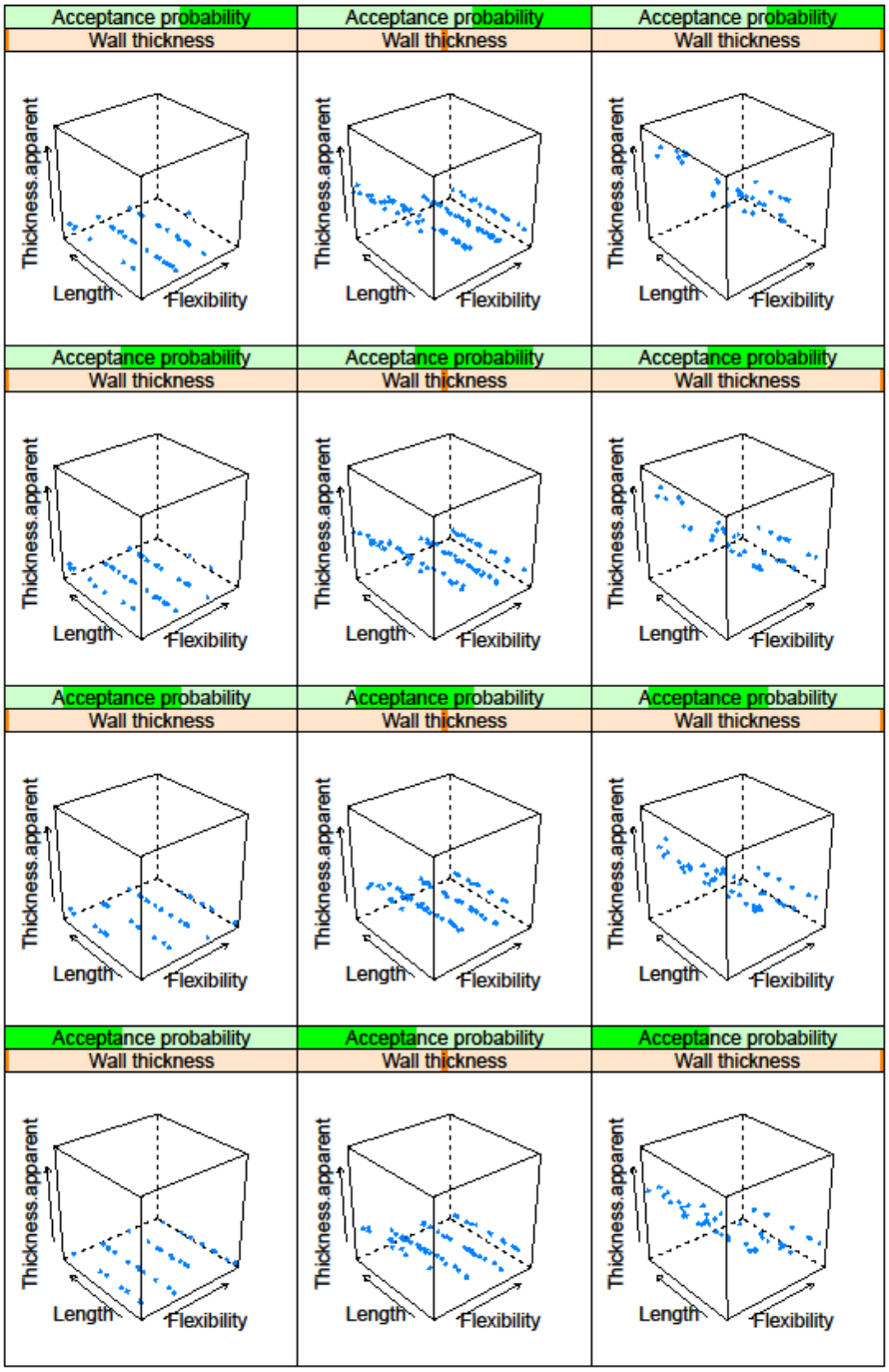

Figure 9. Evolution of thickness with fiber flexibility, dimension and formation acceptance probability

These interesting results deserve further analysis and exploration, namely in terms of structure optimization regarding final end uses.

Conclusions

This is a simulation study were experimental data was used to define a realistic input range. The information about the range of fiber morphology dimensions coming from experimental data was used as an input in the computational plan of simulations. A Latin hypercube computer experiments design was implemented for 1000 simulations, and the resulting networks structures were classified using regression trees and presented with multifactor graphical representation. It was possible to separate the influence of fiber flexibility and fiber dimensions on web structure, using regression trees.

Analyzing the regression trees results we conclude that fiber flexibility have a determinant influence on final web structural properties: fiber flexibility appears at the first split in all de decision trees.

Furthermore, simulations indicate that nanofibers morphology and network formation have a determinant effect on the resulting nanowebs structure and this can be studied using the developed simulator. In a scale where measurements are still challenging, simulations studies can be determinant to improve and optimize material properties.

References

[1] Jayaraman, K. *et al.*, Recent advances in polymer nanofibers, J. Nanosci. Nanotechol. 4, 2004, pp. 52-65.

[2] Rutledge, G.C. and Fridrikh, S.V, Formation of fibers by electrospinning, Adv. Drug Del. Rev., 59, 2007, pp. 1384-1391.

[3] Fridrikh, S.V. *et al.*, Controlling the fiber diameter during electrospinning, Phys. Rev. Lett., 90, 2003, pp. 1-4.

[4] Koombhongse, S. *et al.*, "Flat polymer ribbons and other shapes by electrospinning", J.Polym. Sci., B39, 201, pp. 2598-2606.

[5] Kallmes, O. and Corte, H., Tappi J., 43(9), 1960, pp. 737.

[6] Eichhorn, S.J. and Sampson, W.W., Statistical geometry of pores and statistics of porous nanofibrous assemblies, J.R. Soc. Interface, 2, 2005, pp. 309-318.

[7] Deng, M. and Dodson, C. "Paper: an engineered stochastic structure", Tappi Press, Atlanta 1994.

[8] Dodson, C. and Sampson, W., J. Statist. Phys., 96, 1999, pp. 447.

[9] Sampson, W. Proc. 12th FRS, Oxford, 2001, pp. 1205-1288.

[10] Wang, H. and Shaler, S., J. Pulp Pap. Sci., 24(10), 1998, pp. 314.

[11] Niskanen, K. and Alava, M., Phys. Rev. Lett., 73(25), 1994, pp. 3475.

[12] Alava, M. and Niskanen, K., Reports on Progress in Physics, 69(3), 2006, pp. 669.

[13] Niskanen, K., Nilsen, N., Hellen, E., Alava, M., Proc. 11th FRS, Cambridge 1997, pp. 1273-1293.

[14] Curto, J., Conceição, E., Portugal, A., Simões, R., "Three dimensional modeling of fibrous materials and experimental validation", ACE-X2010, Proc. 4th International conference on advanced computational engineering and experimenting, 2010.

[15] Conceição, E., Curto, J., Simões, R., Portugal, A., Proceedings ComplMAGE 2010, 2nd International Symposium on Computational Modeling of Objects Represented in Images, vol. 6026 of Lecture Notes in Computer Science, Springer, Berlin 2010, pp. 299–310.

[16] Provatas, and Uesaka, T., J. Pulp Pap. Sci., 29(10), 2003, pp.332.

[17] Provatas, N., Haataja, M., Asikainen, J., Majaniemi, J., Alava, M., Ala-Nissila, T., "Physicochemical and Eng. Aspects" Fiber, Colloids and Surfaces, 165, 2000, pp. 209-229.

[18] Santner, T.J., Williams, B.J., Notz, W.I., "The design and analysis of computer experiments", Springer series in statistics, Springer-Verlag, New York, USA, 2003.

[19] Fang, K.-T., Li, R., Sudjianto, A.,"Design and modeling for computer experiments", Computer science and data analysis series, Chapman & Hall/CRC, London, UK, 2005.

[20] Hawkins, D. M., Recursive Partitioning., WIREs Comp. Stat., 1, 2009, pp. 290–295.

[21] Breiman, L., Friedman, J. H., Olshen, R. A., Stone, C. J., Classification and Regression Trees, Wadsworth, Belmont, CA, 1984.

The fiber properties influence on a three dimensional web model: reinforced office paper and cellulose nanowebs case studies

Curto, J.M.R. [1], Conceição, E. L.T.[2], Portugal, A.T.G.[2] and Simões, R.M.S.[1]
[1]Textile and Paper Materials Research Unit,
Chemistry Department, University of Beira Interior (UBI)
[2] Research Centre for Chemical Processes Engineering and Forest Products,
Chemical Engineering Department, University of Coimbra (UC)

Abstract

This article presents a computational model and some simulation results for fibrous materials such as paper and nanoclellulosic web materials. To obtain a better understanding of the influence of fiber properties on the paper structure a novel paper model was developed. This is a physically based model where the web is formed by the sequential deposition of individual fibers. This model is a three dimensional web model that includes the fiber model with a resolution up to 0.05 μm for paper, and 0.05nm for cellulosic naonofibers.
For the case of paper, laboratory handsheets were produced to study the network formation and resulting porous structure was characterized.
The computational simulator was used to investigate the relative influence of fiber properties, such as fiber flexibility and fiber dimensions, for the macro and nanosacle materials.

Keywords: 3D structure model, cellulose fibers, nanocellulose fibers, network materials modeling, fiber flexibility

Chapter 5 Conclusions and Future Work

The properties of stochastic fibrous materials like paper and nanowebs are highly dependent on those fibers from which the network structure is made. Advanced materials like composites, every day materials like paper, or new material like nanowebs used as scaffolds in tissue engineering, filtration and sensors consist of fibrous porous structures. The optimization of the final material properties is a difficult task, especially due to the different fiber properties, contributing in opposite directions, and the influence of various process operations as well as the complexity of the final network structure.

This work contributes to a better understanding of the effect of fiber properties on the network structural properties, using an original 3D fibrous material model with experimental validation, and its application to different fibrous materials: reinforced *Eucalyptus* office paper and nanofibrous networks.

To establish the relationships between the fiber and the final structural material properties, an experimental laboratorial plan has been executed for three different pulp fibers and a physical based 3D model has been developed and implemented. The experimental plan was dedicated to an important Portuguese material: the reinforced *Eucalyptus* based office paper. Office paper is the main Portuguese paper industry product. This paper is mainly produced from *Eucalyptus globulus* bleached Kraft pulp with a small incorporation of a softwood pulp, called reinforcement pulp, to increase paper strength and enhance runnability. The contribution of different reinforcement pulp fibers with different biometry and coarseness to the final paper properties was accessed. The two extremes of reinforcement pulps are represented by a *Picea abies* Kraft softwood pulp, usually considered the best reinforcement fiber, and the Portuguese pine *Pinus pinaster* Kraft pulp. The Portuguese fiber exhibits higher coarseness (45%), length (13%) and width (15%) than the market softwood. One of the goals was to quantify how the different reinforcement pulps and process operations will contribute to final paper properties. To obtain that, several levels of incorporation were tested and process operations like beating and drying studied. Paper properties have been found to be non linear in relation to pulp mixture proportions. The conclusions pointed out that, with the optimal beating, the Portuguese Pine improves tearing and tensile strength of the *Eucalyptus* based paper being possible to obtain equivalent or greatest performance than using the market pulp.

Nevertheless its recognized importance, there is a lack of information about fiber flexibility and its evolution along the pulping process and stock preparation. This study contributes to a better understanding of fiber flexibility as a key factor and presents experimental values for the most important fibers and process operations: bleaching, beating and drying. Fiber flexibility was determined experimentally using the Steadman and Luner method with a computerized acquisition device. An experimental pulp and paper evaluation was obtained in

order to determine the fiber flexibility influence on paper properties. Results indicated that beating had a major effect on fiber flexibility. *Pinus pinaster*, having the thickest fiber wall presents the major change with a rise of $14x10^{11}N^{-1}m^{-2}$, while increasing $4x10^{11}N^{-1}m^{-2}$ with bleaching and diminishing $3x10^{11}N^{-1}m^{-2}$ with drying.

We concluded that, when comparing two reinforcement fibers, the information about fiber flexibility and biometry is determinant to predict paper properties. The values presented correspond to the two extremes of fibers available as reinforcement fibers, regarding wall thickness, beatability and flexibility values. *Pinus pinaster* is the thickest wall fiber, with an average wall near to double, and consequently less flexible than the thinner wall fibers: *Pinus sylvestris* and *Picea abies*. Experimental results for the evolutions of paper properties, like paper apparent density, air permeability, tensile and tear strength, with fiber flexibility, for the two reinforcement fibers, constitute valuable information, also applicable for other reinforcement fibers, with fiber walls dimensions in this range.

Another important achievement is the development of a network fibrous materials model using key fiber properties. The computational model is implemented for fibrous materials such as paper and nanofibrous materials. This is a physically based model where the network is formed by the sequential deposition of individual fibers. The model includes key papermaking fiber properties like morphology, flexibility, and collapse and process operations such as fiber deposition, network forming and densification. This model is a three dimensional model that includes a detailed fiber model. In the case of paper fibers the fiber microstructure is considered, that is, lumen and fiber wall thickness, with a resolution up to 0.05 μm. The model has shown good prediction capability for structural properties like paper thickness. Simulation studies constitute an important tool to separate the influence of fiber properties like fiber flexibility and fiber collapse on the structure densification that occurs with beating.

The 3D network model was modified to model nanofibrous materials and implemented for Polyamide-6 electrospun and cellulose nanowebs. In the case of the nanofibrous materials, the resolution obtained is 0.05nm. When we are modeling materials such as paper, non-woven textiles and fibrous filters, fibers have finite length. For electrospun networks, because of the fiber continuous formation process, fibers can be assumed to have infinite length. This is the major modification to model such networks. Therefore we have modeled these structures as a random network of infinite lines, implemented mathematically as lines occupying all the sampling lattice, that represent the longitudinal axes of fibers and pass through points, distributed according to a point Poisson process, in the plane with uniformly distributed orientation. The influence of computational fiber flexibility and dimensions were investigated. For the Polyamide-6 electrospun network experimental results were compared with simulation results and similar evolution was observed. For cellulose nanowebs the simulation study used literature data to obtain the input information for the nanocellulose fibers. For both cases, the design of computer experiments was done using a space filling

design, the Latin hypercube sampling design, and the simulations results were organized using regression trees.
Both experimental characterization and computational modeling contributed to study the relationships between the polymeric fibers and the network structure formed.

In future work we intend to use the paper model to study the influence of fillers addition, fines and different pulp mixtures. For oriented structures, like commercial paper, which has more fibers in the machine direction, it can be interesting to use the Equivalent Pore model from Silvy (1980), jointly with this structural model (Shaffnit, Silvy and Dodson, 1992; Silvy, 1980).
We also intend to model other nanostructured materials, as well as to continue the work already initiated with cellulose and electrospun nanofibers. Considering that nanomaterials are pointed as key materials for the future (Barnes *et al.*, 2007; Paiva *et al.*, 2007; Ma *et al.*, 2005 and Silva, *et al.*, 2010) we expect that the developed 3D nanostrucuture simulator becames an important tool to study these materials. Particularly in the nanoscale, measurements are still difficult to obtain, and simulation studies can give an important contribution to enhance new materials.

References

ALAVA, M. and NISKANEN, K., 2006. The physics of paper. *Reports on Progress in Physics*, vol.69 no.3 (2006): pp. 669-723.

BARNES, C.P., SELL, S.A, BOLAND, E.D., SIMPSON, D.G. and BOWLIN, G.L., 2007. Nanofiber technology: Designing the next generation of tissue engineering scaffolds. *Advanced Drug Delivery Reviews,* vol.59 (2007): pp. 1413–1433.

BATCHELOR, W.J., KURE, K. and OUELLET, D., 1999. Refining and the development of fiber properties. *Nordic Pulp and Paper Research Journal*, vol.14 no.4 (1999): pp. 285-291.

BERGLUND, L.A. and PEIJIS, T., 2010. Cellulose biocomposites – from bulk molding to nanostructured systems. *MRS bulletin*, vol.35 (2010): pp. 201-207.

BLOCH, J.-F. and ROSCOAT, S.R., 2009. Three-dimensional structural analysis. 14th Fundamental Research Symposium, Oxford, session5 (2009): pp. 599-664.

BOCHKAREVA, L.V., KIREITSEU, M.V., TOMLINSON, G.R, ALTENBACH, H., KOMPIS, V. AND HUI, D., 2005. Computational simulation and 3D virtual reality engineering tools for dynamical modeling and visualization of composite nanomaterials. ENS'05 Paris, France, 14-16 December 2005, TIMA Editions, (2005): 6 pages. ISBN: 2-916187-02-2.

CHENG, Q. and WANG, S., 2008. A method for testing the elastic modulus of single cellulose fibrils via atomic force microscopy. *Composites: part A*, vol.39 (2008): pp. 1838-1843.

CHHABRA, R. and SHAMBAUGH, P.L., 2004. Probabilistic model development of webs structure formation in the melt blowing process. *INJ Fall*, International Nonwovens Journal (2004): pp. 24-34.

CHOWDHURY, M. and STYLIOS, G., 2010. Effect of experimental parameters on the morphology of electrospun Nylon 6 fibers. *International Journal of Basic & Applied Sciences IJBAS-IJENS*, vol.10 no.6 (2010): pp. 116-131.

CLARK, J. d'A, 1985. Pulp technology and treatment for paper, 2nd ed,, Miller Freeman Publications, San Francisco (1985): PP. 187.

CONCEIÇÃO, E.L.T., CURTO, J.M.R., SIMÕES, R.M.S. and PORTUGAL, A.T.G., 2011. Parallelization of a parameter estimation problem in a 3D model of paper. In Proceedings of the "Congresso de Métodos Numéricos de Engenharia", CMNE, APMATC, Coimbra, Portugal, 14-17 July, vol.1 (2011).

CONCEIÇÃO, E.L.T., CURTO, J.M.R, SIMÕES, R.M.S and PORTUGAL, A.T.G., 2010. Coding a simulation model of the 3D structure of paper. In Proceedings of the 2nd International Symposium on Computational Modeling of Objects represented in Images, CompIMAGE 2010, USA. *Lecture Notes in Computer Science*, Barneva; R.P. *et al*. (Eds.), Springer-Verlag Berlin, vol.60 no.26 (2010): pp. 299–310. ISBN: 978-3-642-12711-3. ISI Document Delivery No.: BPJ99.

CRESSON, T., 1995. Wet fiber flexibility: a measurement whose time has finally come, World Pulp and Paper Report, (1995).

CURTO, J.M.R, CONCEIÇÃO, E.L.T., PORTUGAL, A.T.G. and SIMÕES, R.M.S., 2011a. The fiber properties influence on a 3D web model: paper and cellulose nanoweb case studies. In Proceedings of the 5th International Conference on Advanced Computational Engineering and Experimenting, ACE-X2011, Algarve, Portugal (2011). Best Paper Young Scientist Award, Springer.

CURTO, J. M. R., HEKMATI, A.H., DREAN, J.Y, CONCEIÇÃO, E.L.T., PORTUGAL, A.T.G., R. M. S. SIMÕES, R.M.S. and M. J. SANTOS SILVA, M.J., 2011b. Three dimensional polyamide-6 nanowebs modeling and simulation. In Proceedings of the 11th World Textile Conference, AUTEX 2011 (Association of Universities for Textiles), Mulhouse, ENSISA (École Nationale Supérieure d'Ingénieurs Sud Alsace), France, June, vol.2 (2011): pp. 639-643. ISBN: 978-2-7466-2858-8.

CURTO, J.M.R, CONCEIÇÃO, E.L.T., PORTUGAL, A.T.G. and SIMÕES, R.M.S., 2011c. Three dimensional modeling of fibrous materials and experimental validation. *Materialwissenschaft und Werstofftechnik, Materials Science and Engineering Technology*, Wiley-vch, Germany, Wiley-Blackwell, USA, vol.42 no.5 (2011): pp. 370-374. ISSN: 0933-5137 (Print). ISSN 1521-4052 (Online). ISI IDS no.: 762EM.

CURTO, J.M.R., CONCEIÇÃO, E.L.T., PORTUGAL, A.T.G. and SIMÕES, R.M.S., 2011d. The influence of *Eucalyptus* and reinforcement fibers flexibility on paper properties: experimental and 3D paper model evaluation. In Proceedings of the 5th ICEP - International Colloquium on *Eucalyptus* Pulp held in May 9-12, Porto Seguro, Brazil (2011).

CURTO, J.M.R, CONCEIÇÃO, E.L.T., PORTUGAL, A.T.G. and SIMÕES, R.M.S., 2010a. Comparative study of fibers for *Eucalyptus globulus* based paper using experimental characterization and 3D paper modeling. In Proceedings of the 2nd "Simpósio de Materiais Texteis e Papeleiros", Universidade da Beira Interior, Covilhã, Portugal (2010). ISBN: 978-989-654-074-6.

CURTO, J.M.R, CONCEIÇÃO, E.L.T., PORTUGAL, A.T.G. and SIMÕES, R.M.S., 2010b. Three dimensional modeling of fibrous materials and experimental validation, ACE-X2010. In Proceedings of the 4th International Conference on Advanced Computational Engineering and Experimenting, Paris, France (2010).

CURTO, J.M.R, CONCEIÇÃO, E.L.T., PORTUGAL, A.T.G. and SIMÕES, R.M.S., 2010c. The fiber properties influence on a three dimensional paper model. In Proceedings of the XXIII Tecnicelpa conference and exhibition / VI CIADICYP, vol.1 (2010): pp. 123.

CURTO, J.M.R, GIL, C., CONCEIÇÃO, E.L.T., PORTUGAL, A.T.G. and SIMÕES, R.M.S., 2009a. "Estudo comparativo de incorporação de fibra de *Pinus pinaster* branqueada no papel de *Eucalyptus globulus*". *Revista Pasta e Papel* (2009): pp. 52-57.

CURTO, J.M.R, CONCEIÇÃO, E.L.T., PORTUGAL, A.T.G. and SIMÕES, R.M.S., 2009b. The fiber coarseness and collapsibility influence on a three dimension paper model. In Proceedings of the 63rd Appita annual Conference and Exhibition, Melbourne, Australia, 19-22 April (2009): pp. 303-310. ISBN: 9780975746952.

CURTO, J.M.R, CONCEIÇÃO, E.L.T., PORTUGAL, A.T.G. and SIMÕES, R.M.S., 2007a. "Modelo de papel 3D em MATLAB utilizando autómatos celulares". In Proceedings of "Engenharias'07: 4.ª Conferência de Engenharia", UBI, Covilhã, Portugal, November, vol.1 (2007): pp. 8-12.

CURTO, J.M.R, GIL, C., CONCEIÇÃO, E.L.T., PORTUGAL, A.T.G. and SIMÕES, R.M.S., 2007b. *Pinus pinaster* as reinforcement pulp on *Eucalyptus* based paper. In Proceedings of the 22nd "Encontro Nacional da TECNICELPA", Tomar, Portugal (2007): pp. 29-35.

CURTO, J.M.R and SIMÕES, R.M.S., 2005. "Contribuição para o estudo do potencial papeleiro do *Pinus pinaster* como fibra de reforço". In Proceedings of the 20th "Encontro Nacional da TECNICELPA", Tomar, Portugal (2005): pp. 263-272.

CURTO, J.M.R., SIMÕES, R.M.S. and SILVY, J., 2003a. The influence of beating, bleaching and drying in the Wet Fiber Flexibility of *Pinus pinaster* kraft pulp. International Symposium of Wood and Pulp Chemistry, ISWPC, 8-12 June, Madison, EUA, vol.III (2003): pp. 287-294.

CURTO, J.M.R, SIMÕES, R.M.S. and SILVY, J., 2003b. The influence of beating, bleaching, drying in the Wet Fiber Flexibility of the Portuguese softwood kraft pulp (*Pinus pinaster*), COST European E11: Characterization methods for fibers and paper, 4-5 October, Hanasaari, Espoo, Finland (2003): pp. 89-92.

CURTO, J., SIMÕES, R., SANTOS SILVA, M. and SILVY, J., 1998. Wet Fiber Flexibility of paper making materials "Estudo da flexibilidade húmida de diferentes materiais fibrosos utilizados na fabricação do papel". In Proceedings of the 16th "Encontro Nacional da TECNICELPA", Covilhã, Portugal, October, (1998): pp. 415.

DEITZEL, J.M., KLEINMEYER, J., HARRIS, D. and TAN, N.C.B., 2001. The effect of processing variables on the morphology of electrospun nanofibers and textiles. *Polymer*, vol.42 (2001): pp. 261–272.

DENG, M. and DODSON, C.T.J, 1994. "Paper: an engineered stochastic structure", Tappi Press, Atlanta, USA (1994). ISBN 0-89852-283-8.

DICKSON, A.R, CORSON, S.R. and DOOLEY, N.J., 2006. Fiber collapse and decollapse determined by cross-sectional geometry. *Journal of Pulp and Paper Science*, vol.32 no.34 (2006): pp. 1-5.

DJERBI, S., 2005. Cellulose synthesis in *Populus*: identification, expression analyses and in vitro synthesis, University dissertation from Stockholm, KTH (2005).

DODSON, C.T.J. and SAMPSON, W.W., 2009a. Intrinsic correlation in planar Poisson line processes. *Appl. Math. Lett.*, vol. 22 no.7 (2009): pp. 981-987.

DODSON, C.T.J. and SAMPSON, W.W., 2009b. Structural invariance of stochastic fibrous networks. In Advances in Pulp and Paper Research, Oxford 2009, Trans. XIVth Fund. Res. Symp. (S.J. I'Anson, ed.), FRC, Manchester, (2009): pp. 665.

DODSON, C.T.J. and SAMPSON, W.W., 2008. Stochastic Fiber Networks. In Information Geometry: Near Randomness and Near Independence, Arwini, K.A. and Dodson, C.T.J. (Eds.), Springer-Verlag Berlin, (2008).

DODSON, C.T.J. and SAMPSON, W.W., 2007. Planar line processes for void and density statistics in thin stochastic fiber networks. *J. Statist. Phys.*, vol.129 no.2 (2007): pp. 311-322.

DODSON, C.T.J. and SAMPSON, W.W., 2005 Effect of correlated free fiber length on pore size distribution in fiber mats. *FRS Cambridge*, (2005): pp. 943-960.

DODSON, C.T.J., HANDLEY, A.G., OBA, Y. and SAMPSON, W.W., 2003. The pore radius distribution in paper. Part I: The effect of formation and grammage. Appita Journal vol.56 no.4 (2003): pp. 275-280.

DODSON, C.T.J., OBA, Y. and SAMPSON, W.W., 2001. On the distributions of mass, thickness and density in paper. *Appita Journal*, vol.54 no.4 (2001): pp. 385-389.

DODSON, C. AND SAMPSON, W., J., 1999. *Statist. Phys.*, vol.96 (1999): pp. 447.

DODSON, C.T.J., 1998. On the distribution of pore heights in layered random fiber networks. EC COST E11, Geometrical characterization of paper, Brussels, 12, 13 Nov. (1998) pp. 1-6.

DODSON, C.T.J. and FEKIH, K., 1991. The effect of fiber orientation on paper formation. *Journal of Pulp and Paper Science*, vol.17 no.6 (1991): pp. 203-206.

EICHHORN, S.J. and SAMPSON, W.W., 2005. Statistical geometry of pores and statistics of porous nanofibrous assemblies. *J. R. Soc. Interface* vol.2 no.4 (2005), pp. 309–318.

EICHHORN, S.J. and SAMPSON, W.W., 2010. Relationships between specific surface area and pore size in electrospun polymer fiber networks. *J. Roy. Soc. Interface*,vol.7 no. 45 (2010): pp. 641-651.

FANG, K.-T., LI, R., SUDJIANTO, A., 2005. Design and modeling for computer experiments, *Computer science and data analysis series*, Chapman & Hall/CRC, London, UK, (2005).

FENGEL, D. and WEGENER, G., 1989. Wood chemistry, ultrastucture, reactions, Walter de Gruyter, Berlin and New York, (1989).

FARNOOD, R.R., DODSON, C.T.J and LOEWEN, S.R., 1995. Modeling flocculation. Part I: random disk model. *Journal of Pulp and Paper Science*, vol.21 no.10 (1995): pp. 348-355.

FOELKER, Celcius., 2002. Advances in *Eucalyptus* fiber properties and paper products.

FRIDRIKH, S.*V. et al., 2003.* Controlling the fiber diameter during electrospinning, *Phys*. Rev. Lett., vol.90, (2003): pp. 1-4.

GATENHOLM, P. and KLEMM, D., 2010. Bacterial nanocellulose as a renewable material for biomedical applications. *MRS bulletin*, vol.35 (2010).

GORRES, J., AMIRI, R., WOOD, J.R. and KARNIS, A., 1996. Mechanical pulp fines and sheet structure. *Journal of Pulp and Paper Science*, vol.22.no.12 (1996): pp. 491-496.

GORRES, J., CRESSON, T. and LUNER, P., 1989. Sheet formation from flocculated structures. *Journal of Pulp and Paper Science*, vol.15 no.2 (1989): pp. 55-59.

GRAFE, T. and GRAHAM, K., 2003. Polymeric nanofibers and nanowebs: a new class of nonwovens. *INJ Spring* (2003) pp. 51-55.

GRAFE, T. and GRAHAM, K., 2003. Nanofiber webs from electrospinning. Nonwovens in filtration -5th International Conf. Stuttgard, Germany, (2003).

HELLÉN, E.K.O., KETOJA, J.A., NISKANEN, K.J. and ALAVA, M.J., 2002. Diffusion through fiber networks. *Journal of Pulp and Paper Science*, vol.28. no.2 (2002): pp. 55-62.

HELLÉN, E., 2002. Non equilibrium dynamics in fiber networks, aggregation, and sand ripples. Dissertation for the degree of Doctor of Science in Technology, Helsinki University of Technology, Espoo, Finland (2002).

HEYDEN, S. and GUSTAFSSON, P.J., 1998. Simulation of fracture in a cellulose fiber network. *Journal of Pulp and Paper Science*, vol.24 no.5 (1998): pp. 160-165.

HIGGINS, H.G., DE YONG, J. BALODIS, V., PHILLIPS, F.H. and COLLEY, J., 1991. The density and structure of hardwoods in relation to paper surface characteristics and other properties. Process Engineering Handbook, Appendix, Tappi Press, Atlanta, (1991): pp. 77-81.

HONKASALO, J., 2004. Behavior of different furnishes mixtures in mechanical printing papers. Dissertation for the degree of Doctor of Science in Technology, Helsinki University of Technology, Espoo, Finland (2004).

HOSSEINI, S.A. and TAFRESHI, H.V., 2010. 3-D simulation of particle filtration in electrospun nanofibrous filters. *Powder Technology*, vol.201 (2010): pp. 153-160.

HUANG, Z., ZHANG, Y.-Z, KOTAKIC, M. and RAMAKRISHN, S., 2003. A review on polymer nanofibers by electrospinning and their applications in nanocomposites. *Composites Science and Technology*, vol.63 (2003): pp. 2223–2253.

I'ANSON, S.J., SAMPSON, W.W. and SAVANI, S., 2008. Density dependent influence of grammage on tensile properties of handsheets, *Journal of Pulp and Paper Science*, vol.34 no.3 (2008): pp. 182–189.

I'ANSON, S.J., SAMPSON, W.W. and SEVAJEE., 2007a. New perspectives on the influence of formation and grammage on sheet strength. Paptac. (2007): pp. 1-4.

I'ANSON, S.J., CONSTANTINO, R.P.A., HOOLE, S.M. and SAMPSON, W.W., 2007b. Estimation of the profile of cross-machine shrinkage of paper. Meas. Sci. Tech. 19:015701 (2007).

I'ANSON, S.J., KARADEMIR, A. and SAMPSON, W.W., 2006. Specific Contact Area and the Tensile Strength of Paper. *Appita Journal* vol. 59 no. 4(2006): pp. 297 -301.

I'ANSON, S.J. and SAMPSON, W.W., 2007. Competing weibull and stress-transfer influences on the specific tensile strength of a bonded fibrous network. *Composites Science and Technology*, vol. 67 no.7 (2007): pp. 1650-1669.

JAYARAMAN, K. *et al.*, 2004. Recent advances in polymer nanofibers, *J. Nanosci. Nanotechol.*, vol.4, (2004): pp. 52-65.

KALASKAR, D., GOUGH, J.E., ULIJN, R.V., SAMPSON, W.W., SCURR, D.J., RUTTEN, F.J., ALEXANDER, M.R., MERRY, C.L.R. and EICHHORN, S.J., 2008. Controlling cell morphology on amino acid modified cellulose. *Soft Matter*, vol.4 no.5 (2008): pp. 1059-1065.

KALLMES, O. and Corte, H., 1962. Formation and structure of paper. Ed. F. Bolam, Technical section, B.P. & B.M.A., London. (1962): pp. 351-368.

KALLMES, O. and Corte, H., 1960. The structure of paper. I - The Statistical Geometry of an Ideal Two Dimensional Fiber Network. *Tappi Journal.*, vol.43 no.9 (1960): pp. 737-752.

KATAJA, M., HILTUNEN, K. and TIMONEN, J., 1992. Flow of water and air in a compressible porous medium. A model of wet pressing of paper. *J. Phys. D: Appl Phys.*, vol.25 (1992): pp. 1053-1063.

KIM, H., KIM, D.-W., and SEO, M.H., 2005. A Simulation method for modeling the morphology and characteristics of electrospun polymeric nanowebs. *Macromolecular Research*, vol.13 no. 2 (2005): pp. 107-113.

KOOMBHONGSE, S. *et al.*, 2001. Flat polymer ribbons and other shapes by electrospinning, *J.Polym. Sci.*, B39 (2001): pp. 2598-2606.

KORNEV, K.G., REN, X. and DZENIS, Y., 2009. Controlling liquid release by compressing electrospun nanowebs, *Journal of Engineered Fibers and Fabrics*, vol.4 issue 2 (2009): pp. 14-21.

KUGGE, C., BELLANDER, H. and DAICIC, J., 2005. Pressure filtration of cellulose fibers. *Journal of Pulp and Paper Science*, vol.31 no.2 (2005): pp. 95-100.

KWONG, K. and FARNOOD, R., 2007. Modeling the compression of three-dimensional fiber networks using dynamic finite-element analysis. *Journal of Pulp and Paper Science*, vol.33 no.2 (2007): pp.1-6.

LIPPONEN, A., LEPPÄNEN, T., ERKKILÄ, A.-L. and HÄMÄLÄINEN, J., 2008. Effect of drying on simulated cockling of paper, *Journal of Pulp and Paper Science*, vol.34 no.4 (2008): pp. 226-233.

LUNER, P., 1986. Wet Fiber Flexibility as a Index of Pulp and Paper properties, 1986 PIRA International Conference on "Advances in Refining Technologies", Birmingham, England, vol.1, Session 1, Paper 3 (1986).

LUUKKO, K. and PAULAPURO, H., 1999. Mechanical pulp fines: effect of particle size and shape. *Tappi Journal* vol.82 no.2 (1999): pp.95-101.

MA, Z., KOTAKI, M., INAI, R. and RAMAKRISHNA, S., 2005. Potential of nanofiber matrix as tissue-engineering scaffolds. *Tissue Engineering*, vol.11 no.1/2 (2005): pp. 101-109.

MAKELLA, P., NORDHAGEN, H. and GREGERSEN, O.W., 2009. Validation of isotropic deformation theory of plasticity for fracture mechanics analysis of paper materials. *Nordic Pulp and Paper Journal* vol.24 no.4 (2009): pp. 388-402.

MAZE, B., TAFRESHI, H.V., WANG, Q.B. and POURDEYHIMI, B., 2007. A simulation of unsteady-state filtration via nanofiber media at reduced operating pressures. *Journal of Aerosol Science*, vol.38 (2007): pp. 550-571.

MEIER, H., 1961. Chemical and morphological aspects of the fine structure of wood, Trakemiska cudhninger Svenska Traforskningsinstitutet Stock holm, O Sverige, (1961): pp.37-52.

MIETTINEN, P.P.J., KETOJA, J.A. and KLINGENBERG, D.J., 2007. Simulated strength of wet fiber networks. *Journal of Pulp and Paper Science*, vol.33 no.4 (2007): pp.1-8.

MOLIN, U. and TEDER, A., 2002. Importance of cellulose/hemicellulose-ratio for pulp strength, *Nordic Pulp and Paper Journal* vol.17 no.1 (2002): pp. 14–19.

MORSEBURG, K. and CHINGA-CARRASCO, 2009. Assessing the combined benefits of clay and nanofibrillated cellulose in layered TMP-based sheets. *Cellulose*, vol.16 (2009): pp. 795-806.

MOSS, P.A. and RETULAINEN, E., 1997. The effect of fines on fiber bonding: cross-sectional dimensions of TMP fibers at potential bonding sites. *Journal of Pulp and Paper Science*, vol.23 no.8 (1997): pp. 382-388.

NAKAGAITU, A.N., NOGI, M. and YANO, H., 2010. Displays from transparent films of natural nanofibers. *MRS Bulletin*, vol.35 (2010): pp. 214-218.

NAZHAD, M.M., HARRIS, E.J., DODSON, C.T.J. and KEREKES, R.J., 2000. The influence of formation on tensile strength of paper made from mechanical pulps. *Tappi Journal*. Dec (2000): pp. 1-9.

NILSEN, N., ZABIHIAN, M. and NISKANEN, K., 1998. KCL-Pakka: a tool for simulating paper properties. *Tappi Journal* vol.81 no.5 (1998): pp. 163-166.

NISKANEN, K. and RAJATORA, H., 2002. Statistical Geometry of Paper Cross-Sections. *Journal of Pulp and Paper Science*, vol.28 no.7 (2002): pp. 229-233.

NISKANEN, K., KAJANTO, I. and PAKARINEN, P., 1998. Paper structure. Paper Physics, Papermaking Science and Technology, Fapet Oy e Tappi, Finland (1998).

NISKANEN, K., NILSEN, N., HELLEN, E., ALAVA, M., 1997. KCL-PAKKA: simulation of 3D structure of paper. Proc. 11th FRS, Cambridge (1997): pp. 1273-1293.

NISKANEN, K. AND ALAVA, M., 1994. Planar random networks with flexible fibers *Phys. Rev. Lett.*, vol.73 no.25 (1994): pp. 3475-3478.

PAAVILAINEN, L., 1998. Quality – Competitiveness of Asian short fiber-raw materials in different paper grades. *Know-How Wirw, Jaakko Poyry Magazine* vol. 1/98 (1998): pp. 4-7.

PAAVILAINEN, L., 1994. Influence of fiber morphology and processing on the paper making potential of softwood sulphate pulp fibers. TAPPI Proceedings – Pulping Conference (1994).

PAAVILAINEN, L., 1993a. Importance of cross-dimensional fiber properties and coarseness for the characterization of softwood sulphate pulp. *Paperi ja Puu - Paper and Timber* vol.75 no.5 (1993): pp. 343-351.

PAAVILAINEN, L., 1993b. Conformability – flexibility and collapsibility – of sulphate pulp fibers. *Paperi ja Puu - Paper and Timber*, vol.75 no.9-10 (1993): pp. 689-702.

PAAVILAINEN, L., 1992. The possibility of fractionating softwood sulphate pulp according to cell wall thickness. *Appita Journal* vol.45 no.5 (1992): pp. 319-326.

PAAVILAINEN, L., 1990. Importance of particle size – fiber length and fines – for the characterization of softwood Kraft pulp. *Paperi ja Puu - Paper and Timber* vol.72 no.5 (1990): pp. 516-526.

PAAVILAINEN, L., 1989. Effect of sulphate cooking parameters on the parameters on the papermaking potential of pulp fibers. *Paperi já Puu - Paper and Timber* vol.4 (1989): pp. 356-363.

PAGE, D. H., SETH, R. S., JORDAN, B. D. and BARBE, M.C., 1985. Curl, crimps, kinks and microcompressions in pulp fibres: their origin, measurements and significance. Paper Making Raw Materials: Their Interaction with the Production Process and Their Effect on Paper Properties, Transactions of the 8th Fundamental Research Symposium (ed. V. Punton), September 1985, Oxford, UK, (1985): pp. 183-227.

PAGE, D.H., El-HOSSEINY, F., WINKLER, K. and LANCASTER, A.P.S., 1977. Elastic modulus of single wood fibers. *Tappi Journal*, Vol.60 no.4 (1977): pp.114-117.

PAGE, D.H., 1969. A theory for the tensile strength of paper. *Tappi Journal*, vol.52 no.4 (1969): pp. 674-681.

PAGE, D. H. and Grace, J., 1967. The delamination of fiber walls by beating and refining. *Tappi Journal* vol.50 no.10 (1967): pp. 489-501.

PAIVA, A.T., SEQUEIRA, S.M., EVTUGUIN, D.V., KHOLKIN, A. L. and PORTUGAL, I., 2007. Nanoscale structure of cellulosic materials: challenges and opportunities for AFM. *Modern Research and Educational Topics in Microscopy*, (2007): pp. 726-733.

PATRA, S.N., EASTEAL, A.J. and BHATTACHARYYA, D., 2009. Parametric study of manufacturing poly(lactic) acid nanofibrous mat by electrospinning. *J Mater Sci*, vol.44 (2009): pp. 647–654.

PETIT-CONIL, M, PASSAS, R., CLEUT, J.C. , FOUNIER, R. and VOILLOT, C., 1999. Fiber characterization for understanding the effect of plate pattern on TMP and RMP quality. Cost E11, Characterization methods for fibers and paper, PTS workshop, (1999): pp. 5.1-5.12.

POURDEYHIMI ,B., MAZÉ , B. and TAFRESHI, H.V., 2006. Simulation and analysis of unbonded nonwoven fibrous structures. *Journal of Engineered Fibers and Fabrics*, vol.1 issue 2 (2006): pp. 47-65.

PROVATAS, N. and UESAKA, T., 2003. Modeling paper structure and paper press interactions. *Journal of Pulp and Paper Science*, vol.29 no.10 (2003): pp. 332-340.

PROVATAS, N., HAATAJA, M., ASIKAINEN, J., MAJANIEMI, J., ALAVA, M. and ALA-NISSILA, T., 2000. Fiber deposition models in two and three spatial dimensions. *Colloids and Surfaces A: Physicochemical and Engineering Aspects*, vol.165 (2000): pp. 209-229.

PROVATAS, N., HAATAJA, M., SEPPALA, E., J., MAJANIEMI, J., ASTROM, J., ALAVA, M. and ALA-NISSILA, T., 1997. Growth, percolation, and correlations in disordered fiber networks. *Journal of Statistical Physics* vol.87 no.1/2 (1997): pp. 385-394.

PULKKINEN, I., FISKARI, J. and ALOPAEUS, V., 2010. New model for predicting tensile and density of *Eucalyptus* handsheets based on an activation parameter calculated from fiber distribution characteristics. *Holzforshung* vol.64 (2010): pp.201-209.

RAUVANTO, I., RASA, M. and HENRICSON, K., 2008. Fiber damage in unbleached reinforcement pulp – study on the effects of medium consistency fluidization. *Journal of Pulp and Paper Science*, vol.34 no.2 (2008): pp. 121–128.

REBAI, M. *et al.*, 2010. A Lattice Boltzmann approach for predicting the capture efficiency of random fibrous media. *Asia-Pac. J. Chem. Eng.* (2010).

RUDIE, A.W., 1998. Wood and how it relates to paper products. *Tappi Journal*, vol.81 no.5 (1998): pp. 223-228.

RUNDLF, M., HTUN, M., HOGLUND, H. and WAGBERG, L., 2000. The importance of the experimental method when evaluating the quality of fines of mechanical pulps. *Journal of Pulp and Paper Science*, vol.26 no.9 (2000): pp. 301-307.

RUTLEDGE, G.C. and FRIDRIKH, S.V., 2007. "Formation of fibers by electrospinning", *Adv. Drug Del. Rev.*, vol.59 (2007): pp. 1384-1391.

SAMPSON, W.W., 2009. Modeling Stochastic Fibrous Materials with Mathematica. Springer-Verlag, London, 2009.

SAMPSON, W.W., 2009. Materials properties of paper as influenced by its fibrous architecture. *International Materials Reviews*, vol.54 no.3 (2009): pp. 134-156.

SAMPSON, W.W., 2008. Unified theory for structural statistics of flocculated and random fiber networks. *Journal of Pulp and Paper Science*, vol.34 no.2 (2008): pp. 91-99.

SAMPSON, W.W., and URQUHART, S.J., 2008. The contribution of out-of-plane pore dimensions to the pore size distribution of paper and stochastic fibrous materials. *J. Porous Mater*. vol.15 no.4 (2008): pp. 411.

SAMPSON, W.W., 2007. Statistical modeling of the pore structure of stochastic fiber networks. *Filtration*, vol.7 no.3 (2008): pp.251.

SAMPSON, W.W. and SIRVIÖ, J., 2005. The statistics of interfiber contact in random fiber networks. *Journal of Pulp and Paper Science*, vol.31 no.3 (2005): pp. 127-131.

SAMPSON, W.W., 2004. A model for fiber contact in planar random fiber networks. *Journal of Materials Science*, vol.39 no.8 (2004): pp. 2775-2781.

SAMPSON, W.W., 2002. The determination of the variance of local grammage in random fiber networks by the line method. *Journal of Pulp and Paper Science*, vol. 28 no.8 (2002): pp. 259-261.

SAMPSON, W.W., 2001. Comments on the pore radius distribution in near-planar stochastic fiber networks. *Journal of Materials Science,* vol.36 (2001): pp. 5131-5135.

SAMPSON, W.W., 2001. The structural characterization of fiber networks in papermaking process - a review. Trans. XIIth Fund. Res. Symp. (ed. C.F. Baker), Pulp and Paper Fundamental Research Society, Bury, Oxford, (2001): pp. 1205-1288.

SAMPSON, W.W., and DODSON, C.T.J., 1997. Modeling a class of stochastic porous media. *Appl. Math. Lett.,* vol.10 no.28 (1997): pp. 87-89.

SANTNER, T.J., WILLIAMS, B.J., NOTZ, W.I., 2003. The design and analysis of computer experiments, Springer series in statistics, Springer-Verlag, New York, USA, (2003).

SANTOS, I., GAIOLAS, C., CURTO, J.M.R., SILVY, J., SANTOS SILVA, M. and SIMÕES, R.M.S, 1998. A comparative study on the paper making potential of *Pinus pinaster* and *Pinus sylvestris* kraft pulps, "Estudo comparativo do potencial papeleiro das pastas Kraft de *Pinus pinaster* e de *Pinus sylvestris*". In Proceedings of the 16th "Encontro Nacional da TECNICELPA", Covilhã, Portugal, October (1998): pp.101-112.

SCHARCANSKI, J and DODSON, C.T.J., 1996. A new simulator for paper forming using neural network methods. Appita Journal vol.48 no.5 (1996): pp. 347-350.

SCHAFFNIT, C., SILVY, J. and DODSON, C.T.J., 1992. Orientation density distributions of fibers in paper. *Nordic Pulp and Paper Journal* no.3 (1992): pp. 121-125.

SETH, R.S. and CHANG, B.K., 1999a. Measuring fiber strength of papermaking pulps. *Tappi Journal*, vol.82 no.11 (1999): pp. 115-120.

SETH, R.S., 1999b. Beating and refining response of some reinforcement pulps. *Tappi Journal*, vol.82 no.3 (1999): pp. 147-155.

SETH, R.S. and PAGE, D.H., 1988. Fiber properties and tearing resistance. *Tappi Journal*, vol.71 no.2 (1988): pp. 103-107.

SILVA, T. C. F., HABIBI, Y. and LUCIA, L. A., 2011. Nanofibrillated cellulose-based aerogels: a new chemical approach for tuning their micro-architectures. In Proceedings of the 5th ICEP - International Colloquium on *Eucalyptus* Pulp held in May 9-12, Porto Seguro, Brazil (2011).

SILVEIRA, G., ZHANG, X., BERRY, R. and WOOD, J.R., 1996. Location of fines in mechanical pulp handsheets using scanning electron microscopy. *Journal of Pulp and Paper Science*, vol.22. no.9 (1996): pp. 315-320.

SILVY, J. Etude structurale de milieux fibreux: cas des fibres cellulosiques. PhD, Institut National Polytechnique de Grenoble, France, 1980.

SIRVIO, J. 2008. Fibres and Bonds (Chapter2) In Paper Physics. NISKANEN, K. (Editor), Paperi ja Puu Oy, (2008): pp. 77-78. ISBN: 978-952-5216-29-5. Citation of: JENTZEN, C.A., Tappi Journal vol.42 no.7 (1964): pp.412.

SOSZYNSKI, R.M., 1995. Simulation of two-dimensional nonrandom fiber networks. Oriented rectangles with equidistantly spaced centroids. *Journal of Pulp and Paper Science*, vol.21 no.4 (1995): pp. 127-131.

STEADMAN, R.K. and LUNER, P., 1992. An Improved Test to Measure the Wet Fiber Flexibility of Pulp Fibers. Empire State Paper Research Institute Report 79, Chapter V (1992): pp. 69-85.

STEVANIC, J.S., and SALMÉN, 2008. Interactions among components in the primary cell wall of Norway Spruce (*Picea abies* (L.) Karst.), Effect of a low sulphonation pretreatment, *Journal of Pulp and Paper Science*, vol.34 no.2 (2008): pp. 107–112.

TAN, X. and LI, K., 2008. Adhesion forces between ligno-cellulose surfaces by atomic force microscopy, *Journal of Pulp and Paper Science*, vol.33 no.1 (2008): pp. 1-9.

TAN, E. P. S. and LIM, C. T., 2006. Mechanical characterization of nanofibers – a review. *Composites Science and Technology*, vol.66 (2006): pp. 1102-1111.

TAN, E. P. S. and LIM, C. T., 2004. Physical properties of a single polymeric nanofiber. *Applied Physics Letters*, vol.81 no. 9 (2004): pp. 1603-1605.

TANAKA, A., KETTUNEN, H., NISKANEN, K. and KEITAANNIEMI, K., 2000. Comparison of energy dissipation in the out-of-plane and in-plane fracture of paper. *Journal of Pulp and Paper Science*, vol. 26 no.11 (2000): pp. 385-390.

THOMSON, C., LOWE, R., PAGE, D. and RAGAUSKAS, A.T., 2008. Exploring fiber-fiber interfaces via FRET and fluorescence microscopy, *Journal of Pulp and Paper Science*, vol.33 no.4 (2008): pp.113–120.

THOMPSON, C.J., CHASE, G.G., YARIN, A.L. and RENEKER, D.H., 2007. Effects of parameters on nanofiber diameter determined from electrospinning model. *Polymer*, vol.10 (2007): pp. 6913-6922.

TING, T.H.D, JOHNSTON, R.E. and CHIU, W., 2000. Compression of paper in the z-direction-the effects of fiber morphology, wet pressing and refining. *Appita Journal*, vol. 35 no.5 (2000): pp. 378-384.

VAINIO, A., KANGAS, J. and PAULAPURO, H., 2007. The role of TMP fines in interfiber bonding and fiber-segment activation, *Journal of Pulp and Paper Science*, vol.33 no.1 (2007): pp. 29-34.

VINCENT, R., RUEFF, M. and VOILLOT, C., 2009. 3-D computational simulation of paper handsheet structure and prediction of apparent density, *TAPPI Journal*, vol.8 no.9 (2009): pp. 10-17.

VINNURVA, J., ALAVA, M., ALA-NISSILA, T. and KRUG, J., 1998. Kinetic roughening in fiber deposition. Physical Review E, vol.58 no.1 (1998): pp. 1125-1131.

XU, Y. and PELTON, R., 2005. A new look at how fines influence the strength of filled papers, *Journal of Pulp and Paper Science*, Journal of Pulp and Paper Science, vol.31 no.3 (2005): pp. 147–152.

VAINIO, A., PAULAPURO, H., KOLJONEN, K. and LAINE, J., 2006. The effect of drying stress and polyelectrolyte complexes on the strength properties of paper, *Journal of Pulp and Paper Science*, vol. 32 no.1 (2006): pp. 9–13.

WÄGBERG, L. and ANNERGREN,G., 1997. Physicochemical characterization of papermaking fibers. In *The Fundamentals of Papermaking Materials*, Transactions do 11th Fundamental Research Symposium, vol.1, Pira, UK, Cambridge, (1997): pp. 2-82.

WATHÉN, R. and NISKANEN, K., 2006. Strength distributions of running paper webs. *Journal of Pulp and Paper Science*, vol.32 no.3. (2006): pp. 1-8.

WANG, Q., MAZE, B., TAFRESHI, H.V. and POURDEYHIMI, B., 2006. A case study of simulating submicron aerosol filtration via lightweight. *Chemical Engineering Science*, vol.61 (2006): pp. 4871 – 4883.

WANG, H. AND SHALER, S., 1998. Computer-simulated three-dimensional microstructure of wood fibre composite materials. *Journal of Pulp and Paper Science*, vol.24 no.10 (1998): pp. 314-319.

YAN, D., LI, K. and ZHOU, Y., 2008. Measurement of wet fiber flexibility of mechanical pulp fibers by confocal laser scanning microscopy. *Tappi Journal* (2008): pp. 25-31.

ZHAO, Y. and JIANG, L., 2009. Hollow micro / nanomaterials with multilevel interior structures. *Adv. Mater*. Vol.21 (2009): pp. 3621-3638.